FACTORS AFFECTING THE CORROSIVITY OF PULPING LIQUORS

A Thesis
Presented to
The Academic Faculty

by

Patrick Evan Hazlewood

In Partial Fulfillment
of the Requirements for the Degree of
Doctor of Philosophy in Chemical and
Biomolecular Engineering

Georgia Institute of Technology
May 2006

FACTORS AFFECTING THE CORROSIVITY OF PULPING LIQUORS

Approved by:

Preet M. Singh, Ph.D.
Advisor
Department of Materials Science and Engineering

Jeffery S. Hsieh, Ph.D.
Co-Advisor
Department of Chemical and Biomolecular Engineering

Sujit Banerjee, Ph.D.
Committee Member
Department of Chemical and Biomolecular Engineering

Arthur J. Ragauskas, Ph.D.
Committee Member
Department of Chemistry and Biochemistry

Yulin Deng, Ph.D.
Committee Member
Department of Chemical and Biomolecular Engineering

May 2006

Ideally, science should be married to engineering so as to invent new and better methods of prevention and apply existing methods more intelligently and effectively. However, scientists are sometimes devoted to the pursuit of pure knowledge, with little or no perspective on the possible applications of their work. On the other hand, engineers often apply time-honored methods with little or no understanding of the principles behind them.

-- D.A. Jones[1]
Introduction of Principles and Prevention of Corrosion

It comes with the territory. We hug, we kiss, we love. When people say to me how do you get through life or each day, it's the same thing. To me, there are three things we all should do every day. We should do this every day of our lives. Number one is laugh. You should laugh every day. Number two is think. You should spend some time in thought. Number three is, you should have your emotions moved to tears, could be happiness or joy. But think about it. If you laugh, you think, and you cry, that's a full day. That's a heck of a day. You do that seven days a week, you're going to have something special.

-- James 'Jim' Thomas Anthony Valvano[2]
ESPN Arthur Ashe Courage and Humanitarian Award Address

For my wife, who put up with me the many years of this journey, if

Only she knew how much I appreciated her silent support.

Rare indeed is the love that I have in my heart.

Very rarely have I come across a man as stubborn as my father.

Alas, I too am that man – a fact that embraces me every day.

Now as I move with the wind behind me I accept its grip!

TRUMPET MAN

…A GREAT CONSOLATION FOR US SINCE HE DIED

IS THAT HE AND GABRIEL PLAY SIDE BY SIDE.

WITH THE HEAVENLY CHORUS HE IS NOT ALONE.

THEY PLAY THEIR HORNS NOW BEFORE THE KING'S THRONE.

--R.J. Boudreaux, Jr.[3]
Ode to the Trumpet Man in Memory of Ivan 'John' Douglas Hazlewood, Jr.

ACKNOWLEDGMENTS

I would like to acknowledge the lab work of Lee Hill and Dr. Rallming Yang and conversations with future Dr. Cameron Thomson and Dr. M. Buchanan which contributed to this study. I would especially like to acknowledge the support and encouragement of my research group including co-advisor Dr. Jeff Hsieh; Dr. Jorge Perdomo; future Dr. Vikas Behrani, MS; Pablo Conde; and most importantly the ever present Jamshad Mahmood, MS.

For their active support and encouragement I must both thank and acknowledge Adam Karnofski, MS, MBA; Chris Chang, MS; the future Dr. Jason Montegna, MS; and the steadfast Drs. Lauri Lehtonen and Greg Delozier. Drs. Sharon Driscoll, James Turpin and Reed Welker – *Integritat*!!!

To the parents of my advisor, Dr. Preet Singh, thank you for raising an honorable man. It is due to his support and guidance that I will forever bear the title 'Doctor of Philosophy'. To the family of Dr. Barry Crouse, thank you for allowing me to borrow him for a short while. May his soul rest in peace.

Lastly, but most importantly, I would like to acknowledge the soldiers who have lived and died. They ensured for me the freedom to an educational and career path of my own choosing.

TABLE OF CONTENTS

LIST OF TABLES

LIST OF FIGURES

LIST OF SYMBOLS OR ABBREVIATIONS

GDP. Gross domestic product

PPI. Pulp and paper industry

US. United States of America

WL. White liquor

BL. Black liquor

GL. Green liquor

$\mathbf{E_{CORR}}$. Corrosion potential

OCP. Open circuit potential

$\mathbf{i_{CORR}}$. Corrosion current density

$\boldsymbol{\beta_a}$. Anodic Tafel slope

$\boldsymbol{\beta_c}$. Cathodic Tafel slope

F. Faraday's constant

C. Coulomb

in. Inch; mil = 0.001 in

yr. Year

mpy. Mils/year

m. meter; cm = 0.01 m; mm = 0.001 m; μm = 10^{-6} m, nm = 10^{-9}

AM. Atomic mass

A. Ampere; mA = 0.001 A

g. Gram, mg = 0.001 g

ρ,D. Density

n. number of electrons, e^-

$\mathbf{i_O}$. Exchange current density

π. Pi bond

σ. Sigma bond

pH. $-\log[H_3O^+]$

$\mathbf{C_{10}}$. Carbon chain length of 10

$\mathbf{R_P}$. Polarization resistance

V. Volts; mV = 0.001 V

$\mathbf{E_P}$. Critical potential

SCC. Stress-corrosion cracking

TG. Transgranular

IG. Intergranular

HIC. Hydrogen induced cracking

SSRT. Slow strain-rate test

FIC. Film-induced cleavage

LSP. Localized surface plasticity

$\mathbf{L_0}$. Initial length

$\mathbf{L_1}$. Final length

A_0. Initial cross-sectional area

A_1. Final cross-sectional area

HW. Hardwood

SW. Softwood

RDH. Rapid displacement heating

MCC, EMCC. Modified continuous cook, Extended MCC

i_{CRIT}. Critical current density

°C. Degree Celsius

XRD. X-ray diffraction

W. Weight loss

Area. Area

t. Time

SCE. Standard calomel electrode

sec, s. Second

Arr. Log of Arrhenius constant

R. Gas constant

J. Joule

mol. Mole, mol/L = M

K, T. Degree Kelvin

Ea. Activation energy

CR. Corrosion rate

E_r. Reversible potential

E_o. Standard reversible potential

ox. Oxidation

red. Reduction

[ox]. Activity of oxidized species

a,b. Stoichiometric coefficient

SHE. Standard hydrogen electrode

GC. Gas chromatography

MS. Mass spectrometry

L or **l**. Liter; mL = 0.001 L; 3.86 L = 1 gallon or gal

i.d. Inner diameter

hr. Hour

BLOX. Oxidized Black Liquor

min. Minute

scfh. Standard cubic feet per hour

cc. Cubic centimeter

N_2. Nitrogen gas

TCD. Thermal conductivity detector

FPD. Flame photo detector

SUMMARY

Increased equipment failures and the resultant increase in unplanned downtime as the result of process optimization programs continue to plague pulp mills. The failures are a result of a lack of understanding of corrosion in the different pulping liquors, specifically the parameters responsible for its adjustment such as the role and identification of inorganic and organic species. The current work investigates the role of inorganic species, namely sodium hydroxide and sodium sulfide, on liquor corrosivity at a range of process conditions beyond those currently experienced in literature. The role of sulfur species, in the activation of corrosion and the ability of hydroxide to passivate carbon steel A516-Gr70, is evaluated with gravimetric and electrochemical methods. The impact of wood chip weathering on process corrosion was also evaluated. Results were used to identify black liquor components, depending on the wood species, which play a significant role in the activation and inhibition of corrosion for carbon steel A516-Gr70 process equipment. Further, the effect of black liquor oxidation on liquor corrosivity was evaluated. Corrosion and stress corrosion cracking performance of selected materials provided information on classes of materials that may be reliably used in aggressive pulping environments.

Chapter 1

INTRODUCTION

1.1. PULP AND PAPER INDUSTRY PROCESS CORROSION

Although large steps in understanding corrosion cause and effect relationships have been made in the global Pulp and Paper Industry (PPI) over the last half-century, including the impact of wood species, oxidized sulfur compounds, and materials, fundamental questions regarding the causes of corrosion remain unanswered. The root cause and identification of chemicals involved in the variability of wood species corrosion remain unidentified. Likewise, the identification of new materials that are resilient to modified pulping liquor environments, such as oxidized waste liquors, remain untested and studies investigating the limits of currently used materials are unaccounted for. As previous studies have typically focused on the narrow ranges of industrially processed concentrations of hydroxide and sulfide new process modifications, such as process optimization, and technology implementations, such as gasification, may deliver pulping liquor streams at higher concentrations than previously investigated.

The impact of process equipment corrosion in the pulp mill has always been apparent. Yet, two digester explosions, 1983 Pine Hill, Alabama, no one injured, and 1994 Panama City, Florida, three dead and one seriously injured, brought the importance of understanding corrosion closer to the forefront of planning and expenditures.[4] Currently, scheduled annual or semi-annual inspections of equipment are used to identify and investigate problem areas, including the maintenance and upkeep of equipment. Although scheduled downtimes are built into the operational schedules of individual mills, many mills are plagued with unscheduled downtimes requiring closure of sections and/ or the entire mill for unspecified amounts of time. As any shutdown impacts the revenue stream for a mill, unscheduled downtime also impacts operational scheduling and external customers.

To address these concerns an understanding of process parameters and instabilities is needed. These parameters include process chemistries, wood species used, alkalinity and sulfidity of liquors, process temperatures and flow rates, operational and residual stresses; metallurgy used including stainless steels, duplex stainless steels (includes lean duplex and super duplex), titanium alloys, etc.; closed loop concentrations including bio-organisms; and future changes in the mill. A lack of understanding of corrosion and the parameters

responsible for its activation or inhibition in the pulp mill results in significant losses in capital annually.

According to a congressional study published in 2002, corrosion is a $276 Billion, or 3 – 4% of GDP, problem in The United States of America. Of this amount, it is estimated that total corrosion maintenance costs for the PPI range from $2 – 10 Billion, or ~2 – 6% of total sales, with ~$1 Billion dedicated to corrosion in pulping liquor environments (or pulp mills). Compared to the estimated corrosion expenditures in Petroleum Refining, ~$3.7 Billion, and the Chemical, Petrochemical and Pharmaceutical Industries combined, ~$1.7 Billion, the US PPI is significantly lagging behind other US industries.[5]

Preventive strategies to minimize corrosion costs such as advance design practices for better corrosion management, and advance life prediction and performance assessment methods can be performed now. The application of these strategies can reduce capital costs, improve capital effectiveness, allow for cheaper maintenance, and provide detailed information on the direction of material studies for improved future performance and safety.

1.2. PROBLEM STATEMENT

During the Kraft pulping process wood chips are often weathered in outdoor storage yards prior to cooking in white liquor (WL), which contains sodium hydroxide and sodium sulfide at temperatures up to 180°C. In the weathering process wood chips are affected by heat and moisture and organic extractives may diffuse out of the chips. Also, in many of the current investigations into and implementations of Green Energy projects, fuel production through biomass fermentation, the removal of organic components, including extractives and lignin from the wood chips, is required. In the cooking process the wood's lignin is fragmented into smaller segments whose sodium salts are soluble in the cooking liquor. The concentration of hydroxide and sulfide has increased over the years along with temperatures to improve product yield and quality. In the advent of gasification these concentrations may see further increases as processes are further optimized to recover sulfur and produce caustic. The waste pulping stream, sulfide and organic containing caustic solution, referred to as black liquor (BL) may be oxidized to tie-up odiferous sulfur compounds such as hydrogen sulfide and mercaptans in solution as well as provide increased capacity for capacity limited recovery boilers.

Increased process failures and the resultant increase in unplanned downtime as the result of process optimization programs continue to plague the PPI. The failures are a result of a fundamental lack of understanding corrosion in the PPI, specifically the parameters responsible for its adjustment such as the role and identification of inorganic and organic species. The current work investigates the role of inorganic species, namely sodium hydroxide and sodium sulfide, at a range of process conditions beyond those currently experienced in literature. Clarification of the controlling role of sulfur, in the activation of corrosion and the ability of hydroxide to passivate carbon steel A516-Gr70, is evaluated with gravimetric and electrochemical methods. The impact of wood chip weathering on process corrosion was also evaluated. Gravimetric and electrochemical methods were used to identify the controlling components of wood species in the activation and inhibition of corrosion for carbon steel A516-Gr70 process equipment in BL. Further, a study on BLs from a pulp mill utilizing oxidation is performed with respect to material selection and inorganic constituents providing recommendations for suitable process materials in oxidized BL.

While this study investigates the impact of sulfide containing caustic solutions found in process streams in pulp mills utilizing the Kraft pulping process it is

also applicable to modified Bayer processes used in alumina ore processing, the Gilder-sulfide process used in heavy water production, and hydrocarbon processing for the treatment of acidic impurities such as hydrogen sulfide and mercaptans. Due to the range of concentrations and temperatures investigated here our discussion will focus on the PPI, specifically processing solutions referred to as WL and green liquor (GL).

Chapter 2

METHODS FOR CORROSION TESTING

When available, the ability to choose between laboratory, or controlled environment, and *in situ* testing is of tremendous benefit in material testing. *In situ* testing allows for investigation of a particular process with a specific set of variables while flexibility of preparation, materials, analysis, and testing setup allow laboratory tests to develop a fundamental understanding of conditions individually or in combination. Although laboratory testing does allow for enhanced control and evaluation of fundamental relationships built-in process variability and increased margins of error is often a function of testing *in situ*.

Testing in both laboratory and *in situ* environments allows for gravimetric corrosion and electrochemical analysis. It is even possible to replicate the mechanical behavior experienced by material in any industrial process or equipment as well as the local environmental conditions. Laboratory testing of materials at varying rates of strain in specific environments allows one to study the effect of dynamic stresses whereas gravimetric and electrochemical

studies allow corrosion rate measurements in the laboratory in cases which are difficult to monitor *in situ*.

2.1. CORROSION FUNDAMENTALS

One definition of corrosion is the chemical reaction between a metal or metal alloy and its environment. The majority of metals are extracted from minerals, where they are found in a higher oxidation state, at a lower level of energy. This energy is the driving force for the chemical reactions during corrosion. Corrosion, therefore, is the return of the metal to its thermodynamically favorable state and is an electrochemical process which involves the transfer of electronic charge in aqueous solutions.[1] This electronic transfer is the foundation of electrochemistry.

Electrochemistry of corrosion reactions is based on the mixed potential theory, namely charge conservation. That is for any number of half-cell reactions simultaneously occurring on the surface of a conducting electrode an electrochemical potential is established, E_{CORR}, where the total rate of oxidation current must equal the total rate of reduction current to avoid charge accumulation.[1] E_{CORR}, the corrosion potential, can be measured under open

circuit conditions, referred to as the open circuit potential, OCP, if the passage of current through the electrode is not high enough to polarize the reactions involved.

The oxidation of a metal, the anodic reaction, liberates electrons and increases the oxidation number of the metal. Cathodic reactions, on the other hand, are defined as a reduction, e.g. reduction of hydrogen, in which the consumption of electrons decreases the oxidation number. An example is given in Equation (1) below, where zinc metal reacts with hydrochloric acid to form zinc chloride.

$$Zn + 2HCl \rightarrow ZnCl_2 + H_2 \quad [1]$$
$$Zn + 2H^+ + 2Cl^- \rightarrow Zn^{2+} + 2Cl^- + H_2 \quad [2]$$
$$Zn + 2H^+ \rightarrow Zn^{2+} + H_2 \quad [3]$$
$$Zn \rightarrow Zn^{2+} + 2e^- \text{ anodic reaction} \quad [4]$$
$$2H^+ + 2e^- \rightarrow H_2 \text{ cathodic reaction} \quad [5]$$

In Equation (2) the compounds are separated into their ionic forms, Equation (3) displays the net equation where the like species are removed, and in Equations (4) and (5) the oxidation and reduction of zinc and hydrogen, respectively, is shown to occur.[1,6]

In corroding metal the anodic reaction is consistently in the form of Equation (6) and the oxidation of elemental iron to ferrous ions is given in Equation (7). However, Equation (8) describes another reaction concerning iron ions, a common cathodic reaction where ferric ions are reduced to ferrous ions.[1]

$$M \rightarrow M^{n+} + ne^{-} \quad [6]$$

$$\mathrm{Fe} \rightarrow \mathrm{Fe}^{2+} + 2e^{-} \quad [7]$$

$$\mathrm{Fe}^{3+} + e^{-} \rightarrow Fe^{2+} \quad [8]$$

The anodic and cathodic reactions presented in Equations (4) and (5) proceed at limited rates of reaction each having its own half-cell potential and exchange current density, displayed in Figure 1.[1] If an effort is made to drive the cathodic reaction forward by increasing the availability of electrons the potential at the metal surface becomes more negative. Thus, the negative charge at the surface increases due to the inability of the reaction to increase, accommodating the increased concentration gradient of electrons. This negative potential charge is referred to as cathodic polarization. Conversely, if the zinc in Equation (4) does not liberate a sufficient number of electrons a positive potential charge can occur at the metal surface. If allowed to increase, this charge, defined as anodic polarization, will promote anodic dissolution.

The electron deficiency, anodic polarization, describes a driving force for corrosion via the anodic reaction.[1]

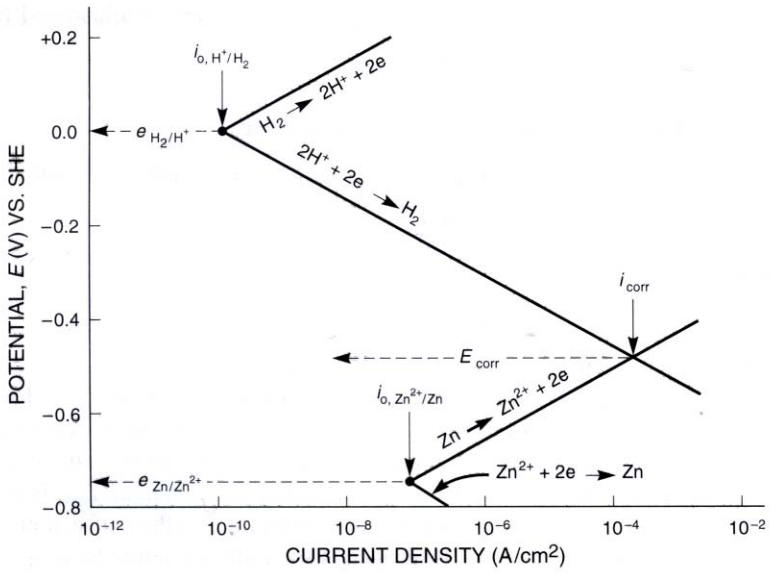

Figure 1. Polarization of anodic and cathodic half-cell reactions for mixed potential, E_{CORR}, and corrosion current density, i_{CORR}, determination.[1,7]

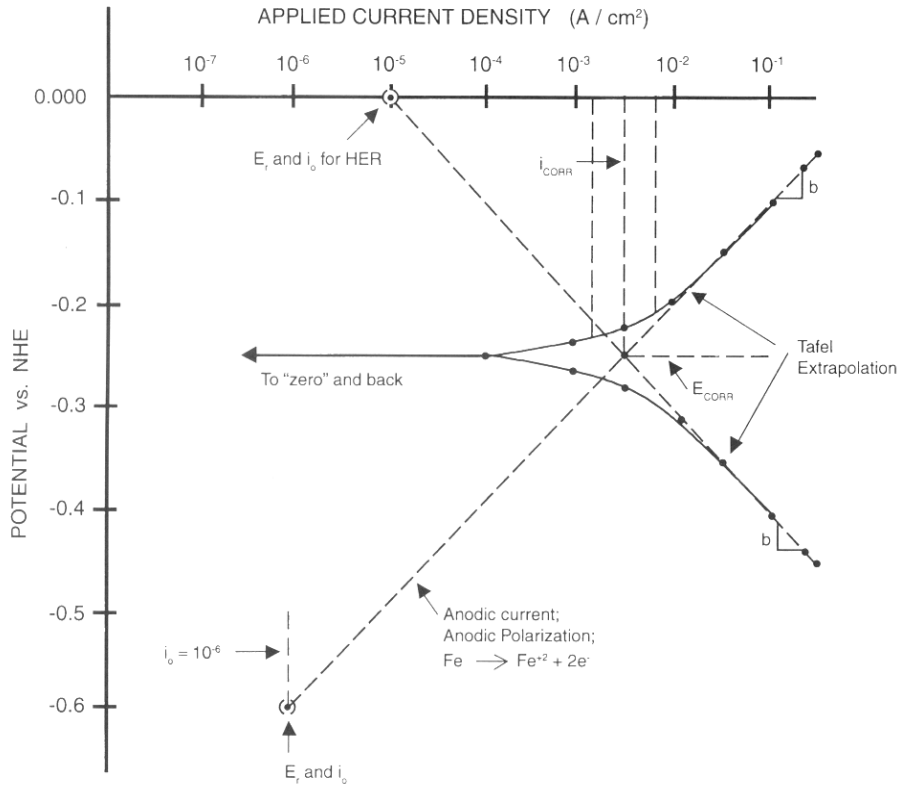

Figure 2. Polarization curve as a result of Evans diagram with inclusion of Evans lines.[8]

In Figure 2, the linear portion of the experimental anodic and cathodic polarization curves are extrapolated, called Tafel extrapolation, for the determination of E_{CORR} and the corrosion current density, i_{CORR},. Additionally, by taking the slope of both lines we determine the Tafel constants, β_a and β_c, anodic and cathodic respectively. An adaptation of Faraday's First and

Second Law allows for the relation of the rate of mass loss or dissolution to the current density with i_{CORR}, described by Equation (9).[8]

$$\dot{m} = \frac{i(AM)}{nF\rho} \qquad [9]$$

Given that 1 Faraday's Constant, F, is equal to 96,485 Coulomb (C), the charge on a single electron is equal to 1.6 x 10^{-19} C/electron and that for every mole of electrons there are 6.02 x 10^{23} electrons we can simplify the estimated mass loss in Equation (9) as a function of length or thickness per time, mils per year, in Equation (10).[8]

$$mpy = \frac{129(AM)(i)}{n\rho} \qquad [10]$$

Where, mpy = penetration rate (mils/yr, 0.001 in/yr or 0.0254 mm/year); AM = atomic mass (g); i = corrosion current density (mA/cm^2); ρ = density (g/cm^3); n = number of electrons lost per atom oxidized.

2.1.1. FILM FORMATION

The polarization of the metal surface due to surface film formation, a surface corrosion product, was clearly described by West:[9]

> *"Although serving as a more or less effective ionic barrier between metal and electrolyte, 'passive' films are sufficiently thin to allow electron tunneling and sustain cathodic reactions such as oxygen reduction and proton reduction. What is more, they do not display the bulk semiconducting properties of simple oxides but tend instead to 'metallic' behaviour and, because of lattice defects, allow a restricted amount of cation conduction and so continued – but slow – anodic dissolution."*

As stated the term 'passive' does not refer to an inactive state. The individual properties of a surface film, which may be composed of multiple layers of varying films or multiple compositions within a single layer at the metal surface, are dependent on system parameters and the introduction of lattice defects consisting of interstitial sites and vacancies.[9,10] The formation of a surface film lowers the electron density in the electrical double layer found at the metal surface, believed to lower the exchange current density, i_o.[9] A reduction in the current density would predict a proportional reduction in

corrosion rate, Equation (10). At lower temperatures diffusion controls, due to limited vacancies in the lattice structure, further restrict the movement of ions across the film. Yet, with higher vacancies available, which may occur at increased temperature, or changes in the oxidation state of the cations in the film, an increase in anodic current may approximate current flowing from an un-passivated metal surface.[9] Additionally, the incorporation of non-stoichiometric metal cations, such as iron, or anions, such as sulfur, into the available oppositely charged vacancies will also affect the passage of electrons across the passive film thereby affecting the passive nature and stability of the film. Surface corrosion products are not the only available mechanism for surface modification and corrosion rate adjustment. The addition of chemical compounds into a system, or compounds native to a system, may also play a role in the passage of electrons from the solution to the metal surface.

2.2. METHODS OF CORROSION INHIBITION

The definition of corrosion inhibitor[11] is: "A substance which retards corrosion when added to an environment in small concentrations." The mechanism of inhibition can be described by three mechanisms which are not mutually exclusive:[12]

1. Adsorption of inhibitors as a thin film onto the surface of a corroding material;

2. Inhibitor induced formation of a thick surface corrosion product;

3. Changing characteristics of the environment through the production of protective precipitates or the removal or inactivation of an aggressive constituent in the system.

Inhibitors can be either organic or inorganic chemicals. It is accepted that the organic molecules generally inhibit corrosion by absorption at the metal-solution interface.[12] The mechanism of absorption is dependent on several factors:[12]

1. Chemical structure of the molecule;

    a. Carbon chain length (many times mistakenly referred to as formula weight in literature), steric strain, solubility, type and number of bonding atoms or groups (π or σ);

2. Chemical composition of the solution, including pH;

3. Metal or alloy composition, surface conditions;

4. Electrochemical potential at the metal-solution interface.

Table 1. Cooling water corrosion inhibition by pyrocatechols with increasing R group.[13]

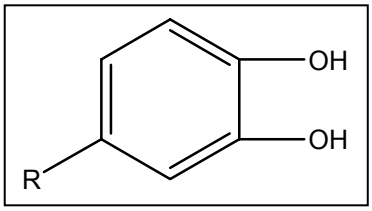

Compound	% Inhibition	R group
Pyrocatechol	-14	-H
4-Methyl Catechol	84	$-CH_3$
4-tert-butyl Catechol	48	$-C(CH_3)_3$
4-n-butyl Catechol	93	$-(CH_2)_3-CH_3$
4-n-hexyl Catechol	96	$-(CH_2)_5-CH_3$

Nathan,[13] in Table 1, demonstrated the importance of structural variations in the stability of inhibitors in cooling tower waters at pH 7. The addition of pyrocatechol, with a -14% inhibition, increased corrosion whereas longer straight chain alkyl groups provided greater efficiencies of inhibition. Nathan,[13] in Table 2 and illustrated in Figure 3, further demonstrates the effect of chelating stability on inhibition as a function of ring size and R-group. Sarcosine, used in the manufacture of biodegradable surfactants, was modified

with a hydrogen and methyl group adjacent to the nitrogen and allowed to form 5, 6, and 7-membered ring surface chelates with carbon steel. Tests with hydrogen adjacent to the nitrogen on a 6-membered ring showed the lowest corrosion rate, the result of a more stable chelating structure, while tests with a methyl group adjacent to the nitrogen in the 5 and 6-membered rings were significantly more stable than the 7-membered chelating structure.

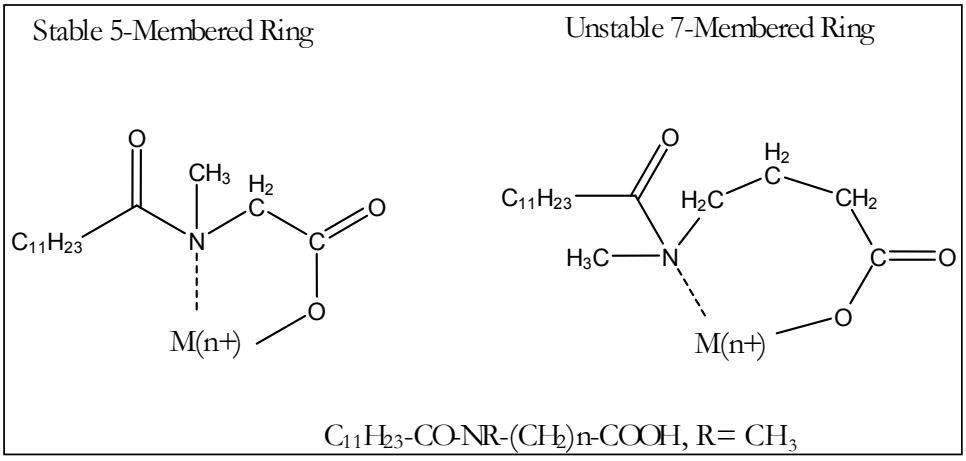

Figure 3. Chelates of 5 and 7-membered sarcosine type rings.[11]

Table 2. Corrosion rate data for 5, 6, and 7-membered sarcosine type compounds.[13]

Corrosion rate, mpy				
n	**Chelate Ring Size**	**R = H**	**R = CH_3**	**Remarks**
1	5-membered	52	2.5	Stable chelate formed
2	6-membered	42.5	5.5	Moderately stable chelate
3	7-membered	104	42	Chelates are unstable

The adsorption of the organic chemical often occurs with at least two mechanisms acting simultaneously:[12]

1. π-bond orbital adsorption;
2. Electrostatic adsorption;
3. Chemisorption.

Although much of literature focuses on acidic or near neutral solutions, in caustic solutions the polar end group acts as the active participant in adsorbing to the metal surface.[12,13,14,15] Additionally, the strength of the bond formed is directly related to the effectiveness of the inhibitor at that site. If the orientation, shape and/ or size of the long chain portion of the molecule, restricts adsorption by other molecules to the metal it will reduce the amount of surface covered and the inhibitor will be reduced in effectiveness. A reduction in inhibitor efficiency with branching of the alkyl chain and increased chain length has been described by Nathan et al.[13,14]

Nathan further postulated that the straighter a chain the more enhanced the ability for chain interlocking and increased coverage. In a thorough review by Metcalf[15] the desired chain length for effective inhibition, using straight-chain

primary aliphatic amines, ranged from C_{10}-C_{21} across a range of solutions. This is a chain length similar to that of naturally occurring fatty acids found in BLs.

2.3. CORROSION MEASUREMENT METHODS

The corrosion current, i_{CORR}, and thus the corrosion rate can also be related to the Tafel slopes, β_a and β_c, shown in Figure 2 using the polarization resistance, which is defined as the slope of the potential-current curve within ± 5 – 10 mV of E_{CORR}, by Equation (11).[16]

$$i_{CORR} = \frac{1}{2.3R_P}\left(\frac{\beta_A\beta_C}{\beta_A + \beta_C}\right) \qquad [11]$$

Where, R_P = Polarization resistance.

However, the logarithmic nature of the current density axis, used for polarization studies, amplifies errors in Tafel extrapolations. Inadequate selection of the slopes to be used can alter the calculation for corrosion current density by an order of magnitude. For best results it is recommended that at

least one of the branches of the polarization curve should exhibit Tafel, linearity on a semi-logarithmic scale, over at least one order of magnitude of current density. Additionally, the extrapolation should start at no less than 50 to 100 mV away from E_{CORR}. Other texts offer advice for extrapolations to begin as low as 25 mV from E_{CORR} providing a glimpse of the intricacies and confusion in Tafel extrapolations.[8,16] Performing the extrapolation according to the above standards provides a small buffer for error.

Several factors lead to non-Tafel behavior so we will begin with the underlying assumptions involved in analyzing a polarization curve:[8,16]

1. Corrosion current is proportional to the change in potential or voltage offset, from E_{CORR}, for one anodic and one cathodic reaction.

2. Polarization resistance estimated by Equation (11) contains the total resistance of the surface corrosion product and solution.

3. The anodic and cathodic reactions are under activation control. Therefore, mass transfer is not a rate limiting reaction which could result in a significantly larger Tafel slope than when under activation control.

4. The entire electrode surface functions simultaneously as both a cathode and an anode with the anodic and cathodic reactions occurring at different sites. If the surface develops a fragile film or pit formation, corrosion may be localized and thus the calculated rate of corrosion is not the rate of uniform corrosion for the sample.

5. No additional electrochemical reactions occur.

Given these assumptions other errors may occur that may lead to an inaccurate determination of the rate of corrosion using electrochemistry and thereby provide misleading results and thus require other methods for analysis:[16]

1. The rate at which the voltage is increased, scan rate, affects the slope of the polarization curve at E_{CORR} and thus the accuracy of R_P.

2. When testing in a solution of low conductivity the uncompensated resistance will increase and therefore magnify the possible error in the estimated R_P.

3. Tafel slope calculations are estimations and may significantly increase the range of error in the estimation of E_{CORR}.

4. The corrosion potential is created by all electrochemical reactions occurring on the corroding surface of the metal. If the electrochemical reactions are not occurring at steady state, or remain constant during the measurement, the voltage-current relationship that defines the polarization curve may reflect differing corrosion phenomena along the curve. In an equilibrated state there would be no corrosion.

In a conductive aqueous solution, the surface of the metal will reach a steady state potential that is dependent upon the availability of electrons and the rate at which they are exchanged by the anodic and cathodic reactions. The steady state potential describes a stable rate of corrosion that can be manipulated by adjusting the surface potential. If the surface potential were to increase above that of the steady state value the corrosion rate would also be expected to increase.[1]

Yet, the relationship of an increased corrosion rate with an increase in potential is not always the case. In many metals the corrosion rate decreases when the potential of the surface becomes greater than the critical potential, E_P, of the metal, shown in Figure 4. This reduction in the corrosion rate is

defined as passivity. Passivity is the result of the formation of a thin hydrated oxide protective film (a corrosion product). This thin fragile film acts as a barrier to the anodic dissolution reaction and is directly related to the oxidizing power, potential, of the solution it contacts. One example of this is the corrosive passivity portrayed by SS304 in aerated salt water and its activity in deaerated salt water.[1]

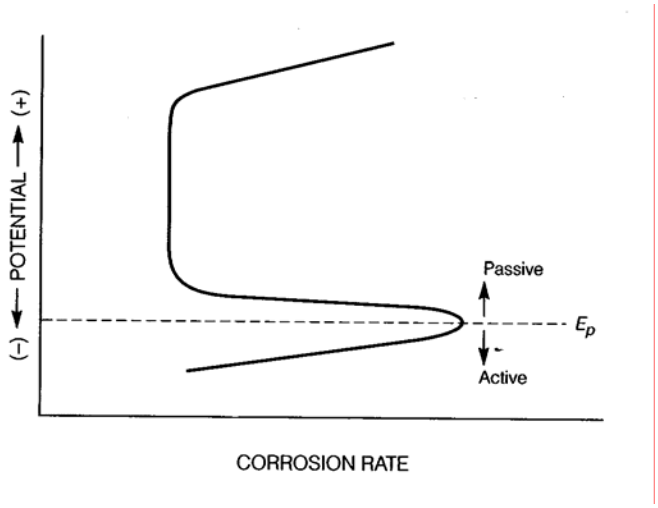

Figure 4. Passivity at oxidizing potentials above the critical potential.[1]

However, passivity does not mean that a metal surface will remain at rest or be unresponsive to its environment. Localized corrosion such as pitting, crevice corrosion, and embrittlement by SCC may occur due to unpredictable breaks

in the passive film found on the metal surface. In an effort to better understand the issues surrounding the embrittlement of metals and the effects of their environment we will turn our focus to SCC.

2.4. STRESS-CORROSION CRACKING

"Stress-corrosion cracking (SCC) is a term used to describe service failures in engineering materials that occur by environmentally induced slow crack propagation. The observed crack propagation is the result of the synergistic interaction of mechanical stress and corrosion reactions."[17] In other words, for a material to undergo SCC differing forces must be combined to embrittle the material in this way. These forces: tensile stress (mechanical stress), a susceptible material, and a corrosive environment (corrosive reactions) are necessary to promote the type of corrosion that has been defined as SCC.

SCC may follow a transgranular, TG, or intergranular, IG, pattern. In TG-SCC the crack will often propagate in specific crystal planes traveling through the grains within the metal. In IG-SCC the boundaries around the grains dictate the path of the crack. The path of a crack may incorporate both patterns and is then called a mixed mode crack. It is believed that the cause of

SCC, in most cases, is due to mechanical fracture with electrochemical dissolution or corrosion, yet it has been shown, in some systems, that anodic dissolution does play a major role in SCC failures.[1]

In order to better understand SCC of metals, anodic dissolution is analyzed using curves of potentiodynamic anodic polarization with metals in the environments they are likely to be placed in. In Figure 5, zones 1 and 2 are defined as cracking zones. It is here at the edges of the passive region, where the passive film is considered the weakest, that much of SCC occurs. Efforts to compare the rate of crack growth in SCC with anodic dissolution currents have shown proportionality in strained samples. However, cracks such as those often found in austenitic stainless steels have been seen with growth rates higher than can be explained using electrochemical dissolution. This latter type of SCC referred to as fast TG cracking is yet another area of SCC that has offered insight to other possible mechanisms of crack propagation that will be discussed further.[1] At this time, what is clear, in SCC failure, is that anodic dissolution of the metal surface is not the only mechanism. However, as we will soon discuss, additional mechanisms proposed for a more complete understanding of SCC material failure offer no apparent universal solution to this much debated topic. In fact, it is both possible and very likely that many

mechanisms occur, depending on environment and material, singly and in conjunction with other proposed mechanisms.

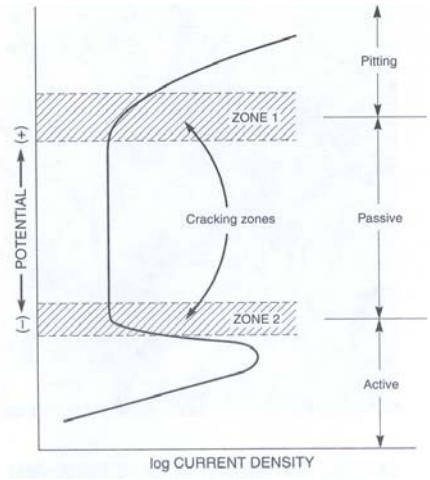

Figure 5. Anodic polarization curve showing zones of susceptibility to SCC.[1]

The prevention of SCC generally requires the removal of one of the three elements mentioned previously: tensile stress, a susceptible material or a corrosive environment. The removal or release of mechanical stresses, changes to material properties and/ or composition, and reduction of oxidizing agents such as dissolved oxygen or the removal of critical species from the environment are all methods employed to reduce the susceptibility of a system

to SCC. Protection of the material using an applied potential, such as cathodic protection, will usually stop SCC but may promote mechanical failure or hydrogen embrittlement or hydrogen induced cracking (HIC).[1]

There are a number of methods used to test material susceptibility to SCC in a given environment, which include exposure of stressed specimens to the environment for a given length of time. However, the most quantifiable method of testing material susceptibility to SCC in an environment is the use of the slow strain-rate test (SSRT). In the SSRT the tested material is subjected to a given environment and is pulled under a constant rate of strain until failure occurs. The benefit of SSRT is the reduction of testing time from months or years of exposure, for a constant load or strain test, to a period of a few days. These tests provide researchers with numerous cracks in the reduced cross-sectional area of the specimen and the final branched crack expected of materials in normal service and laboratory tests. Due to the nature of SSRT as a more aggressive testing procedure than either field or other laboratory tests it is anticipated that the results from SSRT will be conservative, thereby providing the researcher with a set of expectations from which to state his or her findings concerning the reliability of a material in a particular environment.[1]

Although insightful research and analysis have provided us with a much better understanding of SCC and a greater ability to test material susceptibility to SCC a fundamental lack of understanding as to its cause(s) remains. A brief discussion of three mechanisms proposed to answer this fundamental question is given here to offer further insight to some of the complexities involved in finding an answer. The proposed mechanisms: slip-step dissolution, film-induced cleavage, and localized surface plasticity are not the only mechanisms proposed in literature yet they appear to be promoting discussion amongst researchers. Especially amongst researchers that believe that more than one mechanism will be necessary to properly identify the crack initiation, propagation, and growth in SCC.

Slip-step dissolution, one of the originally proposed SCC mechanisms, assumes that tensile stress provides an adequate strain to rupture the surface film at a slip band. A crack then propagates by anodic dissolution of the un-filmed or open surface at the rupture site. There is agreement among most investigators that film rupture is necessary to initiate cracking, yet debate exists concerning the method of SCC growth beyond film rupture. Much of the debate concerns an inability to resolve the appearance of well-defined grain boundaries at the fracture surface rather than the smooth featureless

surface expected of a crack growing by electrochemical dissolution at an un-filmed crack tip.[1]

Film-induced cleavage (FIC) is a mechanism proposed to more clearly explain the discontinuous TG crack growth and high TG crack growth rates. The fundamental point proposed here is that a crack initiated in the brittle surface film will, if at a sufficient velocity, propagate beyond the film and into the metal. Anodic dissolution, therefore, is not required for crack growth, but film formation where a crack may form and penetrate the metal surface. The debate over FIC takes place over the assumption of crack propagation beyond the film layer. Work performed by Fritz, however, showed that in order for a crack to grow beyond the film layer in brass an external anodic potential was required.[1,18]

Localized surface plasticity (LSP) is a mechanism that focuses on the effects of the interaction between the environment and the metal properties. LSP proposes that mechanical creep, which precedes the initiation of SCC, is accelerated by anodic currents and therefore bolstered by common anodic corrosion reactions.[19,20] The accelerated creep is explained by the softening of

the metal due to surface defects, satisfying the normal strain hardening found during primary creep. Thus, corrosion relieves strain hardening resulting in SCC from a defect structure ahead of the crack tip.[21] In an effort to explain discontinuous crack growth it has also been postulated that a brittle crack can burst into the softened crack-tip volume with possible growth beyond the softened region. Yet, an arrested crack-tip must have a defect structure reform at its tip before another burst will occur.[1] This mechanism appears to have answers for many of the questions surrounding SCC in specific material/ environmental systems yet does not explain SCC in most of the systems where embrittlement is evident.

The current understanding of SCC is such that there appears to be no definitive mechanism capable of explaining every SCC failure. However, as has been proposed by numerous researchers it is likely that more than one proposed mechanism will be required to more adequately define SCC whether they are used in conjunction or separately for different analyses. With all of the ongoing debates concerning SCC there are few certainties. Yet one thing is certain, the existence of SCC and its ability to cause failure with little or no warning is of great concern to many industries including that of the PPI.

2.4.1. STRESS-STRAIN CURVES

A characteristic of the particular material being tested, the stress-strain diagram, shown in Figure 6, describes important information about mechanical properties and the mechanical behavior of the material. (It should be noted here that Jacob Bernoulli (1654-1705), a member of the famous Italian engineering family, was the originator of stress-strain diagrams.)[22]

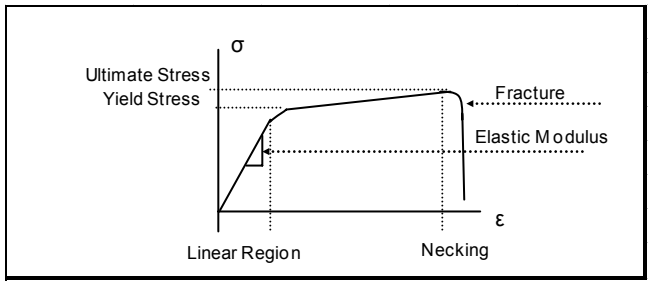

Figure 6. A general description of a stress-strain diagram for a metal in tension.

The method or process of failure depends on the material and the interaction of the material and the environment in which it is tested. Metals that undergo large permanent strains before failure are categorized as ductile. One of the benefits of using ductile materials is that visible distortions will occur if the loads become too large, thereby providing an opportunity for action prior to

material failure. Materials that do demonstrate ductile behavior are, also, capable of absorbing large amounts of strain energy prior to fracture. These more ductile metals are considered to have a higher toughness compared to materials with similar strength characteristics but less ductility. In order to characterize the ductility of a material two common equations are used. The first, Equation (12), the percent elongation in which the change in length of the specimen is divided by its initial length and the second, Equation (13), is the percent reduction in area, a measure of the amount of necking that occurs, where the change in the initial and final cross-sectional area are divided by the initial area.[22]

$$\text{Percent\_Elongation} = \frac{L_1 - L_0}{L_0} * 100\% \qquad [12]$$

$$\text{Percent\_Reduction\_In\_Area} = \frac{A_0 - A_1}{A_0} * 100\% \qquad [13]$$

Where, L_1 = final length; L_0 = initial length; A_1 = final cross-sectional area; A_0 = initial cross-sectional area.

Chapter 3

PROCESS EQUIPMENT CORROSION IN THE PPI

The PPI is based on a concept centuries old, take a fiber source and convert it to paper. Currently the preferred fiber source is predominantly trees. Although clear cutting as a form of harvesting is still performed in certain areas of the world it has become more common to log trees from plantations. In clear cutting, regional woods tend to be used for production often resulting in multiple species and sometimes including both hardwoods (HWs) and softwoods (SWs) in production. Meanwhile, in plantation harvesting controls are placed on the fiber source allowing for the manufacturers to choose specific species, a narrow age range, and specific stands (tree plots). This is of great concern to various manufacturers allowing them to customize their process due to species dependent variations in the fiber length and chemical makeup of the wood. Further, variation in terrain may also affect the makeup of the wood characteristics.

After harvesting the wood the logs are then transported to a chip yard where they are often sorted by age and species and await processing. Transportation

of the logs may include railcar, truck, ship, or river varying in length and duration. Logs may be stored for future use or immediately processed. To begin processing, the logs are commonly stripped of bark and further processed by chipper for uniform chip width and length. Wood chips are sorted and placed in storage in a chip yard or warehouse for use on-site or for transportation to other facilities via railcar, truck, or ship where they will be stored for use. While in storage and transit chips are often subjected to fluctuations in temperature, moisture and time of storage. In storage, some volatile extractives which may lead to process upsets or fluctuations, such as foaming, are removed from the chips in a process often described as weathering. As is often the case, the weathering of chips takes place in chip storage piles as part of the chip inventory build-up.

Prior to processing, wood chips may be treated by fungi, caustic solution, water, steam, or other methods for the removal of organic components such as hemicellulose or lignin to conserve energy and both caustic and sulfide process chemicals. The chips are then processed according to the flowchart in Figure 7. A sulfide containing caustic solution, WL, which may reach or exceed 150 g/L sodium hydroxide and 50 g/L sodium sulfide, is utilized in digesters to cook the chips to a certain brightness and removal of lignin. This

process step occurs in a batch or a continuous digester, which utilizes varying temperatures, streams of caustic and sulfide concentrations, as well as current and countercurrent flow schemes.

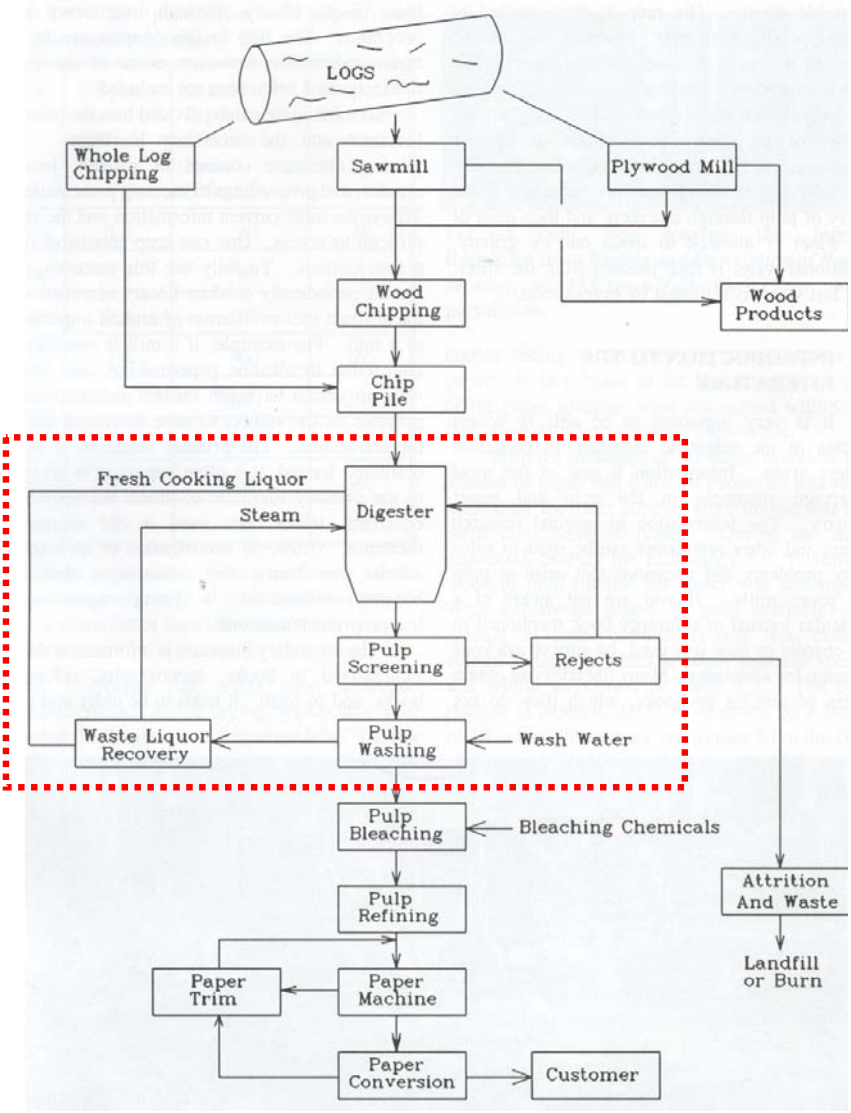

Figure 7. An overview of the chemical and papermaking process in a pulp and paper mill.[23] Highlighted area is that addressed by the present study.

Yet cooking strategies in digesters can differ greatly from mill to mill. Modifications to batch digesters, such as the implementation of Rapid Displacement Heating (RDH), involves pre-impregnation of steam packed chips with weak BLs of varying temperatures.[23] Typically the temperatures increase allowing for a reduction in steam consumption. The result is a higher strength pulp, more consistent hydroxide content for the duration of the cook, and savings due to reduced steam usage. In continuous digesters, Modified Continuous Cooking (MCC) has seen implementation as a countercurrent process with low hydroxide content at the beginning of the cook and higher hydroxide content at the latter stages of the cook. Extended MCC, EMCC, is another method of continuous digester cooking. In both modified cooking processes WL streams are utilized at varying points in the digester to control the level of hydroxide content to produce a more uniform pulp with higher yield and increased brightness and strength.[23]

After removal of the wood chips, now fibers, from the digester the fibers are separated from the waste liquor solution, BL. The fibers are then washed and further processed via brightening steps such as bleaching, if appropriate, and refined prior to utilization in the mill. Refining is a mechanical action

resulting in the maceration and/ or cutting of fibers in preparation for papermaking.[23]

At this stage the BL, referred to as weak, a function of solids concentration, is less than 20% solids. To remove heat energy, recover odiferous and volatile gasses, and allow for higher throughput rates for the recovery boiler the BL undergoes concentration steps via flash tank and evaporators. During these concentration stages oxidation units may also be utilized to tie up sulfur gases, namely hydrogen sulfide and organo-sulfur compounds, such as methyl mercaptans. Keeping these compounds in solution for processing in the recovery boiler reduces sulfur-based odors and chemical make-up requirements for sulfur.[24,25] Oxidation is also used to adjust the viscosity and heating value of the liquor, again allowing for increased throughput in capacity limited recovery boilers. The concentrated BL, now heavy BL, greater than 40% solids, is fired in the recover boiler for heat energy recovery and chemical recycling.

3.1. THE ROLE OF INORGANICS IN PULPING LIQUORS

During the Kraft pulping process, wood chips are cooked in WL, which contains sodium hydroxide and sodium sulfide at temperatures up to 180°C. In this process the wood's lignin is fragmented into smaller segments whose sodium salts are soluble in the cooking liquor, leaving cellulose and hemicellulose in the form of intact fibers needed for papermaking. The concentration of hydroxide and sulfide has increased over the years along with pulping temperatures to improve product yield and quality. Although there are other process streams where hydroxide and sulfide salts may exist with other chemicals, the present study focuses on environmental conditions typically found in different parts of the pulp mill.[26,27] Due to the variability in WL concentration, with trends of higher hydroxide concentrations, which may exceed 150 g/L sodium hydroxide, and higher levels of sulfide, which may exceed 50 g/L sodium sulfide, research in this area has not been comprehensive.[28] The literature has typically focused on concentrations of 100 g/L sodium hydroxide and 30 – 40 g/L sodium sulfide.

Sulfide containing caustic solutions are used or produced in a variety of chemical processes. These include modified Bayer processes used in alumina ore processing, the Gilder-sulfide process used in heavy water production,

hydrocarbon processing for the treatment of acidic impurities such as hydrogen sulfide and mercaptans, and various process streams in pulp mills utilizing the Kraft pulping process.

The dependence of WL corrosivity on the concentration of hydroxide and sulfide, at approximately 100 g/L sodium hydroxide and 30 g/L sodium sulfide, has been described as weak by Yeske.[29] Instead many researchers have focused on other ions which form in most pulping liquors and other industrial processes as a result of hydrolysis or oxidation reactions via Equations (14) and (15).[70] Although the reactions, specifically Equation (15), have been shown to occur at very slow rates when not in an oxidized environment, they are often referred to in literature as the mechanisms for corrosion rate control.[30,70,73]

$$S^{2-} + H_2O \Leftrightarrow HS^- + OH^- \qquad [14]$$

$$S^{2-} + (S_2O_3)^{2-} \Leftrightarrow S_2^{2-} + SO_3^{2-} \qquad [15]$$

Peterman and Yeske[28] investigated the effect of oxidation on chemical concentration for a sulfide containing caustic solution, 100 g/L sodium hydroxide and 35 g/L sodium sulfide, for four week tests. In all cases the concentration of sodium salts analyzed showed change. Yet, testing performed after mixing showed the most significant change in concentration. From the data, it appears evident that the initial variation in concentrations of tested sodium salts was driven by oxidation of the solution during initial mixing and not the proposed equilibrium of the salts according to Equation (15) and supported by the equilibrium constant, $1.6x10^{-4}$, reported by Haegland and Roald.[70]

Wensley and Charlton[67] investigated the role of inorganic sodium salts sulfide, sulfite, thiosulfate and sulfate in the corrosivity of pulp mill liquors, through the potentiostatic polarization study of mild steel. They showed that sulfide and thiosulfate ions act as corrosion activators, impairing the passivation of carbon steel, while sulfite and sulfate ions did not affect passivity, a result previously reported by Kesler.[30] Haegland and Roald demonstrated the ability of polysulfide, shown in Equation (15) in its primary disulfide form, to passivate mild steel when in sufficiently high concentration, above 4 g/L, and activate corrosion at lower concentrations, 1 – 3 g/L.[29,70] The complex

relationship of inorganic salts is also realized in the investigation of thiosulfate and sulfide. Thiosulfate ions at low concentration and in the presence of sulfide have little impact on corrosion rates.[29,70] However, when both are present in sufficient concentrations they inhibit the formation of a passive layer on the metal surface leading to higher corrosion rates.[29,65,67,70,71,72,73,74] The behavior of polysulfide and thiosulfate ions in caustic sulfide solution is similar as an increase in concentration increased the oxidation potential and the rate of corrosion below the passivation potential. Yet, for polysulfide ions an increase in the oxidation potential above the passivation potential formed a stable passive film resulting in low corrosion rates while an increase in thiosulfate ions did not show the ability to increase the potential above that of the passivation potential.[29]

Recently, Singh et al[68] investigated the impact of temperature and concentration of hydroxide and sulfide on liquor corrosivity. The results show that an increase in temperature or in concentration of sulfide or hydroxide results in a decrease in the corrosion potential for austenitic stainless steels, Fe-Cr alloys with ~8% Ni. Depending upon the change in these parameters, the OCP of steels could fall in the range where they are susceptible to SCC.

The resultant potential shift may be due to the formation of hematite, Fe_2O_3, rather than the more stable magnetite, Fe_3O_4, on iron based alloys.

Further defining the relationship of the primary WL constituents and corrosivity will shed some light on the corrosion susceptibility of materials used to construct process equipment, commonly carbon steel.[30,31,32,33]

3.2. THE ROLE OF ORGANICS IN BLACK LIQUOR CORROSIVITY

Significant variation in corrosion rates between process lines at pulp mills, utilizing different tree species, has been reported for a long time.[34] Yet, most of the previously published work has focused on the concentration of inorganic species such as hydroxide and sulfide in pulping liquors. In 1953, MacLean and Gardner[34] demonstrated the effect of organic-metal complexing or sequestering agents in BLs on the corrosion of carbon steel digesters. The organic components come from extractives in the wood chips or are generated from the degradation of lignin, a polymeric phenolic compound, and other heartwood constituents during the pulping process. Niemelä[35,36] analyzed loblolly pine and other BLs which demonstrated that BLs contain a large number of organic constituents which vary from species to species. However,

a number of assumptions were made concerning various fractionations, chemical treatments, and chemical reactions. The concentration of the organic components of BLs depends largely on the wood species used, which individually may contain novel wood species dependent compounds and synthesis pathways. Niemelä[36] characterized more than 700 low-molecular weight organic compounds from Scots pine (*Pinus sylvestris*) BL.

Singh et al[37,38] evaluated corrosivity of BLs from commonly used wood species in the North American PPI and reported the rate of corrosion for carbon steels varied from <0.03 mm/yr to >2.54 mm/yr, depending upon the wood species pulped, under otherwise similar conditions. In general, HW was found to have lower corrosivity compared to the SW species tested. Results from this study indicate that the organic constituents of BL play a significant role in overall variation in the corrosivity among species.[39,40] Although the role of an individual compound is not always certain, organic constituents in BL can be separated into two broad groups: corrosion activators and corrosion inhibitors. Catechol, 1,2-dihydroxybenzene, a breakdown product of lignin, has historically been proposed as a corrosion activator in BLs.[34,37,38,41,42,43,44] Whereas organic extractives, such as resins, tannins, and fatty acids, which show considerable differences in concentration among different species as

well as among differently aged trees,[39,40] are suspected of having some inhibitory properties.

MacLean and Gardner[34] described the ability of 1,2-dihydroxybenzene compounds in phenolic extractives, such as taxifolin or other catechol derivatives, to form stable soluble complexes with iron. These complexes are stable in alkaline solutions and can actively corrode carbon steel during alkaline pulping. Kannan et al[42] confirmed the importance of adjacent hydroxyl groups on aromatic rings showing a significant increase in critical current densities (i_{CRIT}), from 0.1 to 0.44 mA/cm^2, with the addition of 1 g/L of 1,2-dihydroxybenzenes, catechols, for carbon steel during a potentiodynamic polarization study. Other dihydroxybenzenes, m- and p-dihydroxybenzene, which do not have adjacent hydroxyl groups, showed no effect on i_{CRIT}. This result appears to be due to steric strain at the metal-organic molecule interface. Steric strain was identified by Affrossman[45] as a controlling factor when looking at titanium corrosion. In the study, trihydroxybenzenes and dihydroxybenzenes adsorbed more strongly on the titanium metal surface when butyl groups were not attached to the carbon adjacent to the hydroxyl groups. At 30°C, Subramanyan[46] tested corrosion rates for aluminum in the presence of phenolic compounds at 0.01 and 0.1 molar sodium hydroxide.

1,4-dihyrdoxybenzene provided complete inhibition, 100%, at 0.01 molar sodium hydroxide with 1,3- and 1,2-dihydroxybenze compounds providing efficiencies of 98% and 79%, respectively. At higher concentrations of sodium hydroxide the ortho and para compounds continued to protect the metal while the meta-hydroxybenzene realized a marked reduction in inhibition for aluminum, 42% inhibition. Comparison of the inhibition provided to aluminum by phenol in the caustic solution shows a slight reduction in efficiency, 1% for meta and 8% for ortho compounds, when compared to 1,4-dihydroxybenzene for both tested solutions, 97% and 87% with increasing caustic concentration from 0.01 to 0.1 molar sodium hydroxide.

In BLs the addition of 0.64 g/L of catechols was been shown to significantly increase the corrosivity of previously non-corrosive BLs at 170°C. The corrosion rate of carbon steel in a cottonwood BL increased from 0.05 to 35.6 mm/yr and sweetgum BL realized an increase from 0.0 to 221.3 mm/yr.[37] Upon addition of pyrocatechol to synthetic BL, containing only inorganic chemicals, corrosivity of the resulting liquor increased from 0.92 to 11.29 mm/yr. These results indicate that other organic chemicals in the BL may be interacting with added catechol-type compounds in increasing the corrosivity

of BLs compared to that for synthetic BL containing inorganics only. Similarly, the cause of inhibition in some BLs, which appears to be due to organic compounds, is not clear. One compound proposed as having an inhibitory effect in BL is tannin. Tannins have been used as inhibitors in boiler waters and other near neutral environments,[47,48,49] yet may show a more complex effect when present at the high pHs found in BL.[34]

Matamala[47] compared pine and acacia tannins in an anticorrosive paint mixture using a salt fog chamber and reported that tannins from different wood species varied in the capacity to inhibit corrosion. Pine tannins were found to be more effective inhibitors with better adherence to the metallic substance. Tannins have also been described as effective oxygen scavengers.[47,48] Lewis[48] tested tannins in mineral oils as a means of inhibiting oxidation of the media. Although shown to be effective inhibitors and oxygen scavengers, tannins have also been shown to create soluble films resulting in greater susceptibility to corrosion.[49] In near neutral media, a 2% solution of tannin resulted in the formation of a soluble Fe(III) tannate film, whereas with the addition of calcium gluconate and tannin a film with low solubility was formed.[49] The results indicate that the corrosion inhibiting properties of organic compounds depends upon the concentration as well as chemical interaction with other

constituents present in the solution/ environment. Tannins are commonly used as corrosion inhibitors in various industries, including industrial boilers, to protect carbon steel.[47]

Many additional wood compounds are used as corrosion inhibitors for steels in a variety of industries. Derivatized fatty acids, commercial surfactants, have received considerable interest in the petroleum industry as corrosion inhibitors.[50] In the presence of 0.25 molar sulfuric acid and temperatures from 25°C to 55°C the corrosion rate for carbon steel decreased in the presence of the fatty acid compounds.[50] Thermodynamic analysis of adsorption described the tendency for the fatty acid complex to form a stable film on the carbon steel surface. The formation of a protective corrosion product on carbon steel as a result of the addition of fatty acids in solutions has also been proposed in organic solvents evaluated in the presence of C5 to C6 fatty acids at 25°C.[51] The most stable protective film was found on samples tested in the presence of hexanoic acid whereas no protective films were found in the presence of tested C2 to C4 fatty acids.

Yet longer fatty acids chains do not always result in increased protection of the metal. In acidic media C2 to C16 fatty acids were tested from 25°C to 250°C for their inhibitive properties with carbon steel.[52] At 90°C increased fatty chain length from C2 to C16 realized increased inhibition for carbon steel, from ~8 to ~0.1 mm/yr. Although a similar trend was seen from C2 to C16 fatty acids at 250°C, C6 to C12 fatty acids showed unexplained and significant increased rates of corrosion. It was also reported that mixtures of fatty acids in the tested system did not show signs of synergistic behavior. The complexity of identifying chemicals that will act as effective inhibitors is demonstrated by Singh and Gupta.[53] A polarization and gravimetric evaluation of carbon steel in acetic acid and sodium acetate was performed with increasing concentrations of acetic acid increasing the current density, indicating an increased tendency to actively corrode. However, gravimetric tests demonstrated a reduction in the rate of corrosion after reaching a maximum corrosion rate at 20% acetic acid. Abdallah et al[54] evaluated a sulfonated fatty acid in 1 molar hydrochloric acid for its inhibitive properties towards carbon steel. At increased concentration, 100 – 700 ppm, a reduction in current density, 2.24 – 1.00 mA/cm^2, and increase in inhibition efficiency, 77.6 – 90.0%, was realized.

Extractives of organics found in trees have been investigated for wide use in industrial inhibition. Loto et al[55,56,57] have investigated cashew, *Anacardium occidentale*, and mango, *Mangifera indica L.*, extracts for the inhibition of carbon steel in hydrochloric acid and sulfuric acid. After performing a polar solvent extraction, extractives from differing parts of the tree, specifically bark, nuts, fruit, and leaves, were added to the acidic solutions. Extracts of cashew fruits provided the greatest reduction from tested cashew extracts with inhibition efficiencies of 33 – 55%.[55] Mango extracts, when added individually at 1000 ppm for bark and 500 ppm for leaves, also showed promise. However, when added together for a total of 1000 ppm the efficiency of inhibition of carbon steel increased synergistically from ~39% for bark and ~29% for leaves to ~70% for the combined extracts in sulfuric acid.

Although the affect of species dependent corrosion has been known for more than 50 years, and its apparent reliance on the organic composition of the wood, the primary focus of the PPI concerning organic extractives is on pitch formation and not on corrosion. Organic components such as sterols, sterol esters, and waxes have been identified as non-soluble soaps[58] under the alkaline conditions of Kraft pulping and the root cause of pitch problems. On

the other hand, glycerol esters have been shown to completely saponify both fatty and resin acids which then readily dissolve.[59] In some cases the debarking of logs, seasoning of logs, or the seasoning or biological treatment of woods chips with enzymes has been utilized to reduce downstream pitch problems.[60] Therefore the seasoning of wood chips due to the lifetime in the chip pile or during transportation impacts the extractive content in BL. Additionally, moisture and heat can have considerable effects on the amount of extractives removed from wood chips. Until now no significant study has addressed the impact of chip weathering on the corrosivity of BL.

In summary, the complex solution of inorganic and organic chemicals referred to as BL may have multiple corrosion activators and/or inhibitors. Additionally, synergistic reactions between organic chemicals may play a significant role in overall liquor corrosivity.[37,61,69,70] In this study, the role of selected organic constituents identified from the chemical analysis of water extracted wood chips and BL have been systematically evaluated for overall corrosivity towards carbon steel A516-Gr70.

3.3. BLACK LIQUOR OXIDATION

Changes in the general corrosion and SCC susceptibility of used alloys or candidate alloys due to BL oxidation treatment are one concern addressed by the present study. A key component of oxidized BL corrosivity is the extent to which the oxidation is carried out. Depending upon the extent of oxidation, sulfide in the BL may react to form sodium hydroxide and sodium thiosulfate, as shown in Equation (16), or complete oxidation may convert the sulfides into sulfates via the reactions in Equations (16) and (17). Oxidation of both sulfide and thiosulfate to the virtually non-corrosive sulfate ions is therefore desirable. Oxidation may also affect the organic constituents of the liquor.[25] However, if not performed at high efficiencies, oxidation can increase thiosulfate and hydroxide levels, as shown through Equations (16) and (17), and potentially increase the corrosivity of the liquor.[61,62,63,64,65,66]

$$2Na_2S + 2O_2 + H_2O \rightarrow Na_2S_2O_3 + 2NaOH, \quad \Delta G = -806\ \text{kJ}\ @100^{\circ}\text{C} \quad [16]$$

$$Na_2S_2O_3 + 2NaOH + 2O_2 \rightarrow 2Na_2SO_4 + H_2O, \quad \Delta G = -889\ \text{kJ}\ @100^{\circ}\text{C} \quad [17]$$

In a review of the status of oxidation in the pulp and paper industry, Collins[25] reports the apparent benefits of oxidation within the recovery process, noting decreases in corrosion for both vacuum and falling film evaporators following

oxidation of BL. Additionally, it was cautioned that increased sulfidity levels seen in other process streams within the mill, as a result of higher retention of sulfur due to oxidation, would lead to increased rates of corrosion experienced by the respective process equipment.

Wensley and Charlton[67] investigated the role of inorganic chemicals, specifically sulfide, thiosulfate and hydroxide, in the corrosivity of pulping liquors through a polarization study. Sulfide and thiosulfate ions were shown to be corrosion activators, with an ability to impair passivity of carbon steel, while sulfite and sulfate ions did not affect passivity. Recently, Singh et al[68] investigated the impact of changes in hydroxide and sulfide concentrations as well as temperature on corrosivity. At higher temperatures an increase in sulfide or hydroxide concentration resulted in a decrease in the corrosion potential of carbon steel and austenitic stainless steels. A decrease in corrosion potential in the active-passive region can make these alloys susceptible to SCC. The potential shift may also result in the formation of hematite, Fe_2O_3, rather than the more stable magnetite, Fe_3O_4, on iron based alloys and lead to higher corrosion rates of carbon steel. This was demonstrated when Ruus and Stockman[61] showed an increase in corrosion of

carbon steel at 170°C with increasing hydroxide levels during pulping experiments with SW pine.

The complex relationship of inorganic chemicals on liquor corrosivity is realized in the investigation of thiosulfate and sulfide. In the presence of sufficient sulfide, thiosulfate ions, in low concentrations, have little impact on corrosion rates.[61,69,70] However, a further increase in the concentration of thiosulfate can increase the rate of corrosion. This occurs by inhibiting the formation of a passive layer on the metal surface.[71,72,73,74,75]

As stated, oxidation of BL may also affect the organic composition of the liquor. Yet, as discussed by Collins,[76] reports of continued reaction of sulfide with organic constituents in stored oxidized BL resulting in increased levels of hydroxide was more likely the result of the release of caustic with the oxidation of sulfide to thiosulfate. However, the oxidation process may result in the breakdown of lignin in BL and increase the concentration of phenolic compounds, as in catechols, or may further promote the oxidation of phenolic groups to carboxylic acids thus changing the localized interaction of metal and liquor. As reported by Bowers,[77] this may increase the corrosion susceptibility

of pulp mill equipment. The reaction of oxygen with lignin and other organic compounds is prevalent in the early literature regarding oxidation, yet studies relating oxidation of organic compounds to increased rates of corrosion have not been performed.[25]

3.4. MATERIALS USED IN PULP MILL ENVIRONMENTS

Along with carbon steel, austenitic stainless steels SS304 and SS316L are also used in pulp mill equipment.[30,31,32,33] Austenitic stainless steels can also undergo SCC in sulfide containing caustic solutions, depending upon the liquor composition and temperature conditions.[68] Duplex stainless steels DSS2205 and DSS2304 are being used in new pulp mill equipment due to their resistance to general corrosion and SCC. However, their performance in oxidized BLs has not been studied. This study compares the corrosion behavior of selected alloys in both oxidized and non-oxidized BL taken from the same process and cook in a pulp mill. Inorganic constituents of BLs were analyzed to better understand the effects of oxidation on BL and its impact on material behavior.

Although PPI processes continue to implement carbon steel equipment, most pulp mill processes are seeing an increased use of austenitic stainless steel SS304 and duplex stainless steels DSS2205 and DSS2304 compared to carbon steel. With the evolution in material design an increase in initial capital cost has also arisen, a fact offset in the long term by the increased strength and durability of duplex stainless steels. Current research is being conducted on lean duplex stainless such as DSS2101 which consists of reduced quantities of costly nickel and chromium while projected to maintain the strength and durability of DSS2205 and DSS2304. The implementation of lower cost, higher strength, and higher durability materials will provide the PPI with the ability to increase temperature and the concentration range of sodium hydroxide and sodium sulfur compounds currently practiced. With the proposed advent of gasification, and expected variability in sulfur recovery streams, i.e. both high and low sulfidity and polysulfide streams, the implementation of lean duplex stainless steels may be a key to safely unlocking even higher efficiencies from the pulp mill.

Chapter 4

HYPOTHESES

1. The corrosion resistance of carbon steel in alkaline solutions relies on the stability of a passive film on the surface. Increased temperature and concentration of hydroxide and/ or sulfide may shift the potential of carbon steel A516-Gr70 in solution to a range where passivity is not stable. An increase in corrosion rate may result due to a shift in potential into the active region.

2. In BLs, corrosivity depends predominantly on organic constituents. Overall corrosivity depends on wood species pulped with a general trend of lower corrosivity for HW BLs than SW BLs, and therefore a function of organic content in wood chips.

3. Individual organic compounds found in BLs, such as catechols, may activate corrosion whereas other constituents, like tannins, may have an inhibitory effect on carbon steel corrosion. These compounds may act as synergistic or antagonistic corrosion inhibitors for carbon steels in BL.

4. Depending upon the extent, oxidation of BL may result in increased susceptibility of metals to SCC due to increased levels of hydroxide and thiosulfate, reaction products of partial oxidation, in solution resulting in a potential shift to the region of active-passive transition.

Chapter 5

RESEARCH FOCUS

5.1. PULPING LIQUOR CORROSIVITY

In recent years the need for the paper industry to provide greater optimization and utilization of processes has resulted in an effort to drive down costs. Such an effort is generally limited to one key Kraft mill component, the recovery boiler. As the bottleneck for most Kraft mill processes the recovery boiler is the source of energy production, chemical recycling, and waste removal. The boiler is limited by its ability to accept only so much BL and at the same time must continually be operated, outside of scheduled shut downs, in order to avoid costly maintenance and/ or failure.

The required operation also inputs a strain on the remainder of the mill. BL storage tanks are utilized as buffers for process shut downs from both pulp production and boiler operation. Each tank in turn requires additional equipment from pumps to process lines. The result is a process with significant surface area exposed to the harsh corrosive conditions of a sulfide

containing process liquor at high pH and temperatures ranging from slightly above room temperature to 180°C.

Yet mill optimization also affects the front end of pulping liquors. Higher sulfide content, WLs with varying sulfide concentrations for multiple digester entry points, wood chip pre-impregnation with a source that ranges from steam to BL, and increased temperatures are all the result of process optimization programs to improve fiber yield, brightness, and bleachability. The end result is a variety of processes that, on a mill to mill basis, may operate under exceedingly differing conditions.

Chip yards, too, have experienced changes. As timber resources, economic and labor conditions dictate uncertainties in the market place the need to keep adequate inventories is balanced with the desire to optimize cash flow. Wood sourcing is also affected. Regional plantations, forest thinning, and clear cutting continue to operate as the main modes of fiber sourcing. Although increased knowledge in fiber characteristics and product development have encouraged many mills to adopt more stringent sourcing standards this remains far from a universally adapted benchmark. The result is chip storage

and source variations that may lead to process fluctuations not well understood or expected.

The present study investigates the fundamental causes of pulping liquor corrosivity. In Chapter 6, "Corrosion of Carbon Steels in Sulfide Containing Caustic Solutions," corrosivity of carbon steel A516-Gr70 as a function of process parameters temperature, hydroxide concentration, and sulfide concentration is investigated. Corrosion rate, OCP, and surface film characterization are utilized to understand and predict the impact of process parameter changes on corrosion rate. Chapter 7, "Role of Wood Extractives in Black Liquor Corrosivity," investigates the impact of changes in the organic content of the wood pulped on the corrosion rate of carbon steel A516-Gr70. The impact of wood species, age, water extraction and chemical addition are analyzed with electrochemical techniques, chemical analyses, and corrosion rate to understand the fundamental cause in corrosion rate variability.

Whereas, Chapter 8, "Effect of Black Liquor Oxidation on the Corrosion and Stress-Corrosion Cracking of Carbon and Stainless Steels," investigates material susceptibility to BL processed before and after a mill oxidizing unit.

The impact of oxidation, primarily affecting the inorganic constituents of the liquor,[25] and temperature are evaluated with SSRT, OCP, and chemical analyses for carbon steel A516-Gr70, SS304L, DSS2205 and DSS2304.

The focus of this study incorporates many of the arenas of change in the pulp mill with a fundamental investigation in process corrosion. Ranging from wood chips to WLs to oxidized BLs this study addresses the impact of inorganic and organic content as well as temperature on corrosion. Though application of this research does extend to various industrial processes using caustic and sulfide containing caustic solutions, the focus of this work is primarily on the PPI.

Chapter 6

CORROSION OF CARBON STEELS IN SULFIDE CONTAINING CAUSTIC SOLUTIONS

6.1. INTRODUCTION

Corrosion resistance of carbon steels in sulfide containing caustic solutions depends upon the formation of a stable passive film on the metal surface. As processes change operational parameters such as chemical concentrations and temperature the corrosivity of the process environment also changes. New corrosion resistant materials such as duplex stainless steel are being selected for new equipment in pulp mills. Yet, carbon steel continues to be utilized for a significant amount of new and existing pulp mill equipment where it may be subjected to conditions beyond initial design parameters.

The Kraft pulping process continues to realize changes in concentration and temperature to improve product yield and quality. In the last twenty years trends of increased sodium hydroxide concentrations, from 100 – 130 g/L may now exceed 150 g/L, while increased levels of sodium sulfide, formerly below 40 g/L may now exceed 50 g/L. Ever pressing environmental conditions and

improved process technology and material selection are expected to push concentrations even higher. Temperatures, too, have experienced an increase from below 170°C to approaching 180°C in some mills.

Material selection has not always stayed current with technology or process changes. Over the years silicon content of carbon steels has been found to be susceptible to corrosion in sulfide containing caustic solutions, while chromium and molybdenum have also proved susceptible to high alkaline environments.[69] On the other hand, copper and nickel content have shown positive results in their corrosion resistance in sulfide containing caustic solutions.[69] Mill to mill variation, concentration changes within an individual process, and material design (thickness and material selection) have resulted in a range of materials from carbon steels to duplex stainless steels utilized in the industry today.

Due to economic and operational decisions new material purchases realize a similar range of choice. In some processes higher cost corrosion resistant materials are passed over for thicker more susceptible carbon steels. Often maintained or replaced equipment such as pump housing may also be replaced

with carbon steels. In digesters and tanks experiencing high corrosion, carbon steels are weld-overlayed with more resilient stainless or duplex stainless steels.

Prior research in literature was focused on carbon and stainless steels in sulfide containing caustic solutions of 100 – 140 g/L sodium hydroxide and 30 – 40 g/L sodium sulfide with a range of oxidized sulfur compounds. Additionally, significant portions of the literature are focused on comparison of corrosion susceptibility between mills or process lines, containing a variety of unidentified non-process elements, typically utilizing liquors that were transported from the mill to the research facility while stored in a variety of containers and environments. Chemical analyses and testing procedures used were also subject to criticism as many are not clearly identified and thus also incapable of being reproduced.

A systematic study on sulfide containing caustic solutions was performed for temperatures from 25°C to 170°C with sodium hydroxide concentrations of 0 – 200 g/L and sodium sulfide concentrations of 0 – 75 g/L. In this study, the corrosion resistance of carbon steel and its ability to maintain a stable passive

surface film was investigated as a function of electrochemical potential which allows prediction of corrosion behavior in a variety of pulping environments.

6.2. EXPERIMENTAL PROCEDURES

6.2.1. COUPON EXPOSURE TESTS

Corrosion tests were carried out in 4-liter duplex stainless steel autoclaves, testing apparatus is shown in Figures 8 and 9. All gravimetric corrosion tests in this study were carried out for 72 hours at 25°C, 100°C, and 170°C. A minimum of two A516-Gr70 carbon steel corrosion coupons were exposed in each test to verify the reproducibility in corrosion rate measurements. Metal samples were polished to a 1.2-μm finish and cleaned with acetone. Each test sample was weighed and its area was measured before mounting them on electrically isolated Teflon racks to eliminate galvanic effects. Samples were placed in the autoclave making sure that they did not touch the autoclave walls. Test temperature was maintained within 1°C throughout the experiment. Upon completion of the test, the samples were removed from the autoclave and placed on drying racks. Dried samples were stored in air-tight envelopes for further analysis. Tested coupons were examined for visible corrosion features or signs of localized corrosion on the surface or under crevice washers. Surface corrosion products on exposed samples were

characterized by X-ray diffraction (XRD) method. Reaction products on the metal surface were removed and the final weight of each coupon was used to calculate the corrosion rate, Equation (18), in the given test condition.

Figure 8. Duplex stainless steel 2205 autoclaves used for corrosion testing.

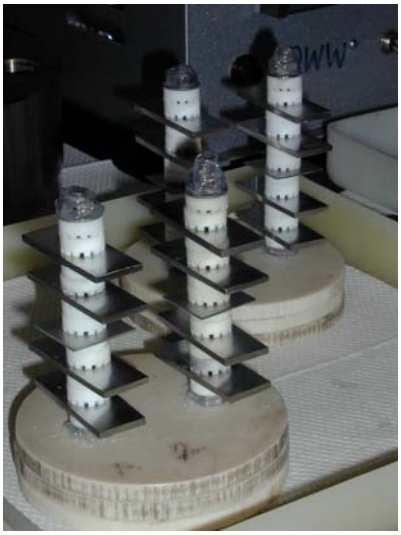

Figure 9. Insulated testing rack with duplicate alloy specimens for each tested solution.

$$\text{Corrosion\_Rate}(mm/yr) = \frac{87.6 * W}{D * Area * t} \quad [18]$$

Where, W = weight loss in mg; D = density in g/cm^3; Area = area is measured in cm^2; t = time in hours.

6.2.2. ELECTROCHEMICAL TESTS FOR CORROSION

Potentiodynamic polarization tests were carried out to study the electrochemical behavior of carbon steels in different sulfide containing

caustic solutions. Tests were performed in 4-liter duplex stainless steel autoclaves at 25°C and 90°C. Cylindrical metal samples were polished to a 1.2-μm finish, cleaned with acetone, weighed and the surface area measured. Test samples were mounted on a polymer coated steel rod, which was protected against corrosion. Carbon steel samples were further insulated from the autoclave material with Teflon fittings. Electrochemical tests were started at the test temperature and the conditions were maintained throughout the test. Potentiodynamic polarization tests were carried out using a platinum foil counter electrode and a saturated calomel reference electrode (SCE). Carbon steel samples were conditioned at cathodic potential for 5 minutes to reduce oxide film on the surface. Potential was scanned in the anodic direction, more positive potentials, at a rate of 1 mV/sec for all tests done in this study.

6.3. RESULTS AND DISCUSSION

Solutions used for these studies varied in caustic concentrations and in the addition of sodium sulfide at temperatures of 25°C, 100°C, and 170°C. Corrosion rates reported in this study represent an average corrosion rate over the entire test duration and not the instantaneous corrosion rate, which may change during the test duration. For gravimetric corrosion tests performed at 25°C, shown in Figure 10, there is a small increase in corrosion rate with an

increase in hydroxide or sulfide concentration, however the effect is not very significant at 25°C. At 100°C, gravimetric corrosion tests, shown in Figure 11, realized significantly increased corrosion rates with both increasing hydroxide and sulfide concentration. Corrosion tests at 170°C, shown in Figure 12, demonstrate a more complex behavior. Increased sulfide concentration corresponded with increased corrosion rates while increased sodium hydroxide concentration above 100 g/L at 37.5 and 75 g/L sodium sulfide demonstrates a reduction in corrosion rate. Temperature also appears to play a significant role in liquor corrosivity above 100°C with corrosion rates increasing an order of magnitude between 100°C and 170°C.

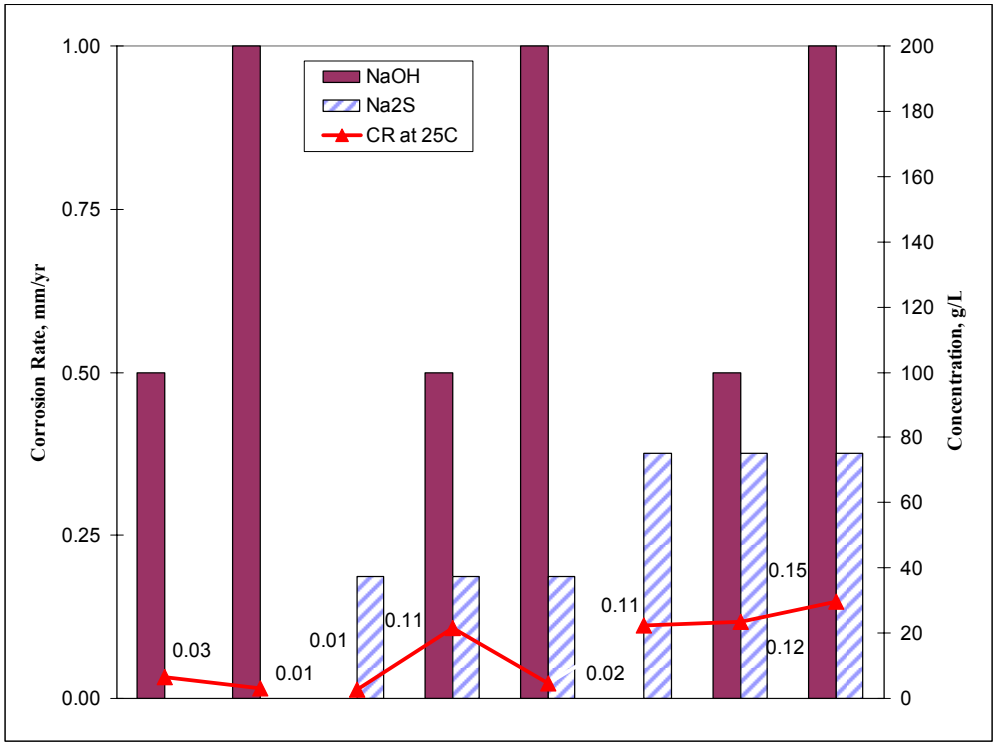

Figure 10. Corrosion rate of A516-Gr70 carbon steel at 25°C as a function of increasing sodium hydroxide concentration at constant sodium sulfide concentration. Corrosion rates in mm/yr.

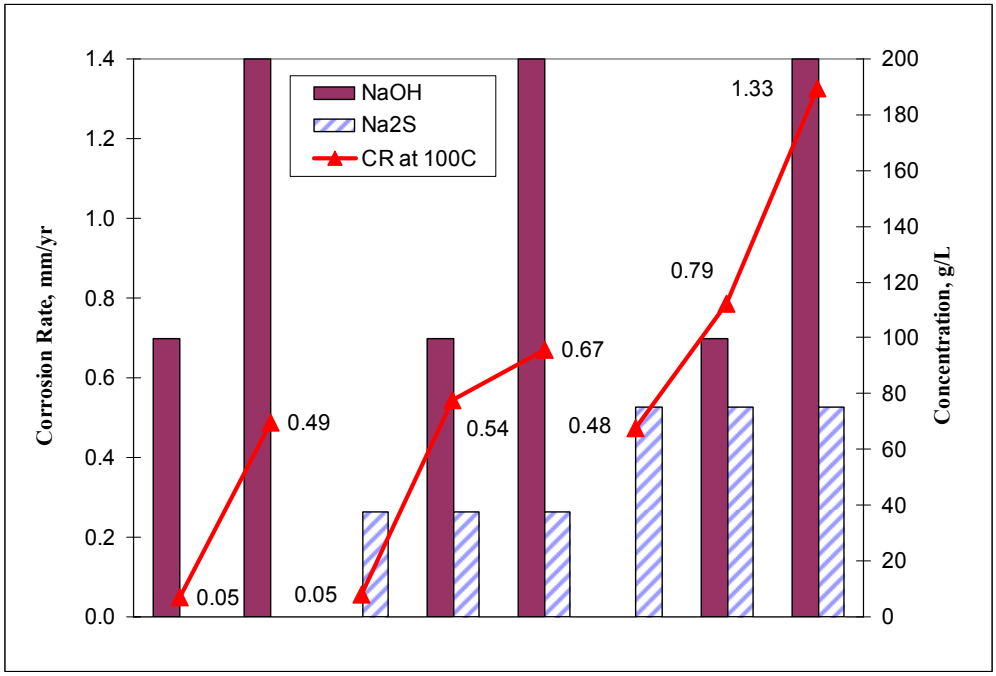

Figure 11. Corrosion rate of A516-Gr70 carbon steel at 100°C as a function of increasing sodium hydroxide concentration at constant sodium sulfide concentration. Corrosion rates in mm/yr.

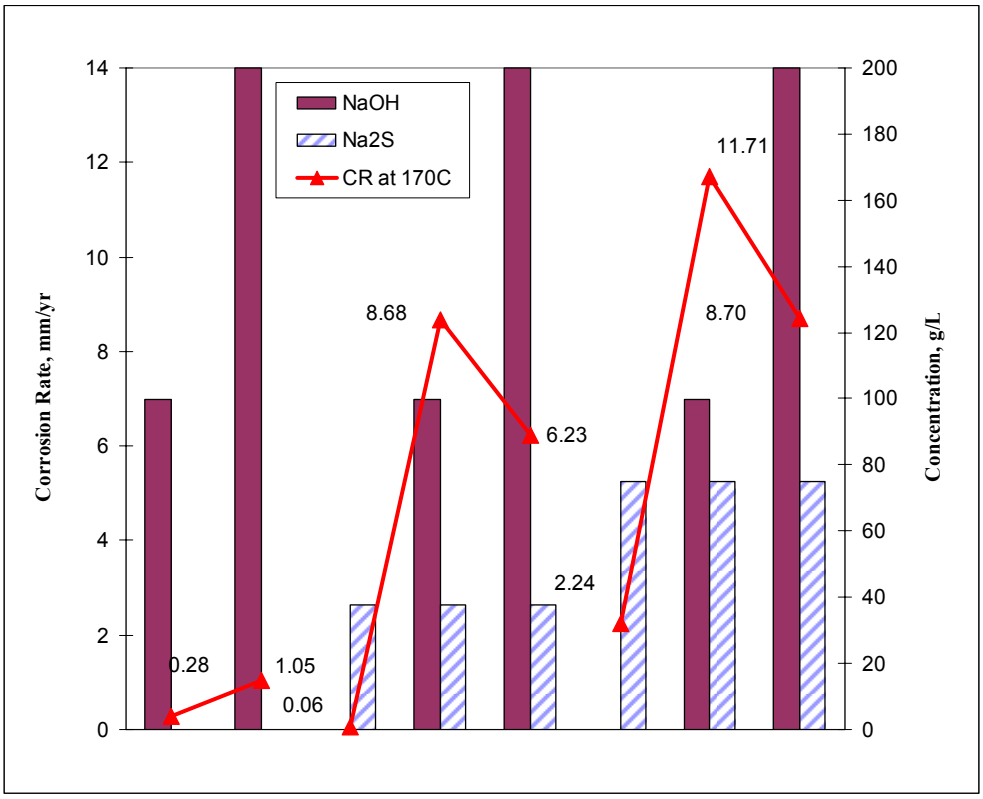

Figure 12. Corrosion rate of A516-Gr70 carbon steel at 170°C as a function of increasing sodium hydroxide concentration at constant sodium sulfide concentration. Corrosion rates in mm/yr.

In all cases shown in Figures 10 – 12, temperature has a more significant affect on corrosion rates in sulfide containing caustic solutions than individual concentrations. However, in solutions containing only hydroxide the metal does not realize significantly increased rates of corrosion with increased temperature. Additionally, in tested solutions containing only initial additions

of 37.5 g/L of sodium sulfide A516-Gr70 also does not realize noteworthy increases in corrosion compared to that of 75 g/L sodium sulfide or sulfide containing caustic solutions. As shown in Equation (19), the hydrolysis of sodium sulfide will produce caustic. The presence of sufficient caustic due to sulfide hydrolysis may explain the increased corrosion realized in a solution of 75 g/L sodium sulfide compared to that of 37.5 g/L sodium sulfide.

$$Na_2S + H2O \rightarrow NaSH + NaOH \qquad [19]$$

6.3.1. CORROSION RATE DEPENDENCE ON TEMPERATURE

The rate of corrosion for carbon steel was found to increase with an increase in temperature and is described by the Arrhenius equation, Equation (20), where Arr = the constant described by the natural log of the Arrhenius constant, R = the gas constant 8.314 J/mol*K, and Ea = the activation energy with units of J/mol. In Figure 13, a plot of the Arrhenius relationship, Equation (20), with the natural log of the corrosion rate, CR, versus inverse absolute temperature, T, shows that the corrosion rate of carbon steel A516-Gr70 in solution increases with increased temperature at an Ea of ~494.8 J/mol.[6]

$$\ln CR = Arr - \frac{Ea}{RT} \qquad [20]$$

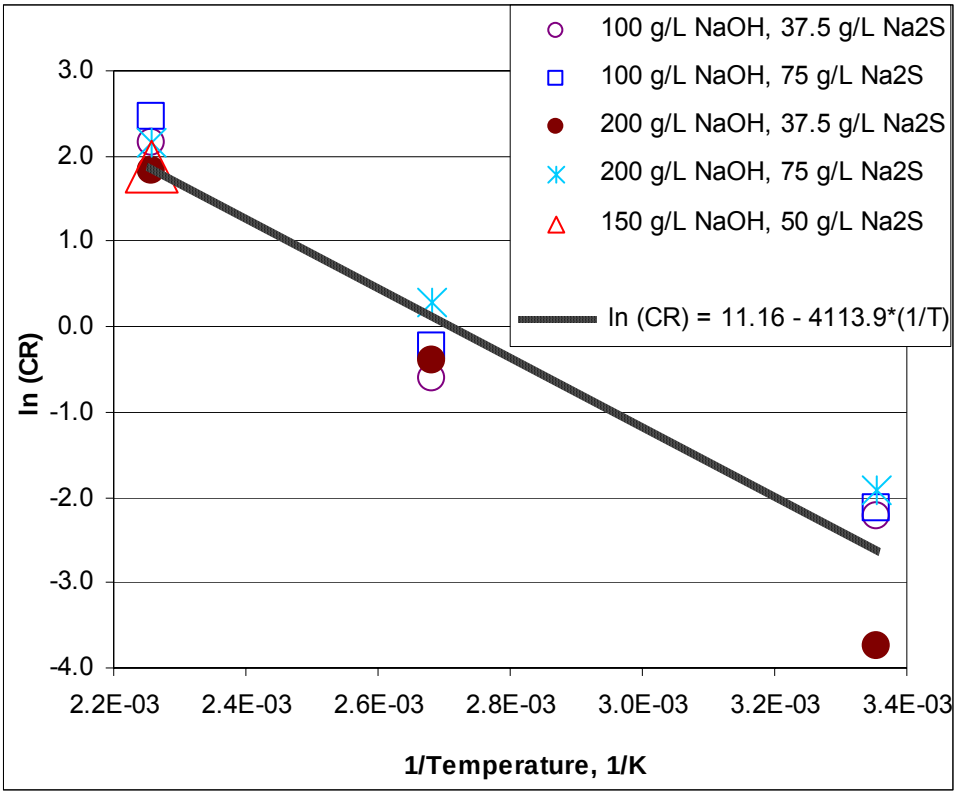

Figure 13. An Arrhenius plot of the corrosivity of carbon steel A516-Gr70 in sulfide containing caustic solutions at 25°C, 100°C and 170°C.

6.3.2. GRAVIMETRIC EVALUATION OF TAFEL METHOD

To investigate the feasibility of electrochemical techniques, namely the Tafel extrapolation method, in corrosion rate evaluation of sulfide containing caustic solutions, electrochemical studies were performed in addition to gravimetric corrosion rate tests at 25°C and 90°C. Electrochemical tests namely

potentiodynamic polarization allow for rapid testing of a solution providing near instantaneous feedback (often in less than an hour compared to the more than two weeks expected of gravimetric testing) and is the basis of the Tafel method. The Tafel method, described in Chapter 2, allows for a quick estimation of the rate of corrosion expected for metal in solution.

The investigation of temperature and concentration changes in sulfide containing caustic solutions allowed for a direct comparison of gravimetric and Tafel methods at 25°C and 90°C. In potentiodynamic polarization tests, potential is scanned in a predetermined range at a fixed rate, typically 1 mV/sec, and the current flowing between the working electrode, carbon steel, and the counter electrode, platinum electrode, is measured. The resulting potential versus log current density curves can be used to calculate corrosion rate by the Tafel extrapolation method. Gravimetric testing, however, allows for reactions at the rest potential and typically takes a long time to measure corrosion rates, especially when corrosion rates are slow.

Potentiodynamic polarization curves for carbon steel samples were analyzed and Tafel regions of the curves were used to calculate corrosion rates. Results

from these measurements are shown in Tables 3 and 4. Corrosion rates calculated from the Tafel extrapolation method in sulfide containing caustic solutions did not exactly correspond to the corrosion rates measured from gravimetric tests. However, general trends of increasing corrosion rates with increased temperature are also seen with the electrochemical tests. Differences in the two methods may be due to sulfur related electrochemical reactions on the electrode surface which were possible along with the metal corrosion reactions.

Corrosion rates for carbon steel A516-Gr70 measured by the Tafel extrapolation method correlated better with the corrosion rate from gravimetric measurements in simple caustic solutions, without addition of sulfide, at 25°C. However, in solutions containing both hydroxide and sulfide, corrosion rates predicted from electrochemical measurements did not correlate with the average measured corrosion rate. At 25°C, Table 3 shows increased corrosion rate with increases in both sulfide and hydroxide concentrations which corresponds to the trend of the gravimetric data. Yet, at 90°C, shown in Table 4, corrosion rates calculated from Tafel extrapolations did not follow the trend of gravimetric data.

Table 3. Corrosion rate for carbon steel A516-Gr70 measured by Tafel slope extrapolation and gravimetric test methods in sulfide containing caustic solutions at 25°C.

NaOH g/L	Na_2S g/L	Tafel Extrapolation CR, mm/yr	Gravimetric Avg. CR, mm/yr
100	0	0.09	0.03
200	0	0.13	0.01
0	37.5	0.44	0.01
100	37.5	--	0.11
200	37.5	2.21	0.02
0	75	1.74	0.11
100	75	2.79	0.12
200	75	8.14	0.15

Table 4. Corrosion rate for carbon steel A516-Gr70 measured by Tafel slope extrapolation and gravimetric test methods in sulfide containing caustic solutions at 90°C.

NaOH g/L	Na_2S g/L	Tafel Extrapolation CR, mm/yr	Gravimetric Avg. CR, mm/yr
100	0	12.79	0.05
200	0	20.93	0.49
0	37.5	--	0.05
100	37.5	12.79	0.54
200	37.5	36.04	0.61
0	75	3.37	0.48
100	75	8.14	0.79
200	75	32.55	1.33

Instead Tafel data anticipates a reduction in corrosion rate with an increase in sulfide content at both 100 and 200 g/L sodium hydroxide. The presence of sulfide, which can participate in redox reactions at the steel surface shifts the polarization potential to increased current density and inhibits the ability of the metal to passivate with the incorporation of sulfide in the iron oxide passive layer.[64,72,78] Further the shift in the polarization curve can reduce the cathodic Tafel slope thereby reducing the corrosion current density used to calculate the corrosion rate, Equation (11), where i_{CORR} = the corrosion current, R_P = the polarization resistance, and β_a and β_c = the anodic and cathodic Tafel slopes, respectively.

$$i_{CORR} = \frac{1}{2.3R_P}\left(\frac{\beta_A\beta_C}{\beta_A + \beta_C}\right) \qquad [11]$$

Other factors affecting the ability of electrochemical techniques to effectively compare rates of corrosion with gravimetric tests include passivity in solution and reference electrode stability. Due to the length of testing, gravimetric corrosion samples have a greater opportunity to passivate resulting in a reduced time period for active corrosion that may be included in electrochemical calculations. Reference electrodes in sulfide containing

caustic solutions have been found to be unstable over time and with increased temperatures. Reference electrodes may be surrounded by solutions different than that of the working electrode, tested metal. Common electrodes such as the Ag/AgCl and Ag/Ag_2S are also subjected to poisoning which inhibits the ability of the electrode to provide a stable response during testing.[79] However, that problem can be solved by using an external reference electrode to avoid poisoning.

6.3.3. COMPARISON OF OPEN CIRCUIT POTENTIAL TO CORROSIVITY

Another electrochemical parameter used to obtain information concerning the thermodynamic activity of the metal in solution is OCP, open circuit potential, represented in Figures 1 and 2 as E_{CORR}, the rest potential or mixed potential of the metal in solution. OCP can be determined from polarization studies or by measuring the potential of the test metal against a reference electrode. OCP provides insight into the oxidizing and reducing power of the solution with concentration and temperature changes and the resulting behavior of the metal in that solution. Electrochemical potential data, in conjunction with the pH of the solution, also allows for calculations of thermodynamically stable surface corrosion products, typically known as Pourbaix diagrams.[80]

To understand the corrosion behavior of carbon steel, as measured by gravimetric methods, OCPs were measured for carbon steel A516-Gr70 samples exposed to different test conditions at 25°C and 90°C. The OCPs were plotted versus corrosion rate in Figures 14 and 15. As shown in Figure 14 an increase in hydroxide concentration at 25°C and 90°C and an increase in temperature at constant concentration correspond to a decrease in OCP of carbon steel A516-Gr70 in solution. The reduction in OCP is predicted by the Nernst equation, Equation (21),[8] and also realized with austenitic stainless steel 304L reported by Singh et al.[68] Results in Figure 14, show that potential increases with an increase in sulfide content at 25°C. Whereas at 90°C the trend reversed itself as an increase in sulfide did yield a decrease in measured OCP. For all compositions tested, the OCP decreased with an increase in temperature.

$$E_r = E_o - \frac{RT}{nF} \ln \frac{[ox]^b}{[red]^a} \qquad [21]$$

Where E_r = the reversible potential in V, E_o = standard reversible potential in V, and $[ox]^b$ = activity of oxidized species, raised to the stoichiometric coefficient *b*.[8]

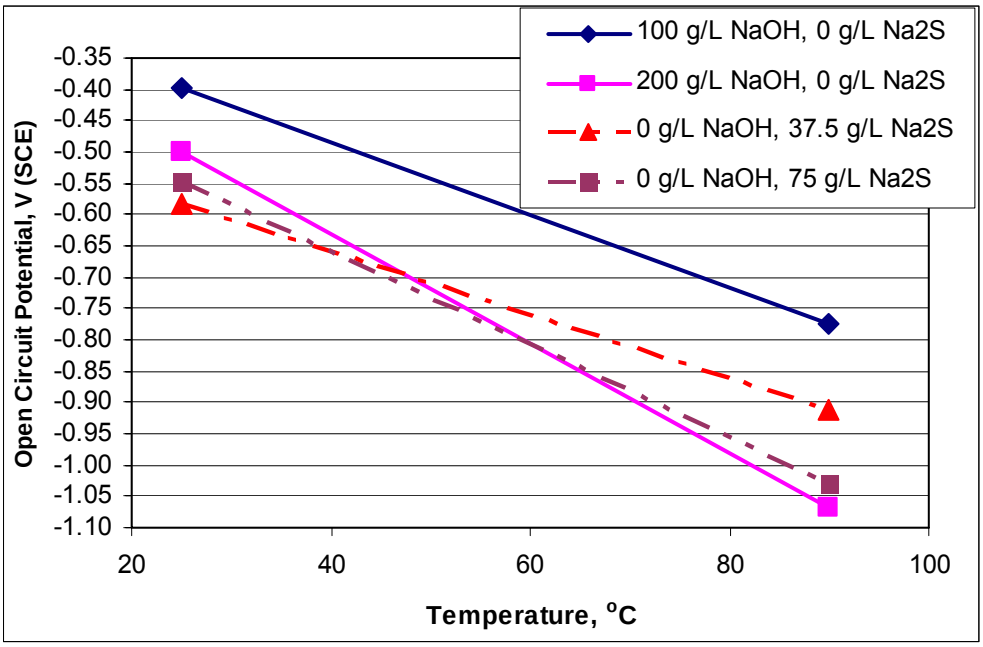

Figure 14. Open circuit potentials for tested concentrations of caustic and sulfide solutions at 25°C and 90°C.

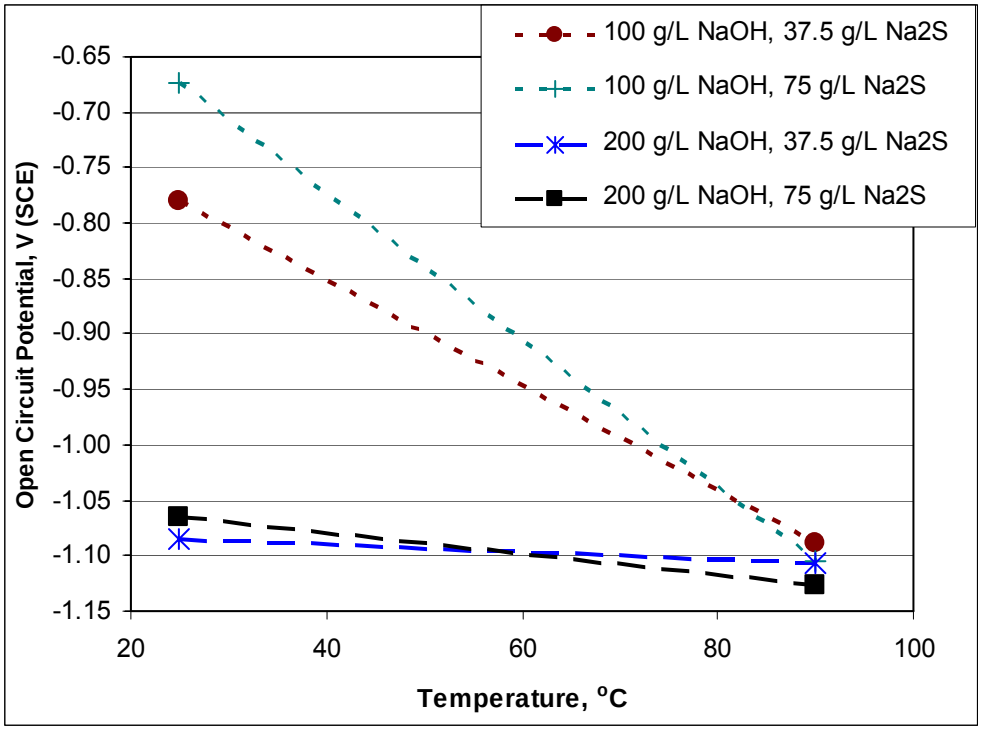

Figure 15. Open circuit potentials for tested concentrations of sulfide containing caustic solutions at 25°C and 90°C.

In sulfide containing caustic solutions, polarization curves result from all possible redox reactions, making it difficult to extract information about metal oxidation reactions from the overall signal. The potentials for several possible reactions, calculated from the data by Biernat and Robins,[81] from 0.2 to -1.8 V (SHE) in a Fe-S-H_2O system at 25°C, 100°C, and 150°C are given in Table 5. Sulfur can also oxidize into various oxidation states including thiosulfate and

sulfate. Thus, OCP in these systems is mixed potential and includes possible sulfur redox reactions. It is difficult to use a simple Tafel approach to extract information of metal oxidation reactions in such a system. However, OCP can indicate thermodynamic tendencies for the metal to form more stable products.[72]

Table 5. Reaction potentials, V (SHE), for an iron-sulfur-water system at 25°C, 100°C, and 150°C.[81]

Reaction Potentials, V (SHE)			
25°C	**100°C**	**150°C**	
-0.906	-0.996	-1.112	$FeS + 2H^+ + 2e^- = Fe + H_2S$
-0.761	-0.795	-0.886	$FeS + H^+ + 2e^- = Fe + HS^-$
-0.787	-0.757	-0.798	$FeS + 2e^- = Fe + S^{2-}$
-0.459	-0.798	-0.899	$Fe_3O_4 + H_2S + 2H^+ + 2e^- = 3FeS + 4H_2O$
-0.907	-1.401	-1.578	$Fe_3O_4 + 3HS^- + 5H^+ + 2e^- = 3FeS + 4H_2O$
-0.817	-1.514	-1.844	$Fe_3O_4 + 3S^{2-} + 8H^+ + 2e^- = 3FeS + 4H_2O$
-0.395	-0.867	-1.090	$Fe(OH)_3 + S^{2-} + 3H^+ + e^- = FeS + 3H_2O$
-0.707	-1.213	-1.462	$FeOOH + S^{2-} + 3H^+ + e^- = FeS + 2H_2O$
-0.709	-1.219	-1.472	$Fe_2O_3 + 2S^{2-} + 6H^+ + 2e^- = 2FeS + 3H_2O$
-0.695	-0.769	-0.780	$FeS_2 + 2H^+ + 2e^- = FeS + H_2S$
-0.542	-0.568	-0.554	$FeS_2 + H^+ + 2e^- = FeS + HS^-$
-0.576	-0.530	-0.465	$FeS_2 + 2e^- = FeS + S^{2-}$
-1.016	-1.202	-1.333	$FeS_2 + 4H^+ + 2e^- = Fe^{2+} + 2H_2S$
-0.612	-0.238	0.002	$FeS_2 + 2H_2O + 2e^- = HFeO_2^- + 2S^{2-} + 3H^+$
-0.592	-0.375	-0.246	$FeS_2 + 2H_2O + 2e^- = Fe(OH)_2 + 2S^{2-} + 2H^+$
-0.457	-0.038	0.224	$3FeS_2 + 4H_2O + 4e^- = Fe_3O_4 + 6S^{2-} + 8H^+$
0.243	0.253	0.244	$Fe^{2+} + 2S^0 + 2e^- = FeS_2$
Concentrations of 10^{-6} M and pH 12 were used in the preparation of this data.			

An OCP more anodic than the E_P yet below the transpassive region indicates the formation of a more stable surface corrosion product and a reduction in the corrosion current density at the metal surface. However, the more stable film may continue to corrode even though at a very low rate compared to the metal without passive film on the surface. At the active-passive transition, within a narrow range of potentials, metals may actively corrode or a passive film may form at the metal surface. In the solutions tested, the OCP for A516-Gr70 was commonly found in the active-passive region. As shown in Figure 16, the determination of measured OCP values shows that there is no linear correlation of corrosion rate for carbon steel A516-Gr70 which is expected of an activation controlled reaction, iron oxidized to ferrous or ferric ions. Although a similar range of OCP values, from approximately -0.40 to -1.15 V (SCE), was measured a significant variation in corrosion rate was realized with increased temperature. As predicted by the Nernst equation,[8] increased temperature will cathodically shift the OCP and may result in the activation of metal in the active-passive region.

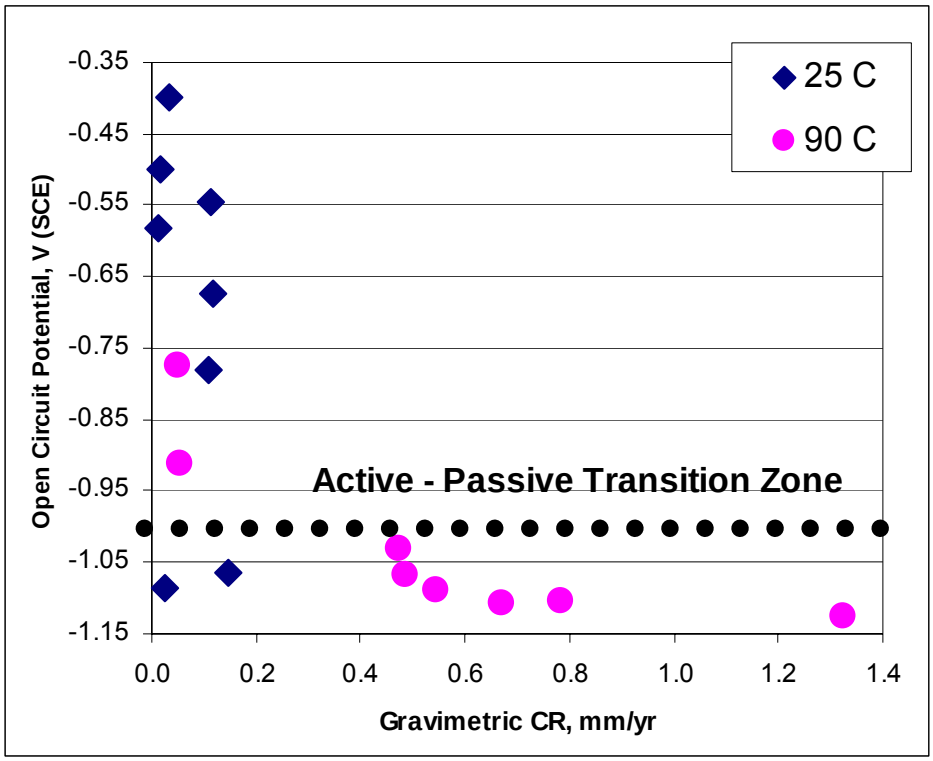

Figure 16. Open circuit potentials and the corresponding measured corrosion rate for carbon steel A516-Gr70 in tested concentrations of sulfide containing caustic solutions at 25°C and 90°C.

Depending upon whether the metal has a tendency to form a protective passive film on the surface or a soluble product, the corrosion rate at a given potential can vary significantly. Figure 16 shows OCP for carbon steel A516-Gr70 versus gravimetrically measured corrosion rate, mm/yr, under different solution concentrations at 25°C and 90°C. It is clear from the results that

above approximately -1.00 V (SCE) the corrosion rates were relatively low whereas below -1.00 V (SCE) the rate of corrosion for carbon steel increased significantly. This behavior corresponds to the formation of Fe_3O_4 in the Pourbaix diagrams,[80] Figures 17 and 18, and is analogous to potentiodynamic polarization behavior of carbon steels in high pH environments where passivity is generally stable above the passivation potential.

Figures 17, 18, and 19 show a potential-pH diagram for a Fe-S-H_2O system at 25°C, 100°C, and 170°C, respectively, derived by a chemical equilibrium and reaction software database.[82] This diagram shows the thermodynamically favored phases that exist for Fe-S-H_2O systems at different pHs and potentials. At the pH range tested, solid iron oxide formations of Fe_2O_3 and Fe_3O_4, and soluble anion compounds FeO_2(-a) and $HFeO_2$(-a) are expected to form depending upon the potential. Comparing Figure 16 with the Pourbaix diagram[80] in Figure 17 indicates that at a pH range of 12.5 – 14, typical for most pulping liquors, the stable phase at the carbon steel surface may be a Fe_2O_3 or Fe_3O_4 film or it can be soluble $HFeOO^-$ ions.

These results can be used to develop an on-line corrosivity probe to monitor the OCP of the system and relate it to the expected corrosion rate of carbon steel A516-Gr70 in pulping liquors and other similar process streams. Environmental conditions such as temperature or changes in solution concentration may stabilize OCP in the region of a soluble product which may lead to higher corrosion rates. If an insoluble film is stable the corrosion rates are low. The protective nature of passive films depends on their stability and the ionic or electronic conductive properties of the passive film. As shown in Figures 17 and 18 the formation of FeS is not thermodynamically favorable above a pH of 11.5. Ionic species of soluble sulfur compounds HS_2O_8(-a), HS_2O_6(-a), HS(-a), and S(-2a) are also not thermodynamically favored above a pH of 10.5.

However, work by Tromans[72] has shown that sulfur is incorporated in Fe_3O_4 film in the region of critical current density, below the active-passive transition region of the polarization curve. Similar results were found in this study. XRD analysis was performed on surface corrosion products of carbon steel A516-Gr70 samples tested in solution at 170°C. Figure 20 illustrates the diffraction pattern for the iron oxide corrosion product at 100 g/L sodium hydroxide at 170°C. A summary of the phases identified for all tested samples

is shown in Table 6 and diffraction patterns are given in Appendix A – X-Ray Diffraction Analysis. The inclusion of multiple crystalline layers and the incorporation of multiple compounds within the same layer were realized within the surface corrosion product of tested samples. It is clear from the results shown in Appendix A and Table 6, that surface films in solutions with sulfide present, contained FeS along with Fe_2O_3 and Fe_3O_4.

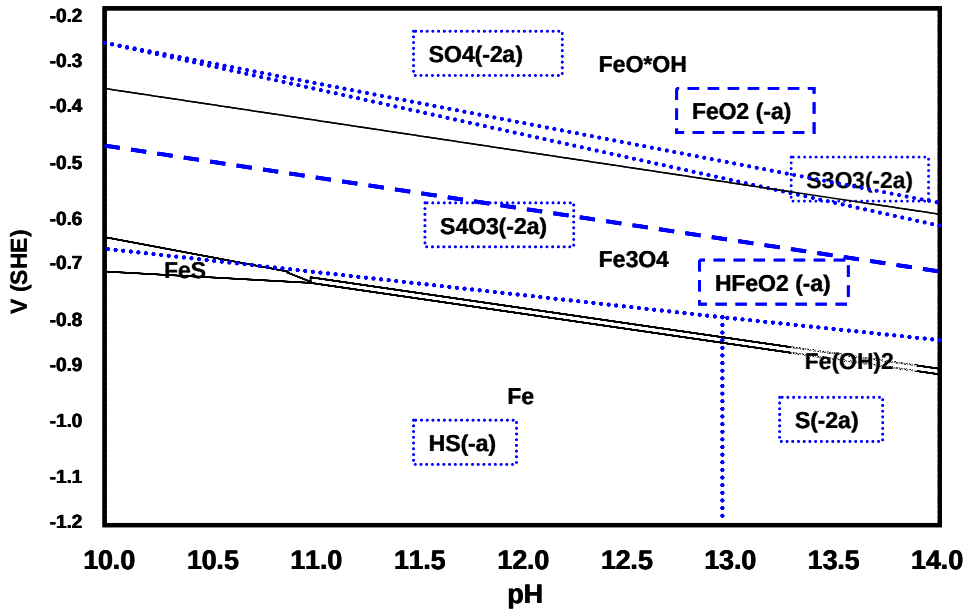

Figure 17. Potential-pH diagram, Pourbaix diagram, of Fe-S-H2O system at 25°C calculated with a stand alone database.[80]

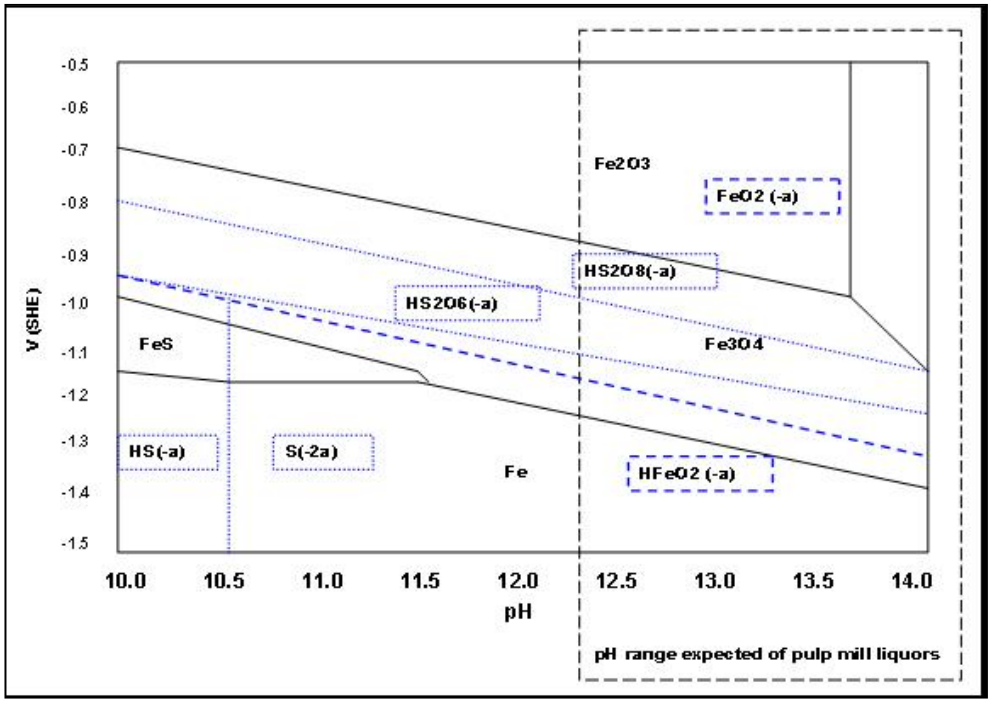

Figure 18. Potential-pH diagram, Pourbaix diagram, of Fe-S-H2O system at 90°C calculated with a stand alone database.[80]

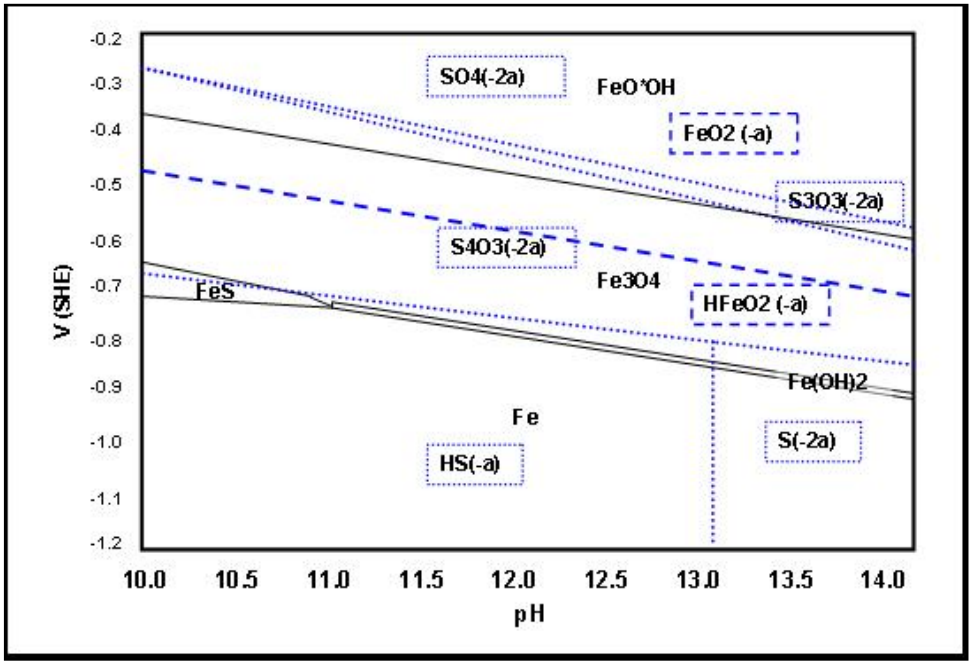

Figure 19. Potential-pH diagram, Pourbaix diagram, of Fe-S-H2O system at 170°C calculated with a stand alone database.[80]

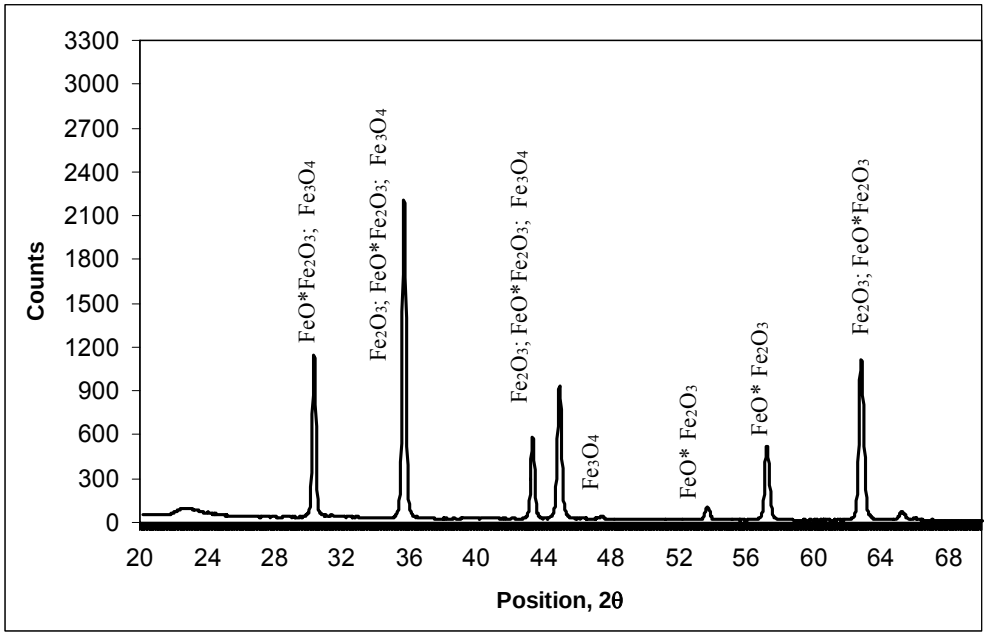

Figure 20. X-Ray Diffraction of surface corrosion product on carbon steel A516-Gr70 in 100 g/L NaOH at 170°C.

Table 6. Crystalline surface corrosion product for carbon steel A516-Gr70 in sulfide containing caustic solutions at 170°C.

NaOH g/L	Na_2S g/L	CR mm/yr	Peaks Identified with XRD
100	0	0.28	{Fe_2O_3, $FeO*Fe_2O_3$, Fe_3O_4}
200	0	1.05	{Fe_2O_3, FeOOH, Fe_3O_4}
0	37.5	0.06	{FeS, Fe_3S_4, Fe_2O_3, Fe_3O_4}
100	37.5	8.68	{FeS, Fe_3S_4, Fe_2O_3, Fe_3O_4}
200	37.5	6.23	{Fe, FeS, Fe_2O_3, Fe_3O_4}
0	75	2.24	{FeS, Fe_3S_4, Fe_3O_4}
100	75	11.71	{FeS, Fe_2O_3, Fe_3O_4}
200	75	8.70	{FeS, Fe_9S_8, Fe_3O_4}

6.3.5. CONCENTRATION EFFECTS AT INCREASED TEMPERATURE

To further investigate the affect of increasing temperature on liquor corrosivity towards carbon steel A516-Gr70 the corrosion rate at 170°C was plotted with increasing hydroxide concentration at constant sulfide content, shown in Figure 21 with complete hydrolysis according to Equation (19). As a result of complete hydrolysis the hydroxide concentration increases by nearly 40 g/L with the addition of 75 g/L of sodium sulfide. Although solution equilibrium will be reached below 100% hydrolysis, it is necessary to point to the increase in caustic with the addition of sulfide. An increase in sodium sulfide from

37.5 to 75 g/L at 170°C and constant initial hydroxide concentration increases the rate of corrosion experienced by carbon steel A516-Gr70. Yet, an increase in added hydroxide from 100 to 200 g/L reduces the corrosion rate when in the presence of initial sulfide at both 37.5 and 75 g/L. The reduction in corrosion rate which occurs at increased hydroxide levels in the presence of sulfide seems to be due to the formation of a more stable film, such as Fe_3O_4, on the metal surface and a corresponding passivation of carbon steel A516-Gr70.

In the presence of sulfide, the diffusion of iron ions from the metal surface at higher concentrations of hydroxide may be limited due to the plugging of passages, or interstitial spaces, within the lattice structure by sulfur compounds.[83] The incorporation of non-stoichiometric sulfur in the anodic vacancies instead of oxygen changes local conductivity and may act as a destabilizing force to the film.[72] The local plugging of passages has been suggested by Shoesmith et al[83] as a mechanism of film passivation.

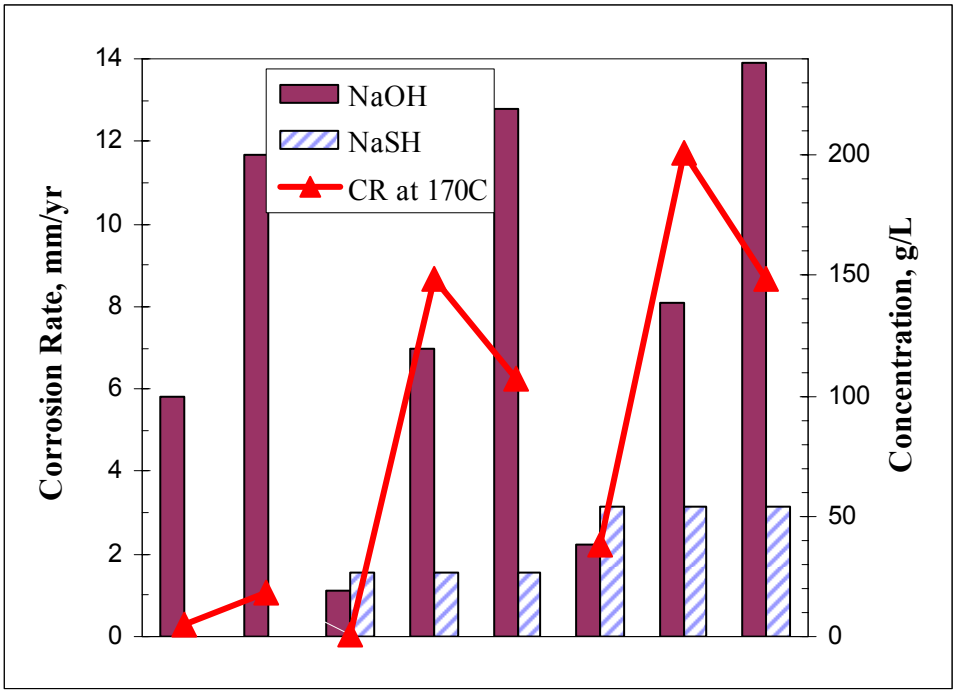

Figure 21. Corrosion rate of A516-Gr70 carbon steel at 170°C as a function of increasing sodium hydroxide concentration at constant sodium sulfide, given as sodium hydrosulfide, $Na_2S + H_2O \rightarrow NaSH + NaOH$.

At 100 g/L sodium hydroxide and both 37.5 and 75 g/L sodium sulfide the OCP may stabilize in a region of a soluble product while an increase in hydroxide shifts the potential to a region of greater stability and a reduction in the corresponding corrosion rate. In the presence of sulfide, the incorporation of FeS into the lattice structure of the surface corrosion product changes the conductivity of the more stable Fe_3O_4. Additionally the formation of multiple

crystalline compounds in the surface corrosion product may result in distinctly different electrical properties across the metal surface and non-uniform corrosion of the metal.

Most of the previously published work[28,30,31,32,33,65,69,70,71,72,73,74,83] studied corrosion rate of carbon steels as a function of specific environmental variables such as temperature, concentration of hydroxide and/ or sulfide and other oxidized sulfur species. Conclusions from previously published studies are contradictory and cannot be compared as exact compositions of solutions were not similar. In the present work it was seen that the affect of all environment parameters on corrosivity could be explained by measuring OCP. The change in OCP determines thermodynamic tendency for a metal to form either a soluble product and corrode or to form an insoluble product which may form a passive film on the surface. Pourbaix diagrams[80] for the selected system, shown in Figures 15, 16, and 17, show thermodynamically stable products at a given pH and potential for iron or carbon steel. Comparison of experimental results with Pourbaix diagrams, in Figures 15 and 16, indicate that, under tested conditions, when OCP was in a region where soluble products are thermodynamically stable, below -1.00 V (SCE), carbon steel A56-Gr70 experienced higher corrosion rates ~0.5 to ~1.3 mm/yr. However,

when the OCP was in the region of thermodynamic stability for insoluble product formation or above the active-passive transition, above -1.00 V (SCE), carbon steel A516-Gr70 realized relatively low rates of corrosion, below ~0.1 mm/yr.

6.4. CONCLUSIONS

- An increase in temperature at a given constant concentration of sulfide containing caustic solution increases the corrosion rate for carbon steel A516-Gr70.

- At all temperatures tested increased sulfide content increased the corrosion rate for carbon steel A516-Gr70.

- At the active-passive transition, a shift in OCP due to a change in concentration or temperature may result in carbon steel A516-Gr70 moving to a region of greater stability, with a reduction in corrosion rate, or to a region of greater solubility, which may increase the corrosion rate.

- In the presence of sulfide the incorporation of FeS into the Fe_3O_4 lattice structure may change the conductivity of the surface film and

destabilize the surface corrosion product leading to increased corrosion rates for carbon steel A516-Gr70.

- An increase in corrosion rate results in these environments due to a shift in OCP values below approximately -1.00 V (SCE). Any parameter change that will result in this OCP shift may change the corrosion behavior of carbon steel. This can provide an indication marker for correlating expected shifts in corrosion rate with rest potentials below the active-passive transition potential.

- In tested environments, OCP values above approximately -1.00 V (SCE) showed relatively low corrosion rates, below ~0.2 mm/yr.

- XRD characterization of surface corrosion products in sulfide containing caustic solutions was not a sufficient tool for the evaluation of passivation and activation of carbon steel A516-Gr70 in sulfide containing caustic solutions.

Chapter 7

ROLE OF WOOD EXTRACTIVES IN BLACK LIQUOR CORROSIVITY

7.1. INTRODUCTION

From digesters to recovery boilers, pulp mill equipment is exposed to an organic waste liquor environment called black liquor (BL). The composition of BL depends on the pulping process as well as on the wood species used in the pulp mill. Variability in the process and wood source may result in high corrosivity waste liquors. Prior research has demonstrated corrosion rates of carbon steel in pulp mill equipment ranging from <0.03 mm/yr to >2.54 mm/yr, depending on wood species pulped.[37,38] The composition of the organic portion of BL depends largely on the wood species used. Organic components in BLs come from extractives in the wood chips or are generated from the degradation of lignin and other wood constituents during the pulping process. Depending upon the wood species used, some BL constituents have been identified to increase the corrosivity of BLs whereas others have been found to act as corrosion inhibitors.

Inhibitors by definition retard system corrosion by changing the local environment through the formation of protective precipitates or the removal or inactivation of aggressive constituents. Inhibitors may also form protective films or surface corrosion products on the metal surface retarding corrosion. Activators, on the other hand, increase corrosion by destabilizing protective films or through the formation of soluble metal chelates with metal components. For both activators and inhibitors, solution composition and potential, pH, metal surface, and chemical structure are interrelated and are responsible for the efficiency of the activation or inhibition of corrosion.

The demonstration of wood species controlling the corrosivity of BLs suggests that wood chips contain chemicals, specifically organic chemicals, which impact the mechanisms of activation and inhibition within the liquors. As hundreds of organic compounds have been identified[35,36] in various BLs the data also suggests a large number of chemicals may be involved in the controlling mechanism. An investigation of the synergistic or antagonistic affects of all currently identified organic chemicals in BL would be a breathtaking endeavor. Fortunately researchers have identified catechol as an activator of corrosion in BL.[34,37] Catechol is a common phenol breakdown product primarily ascribed to lignin but can also be derived from other

polyphenolic compounds such as tannin. In fact the impact of catechol in synthetic BL, containing only inorganics, and BL has shown significant deviation, with the organic compounds in BL acting in a synergistic fashion to activate corrosion.

Catechol activates corrosion, and is a breakdown product of lignin which varies in degree of polymerization from species to species with basic breakdown components and concentrations remaining similar. This also suggests that other compounds in BLs must play a role in inhibition. Species to species variability in BL corrosion is also unlikely due to cellulose and hemicellulose, which have similar chemical structure and breakdown products amongst trees. Deductively organic extractives, which vary in type and concentration from species to species and in concentration between juvenile and mature wood, are the most likely source for compounds exhibiting inhibitory properties in BLs.

Examining organic extractives amongst species provides several difficulties. The first involves pulping chips from the wood species, chemically analyzing the BL, and quantitatively comparing Gas Chromatography/ Mass

Spectrometry (GC/MS) data amongst species with the respective corrosion rates for the individual BLs. Identifying specific concentration changes among several hundred compounds and relating this data to corrosion rate, while keeping in mind the likelihood of synergistic effects, is wrought with inefficiencies. A second difficulty in organic extractive evaluation is using already identified native compounds as additives to BLs. Although a very sterile concept this too is impractical as many compounds are simply unavailable in their native state or identified for specific tree species. A third difficulty is extraction of organics. Commonly used extraction techniques for tree species specific organic analysis include finely ground sawdust and various organic solvents. The use of a sawdust technique may result in a questioning of the comparability of BLs from wood chips and the data from sawdust due to enhanced diffusion and thus expected increases in organic extractives as well as possible material losses. Yet, an even more serious concern is the removal of the utilized organic solvent from the extractives at the conclusion of the extraction procedure. Residual benzene, toluene, acetone, or chloride may negatively impact corrosion tests.

7.2. EXPERIMENTAL PROCEDURES

A schematic of wood chip extraction, wood chip pulping and corrosion testing schemes used in this study is shown by the flowchart in Figure 22.

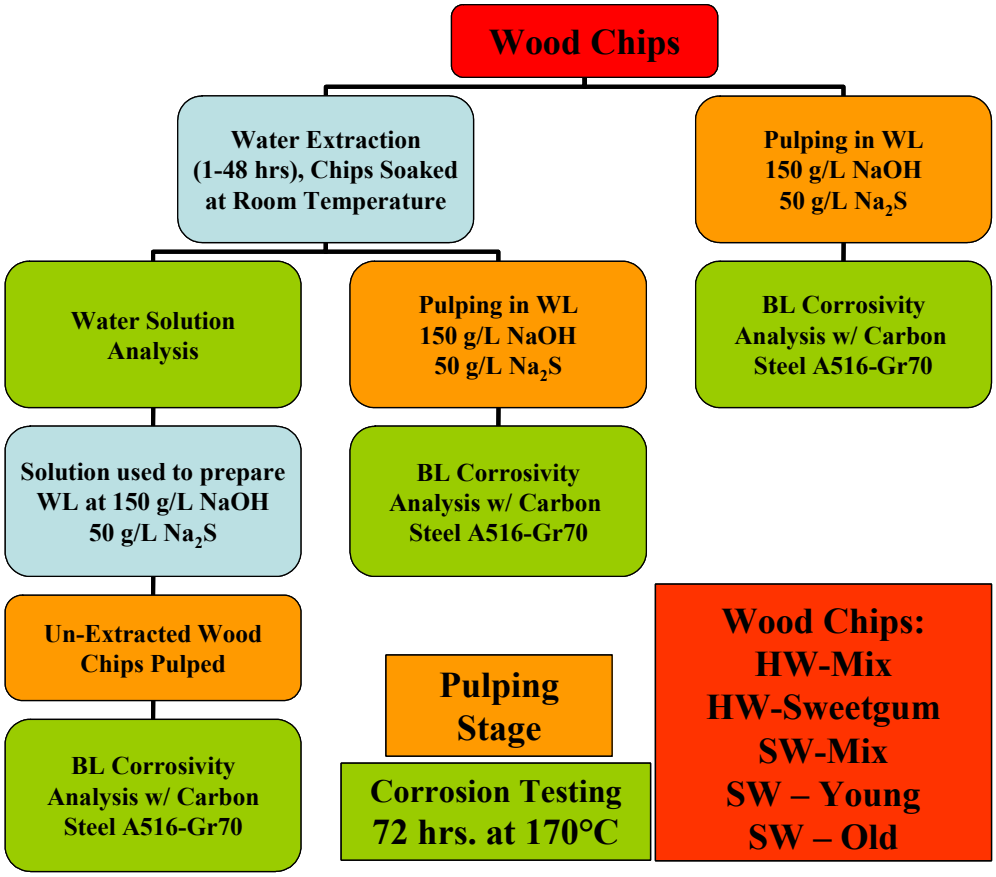

Figure 22. Experimental flowchart for wood extractives corrosion analysis.

7.2.1. RAW MATERIALS

Five groups of wood samples were selected for this study, young (14-16 years) and old (30+ years) softwood loblolly pine (*Pinus taeda*) harvested from a southern plantation, a southern hardwood sweetgum (35 years, *Liquidambar*

styraciflua), a mixture of southern SWs and a mixture of southern HWs used in a southeastern mill. Analysis of southern HW sweetgum is provided in Appendix - B Effect of Wood Chip Storage and Extraction on a Southern Hardwood Sweetgum. The choice of young and old wood chips utilized in this study allowed for an investigation into the affects of tree age, more specifically the concentration of juvenile wood, on BL corrosivity. Juvenile wood is expected to have a greater concentration of organic extractives than that of mature wood, thus the older a tree the lower the concentration of juvenile wood corresponding to an overall decrease in the concentration of extractives.[84,85] The mixed wood chip batches were not analyzed for individual species content.

7.2.2. WOOD CHIP SELECTION AND PULPING

Selected wood chips of 8 – 10 mm thickness from the five groups were pulped in the laboratory. The chemical makeup of the pulping liquor, WL, was 150 g/L of sodium hydroxide and 50 g/L of sodium sulfide. The WL and wood chips, in 4:1 ratio, were added to a laboratory batch digester for pulping. The pulping temperature was ramped to 170˚C over 90 minutes and maintained at temperature for 60 minutes for SW and 45 minutes for HW. The temperature steps were chosen to allow for similar residual inorganic concentrations at the

end of each cook. BL was collected and stored in one-liter plastic containers, completely filled to minimize oxidation during transportation. The BL was transferred to an autoclave for corrosion testing.

7.2.3. GRAVIMETRIC CORROSION INVESTIGATION

Corrosion tests were carried out in 4-liter duplex stainless steel autoclaves. All corrosion tests in this study were gravimetric and carried out at 170˚C for 72 hours. At least two metal samples, made out of A516-Gr70 carbon steel, were exposed in each test to check the reproducibility of our results. Metal samples were polished to 1.2-μm finish and cleaned with acetone. Each sample was weighed and its area measured before mounting on electrically isolated Teflon testing racks to eliminate galvanic effects. Upon conclusion of a test, the samples were removed from the autoclave and placed on a drying rack for further analysis. Reaction products on the metal surface were removed and final weight determined to calculate material loss and corrosion rate under each condition.

7.2.4. WOOD EXTRACTIVE SEPARATION

The technique chosen for the investigation of the role of organic extractives in BL corrosivity was the use of wood chips submerged in cold water. Although the water extraction does involve some hydrolysis of the wood chips which may result in the breakdown of some compounds, such as lignin, the impact of the cold water extraction is expected to be minor. Additionally, a water extraction provides for the ability to pulp the wood chips, adjusting for added water content, resulting in comparison data of wood chips from the same tree with and without extractive treatment.

In a series of tests, water was used to extract organics from selected wood chips generally following TAPPI Test Method T207 om-93.[86] Extractions were performed by fully submerging wood chips in water at room temperature for test duration. Upon completion of extraction, chips were removed from the solution and excess water was removed. Extractions were performed in this manner to investigate the correlation between wood-specific organics and BL corrosivity and the relation to water extracted organics. Wood chips were extracted in water at room temperature for 1, 6, 24, and 48 hours to verify time dependent diffusion of the extractives. The extracted solution was placed in plastic bottles and stored in a cold room at 4˚C until further testing. Wood

chips after extraction, extracted chips, were immediately used for pulping to produce BL with reduced extractive content. The resulting BL from the extracted chips has been referred to as extracted BL.

7.2.5. WOOD EXTRACTIVE ANALYSIS

Wood extractives removed by the water submersion method were analyzed using capillary ion electrophoresis, GC/MS, and total organic carbon content. An aliquot of approximately 0.5 mL of cold water wood extracts was taken for ion electrophoresis analysis. The instrument was a Waters Capillary Ion Analyzer equipped with a hydrodynamic sampling system and indirect UV measurement at 254 nm. The analyzer was operated with a buffer electrolyte of 2.75 mM n-tetradecyltrimethylammonium bromide, 5 mM sodium chromate, 10 mM 2-(N-cyclohexylamino)ethane sulfonic acid at a temperature of 25°C and voltage of 14 kV.

Aliquots of cold water wood extracts for GC/MS analysis contained an internal standard, 2.8 mg heptadecanoic acid in 1 mL dichloromethane, and were freeze dried. The dried residues were derivatized with the addition of MSTFA (N-Methyl-n-trimethylsilyl-trifluoroacetamide). The GC/MS

instrument was a Hewlett-Packard 5890 II Gas Chromatograph equipped with a Hewlett-Packard 5971A Mass Selective Detector. A DB-5 J&W capillary column (60 m x 0.25 mm i.d., 0.25 μm film thickness) was used for the separation. The chromatograph was operated with an initial temperature of 150˚C and initial time of 2 minutes. The temperature was raised at 10˚C per minute with a final temperature of 275˚C and final time of 30 minutes. The injection temperature was 250˚C with a solvent delay time of 8 minutes. The identification of individual compounds was made by comparison of mass spectra from the test sample with spectra from chemical standards and the laboratory database. The concentration of the identified compound was calculated based on the area of the selected ion peak and the response factor derived from known pure compounds.

Total organic carbon content was determined by using a UIC carbon analysis system. To identify inorganic carbon the system monitored the carbon dioxide generated from the acid degradation of carbonate and measured the total carbon content by monitoring the carbon dioxide generated from the combustion of chemical standards at 900°C. The concentration of total organic carbon was obtained from the difference between the total carbon content and the inorganic carbon content in solution.

In further tests, identified extractives were also added to BL to investigate their role in corrosion activation or inhibition of carbon steel A516-Gr70 in BL. Additions were carried out in BL during autoclave induction to minimize oxidation of the liquor. These tests were performed to evaluate the role of selected compounds in BL corrosivity.

7.2.6. ELECTROCHEMICAL TESTING IN EXTRACTED BLACK LIQUOR

The potentiodynamic polarization method as described in Appendix – C Electrochemical Effects of Water Extraction was used to investigate the effect of extractive addition on the polarization behavior of carbon steel A516-Gr70. The addition of chemicals to BL was carried out during autoclave induction to minimize oxidation of the liquor. In these tests, the potential was scanned at a rate of 1 mV/s at 25°C and 90°C using a standard calomel electrode as a reference electrode. Current flowing through the corrosion cell was recorded at each potential. A platinum counter electrode was used in these tests.

7.3. RESULTS AND DISCUSSION

7.3.1. WOOD SPECIES AND AGE DEPENDENT CORROSION

Corrosion rates for A516-Gr70 carbon steel samples tested in SW and HW BLs are listed in Table 7 and plotted in Figure 23. It is clear from these results

that BL from the pulping of the HW mixture (HW-Mix) was less corrosive (~0.09 mm/yr) to carbon steel compared to the BL obtained from SW. Even within SW species, the BL from young pine resulted in a corrosion rate of ~1.55 mm/yr compared to a corrosion rate of ~6.23 mm/yr for old pine at 170˚C after 72 hours of exposure. BL from a mixture of SW (SW-Mix) species produced a corrosion rate of ~9.13 mm/yr for A516-Gr70 steel at 170˚C after 72 hours of exposure. From this data it may be possible to broadly generalize rates of corrosion for HW and SW species studied based on their organic extractives content. HWs which typically have a higher concentration of extractives, resulted in the lowest corrosivity in our tests. In comparison, SWs whose extractive content has been shown to decrease with age showed an approximately four fold increase in corrosivity when pulping young versus old pine.[39] As shown in Figures 24 and 25, the HW-Mix BL exposure resulted in very low corrosion rates and a clear iron oxide film on the metal surface similar to that of the untested coupon blank.

Table 7. Corrosivity of black liquors for *Pinus taeda* and mixtures of softwoods and hardwoods.

Wood Source	Wood Species	Corrosion Rate (mm/yr)
Mill A	SW-Young	1.55
Mill A	SW-Old	6.23
Mill B	SW-Mix	9.13
Mill B	HW-Mix	0.09

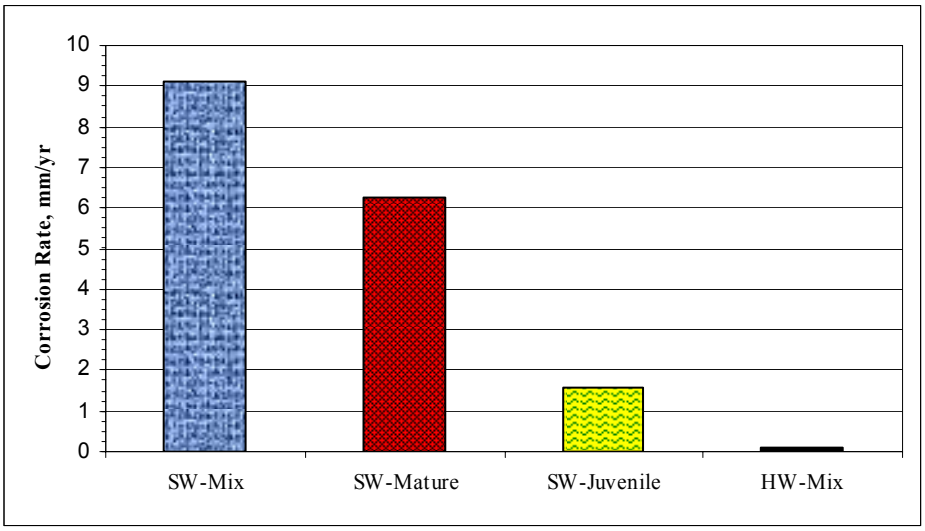

Figure 23. Corrosivity of black liquors for *Pinus taeda* and mixtures of softwoods and hardwoods to carbon steel A516-Gr70 at 170°C for 72 hours.

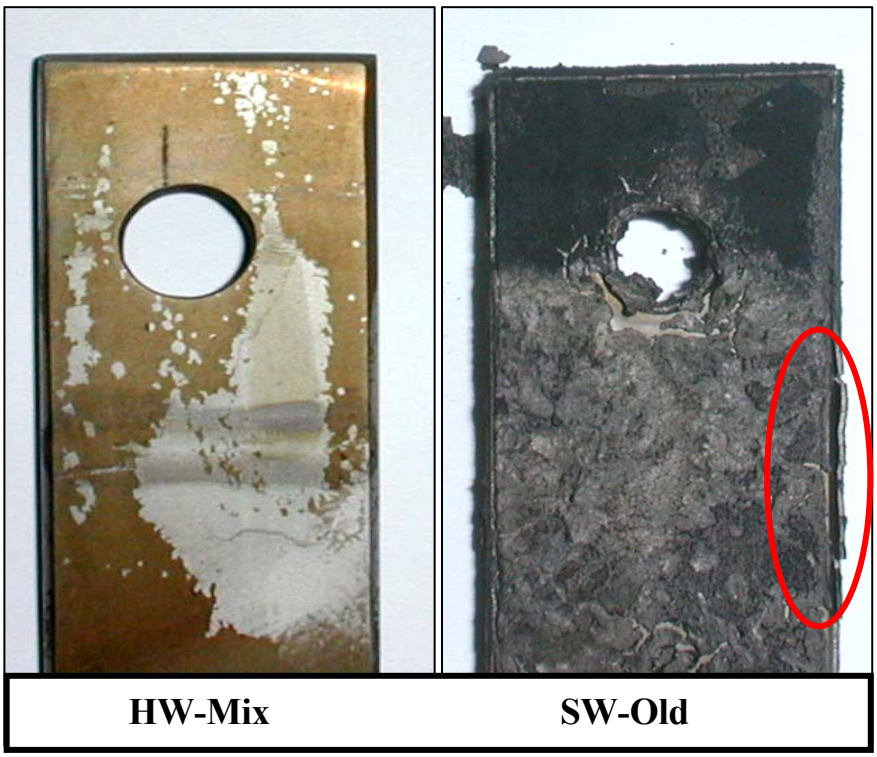

Figure 24. Carbon steel (A516-Gr70) coupons tested in mixed hardwood and old softwood black liquors at 170°C for 72 hours. The corrosion product film is highlighted for SW-Old.

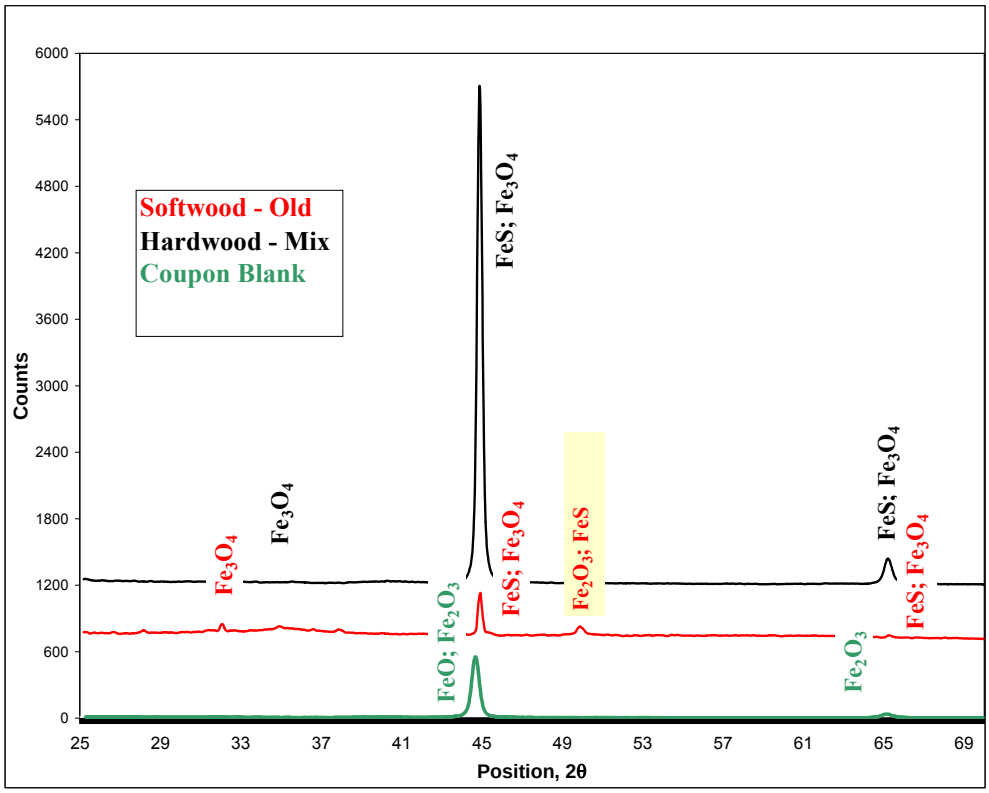

Figure 25. X-Ray Diffraction of surface corrosion product on carbon steel A516-Gr70 in Hardwood and Softwood black liquors. Diffraction pattern of a carbon steel sample prior to testing (Coupon Blank) is included.

7.3.2. EXTRACTIVE DEPENDENT CORROSION IN BLACK LIQUOR

The correlation between the relative corrosivity of BL and water extractable components in wood was further investigated. Water extractable organic constituents from the wood chips were removed using a modified cold water extraction method for 6 and 48 hours. Wood chips, after removal of

extractives, were pulped and corrosion tests were carried out in the resulting BL. Table 8 shows the corrosion rate for A516-Gr70 carbon steel in BL of extracted wood chips tested at 170°C for 72 hours. Pulping after a 6 hour extraction for HW-Mix chips led to an increase in the BL corrosivity of nearly twenty times compared to the corrosion rates for unextracted BL, as shown in Table 7 and Figure 23. The corrosivity of extracted HW-Mix BL was similar to the corrosion rate for unextracted young SW (SW-Young). After a 48 hour extraction, BL from HW-Mix chips caused carbon steel to corrode at ~5.08 mm/yr compared to ~0.09 mm/yr for liquors without extraction. HW-Mix wood chips were treated with a 48 hr water extraction and BLs tested for corrosivity towards carbon steel A516-Gr70 on three separate occasions during this study, corrosion rates for all tests were above 5 mm/yr. SW-Young wood chips were also extracted to see the affect of water extracted organics on its BL corrosivity. Liquors for SW-Young and HW-Mix, after a 48 hr extraction, showed comparable rates of corrosion and approached that of unextracted old SW (SW-Old BL), ~6.23 mm/yr. From this data it is evident that the removal of organic extractives from HW-Mix as well as SW-Young wood chips had a significant effect on increasing the overall corrosivity of resulting BLs.

Table 8. Corrosivity of black liquors prepared with chips having undergone cold water extraction.

Wood Source	Wood Species	Extraction Time (hr)	Corrosion Rate (mm/yr)
Mill B	HW-Mix	6	1.74
Mill B	HW-Mix	48	5.08
Mill A	SW-Young	48	5.42

7.3.3. WATER EXTRACTION AND BLACK LIQUOR CORROSION

To examine the effect of extractives on the corrosivity of carbon steel, both HW-Mix and SW-Mix chips were extracted for 48 hours. The corrosivity of the resulting extracted solution, containing organic wood extractives, from both chip groups was tested individually by exposing A516-Gr70 coupons in these solutions at 170°C for 72 hours. HW-Mix and SW-Mix extracted solutions exhibited low corrosivity towards carbon steel, as shown by the results in Table 9. Comparing results in Tables 8 and 9 indicates that the extraction solution from both HW-Mix and SW-Mix were relatively non-corrosive with corrosion rates ranging from 0.03 to 0.05 mm/yr. The removal of water soluble extractives from the wood chips, however, resulted in a significant increase in the corrosivity of resultant BLs. These results point to the inhibitory effect of chemicals removed from the chips by water extraction.

The impact of the pulping process on extractives was further examined. HW-Mix chips contained more extractives and their BLs were found to be less corrosive than that for SWs. Tests were done to see if water soluble extractives from the HW-Mix chips could be used to reduce corrosivity of the SW BLs. HW-Mix chips were extracted for 48 hours and the extracted solution was used in the preparation of WL (150 g/L of sodium hydroxide and 50 g/L of sodium sulfide) for the pulping of SW-Mix chips. A516-Gr70 carbon steel coupons were tested in the resultant BL at 170°C for 72 hours. The corrosion rate for this liquor, with HW-Mix extractives, was ~3.32 mm/yr compared to the corrosion rate of ~9.13 mm/yr in SW-Mix BL, without any addition of extractives, shown in Table 7. Suppression of SW-Mix corrosivity by greater than 60% using HW-Mix extractives further indicates that these chemicals have an inhibitory effect towards carbon steel corrosion under tested conditions. These results also indicate that water extracted chemicals may not completely degrade during the pulping process and may effectively inhibit carbon steel corrosion in BL, depending on their concentration in the BL.

Table 9. Corrosivity of organic extractives in solution and their effect on softwood black liquor corrosivity.

Test Solutions	**Corrosion Rate (mm/yr)**
HW-Mix Extraction Sol. (48 hr)	0.03
SW-Mix Extraction Sol. (48 hr)	0.05
BL of SW-Mix *(pulped with added HW-Mix Extraction Sol.-48 hr)*	3.32

7.3.4. ANALYSIS OF ORGANIC EXTRACTIVES IN WATER EXTRACT

An attempt was made to identify the chemicals in SW-Young and HW-Mix extractives that may affect the rate of corrosion in BL, water extractions were carried out for up to 48 hours. The characterization of water extracted chemicals was done using GC/MS with a standardized library database. Results from the chemical analysis of SW-Young and HW-Mix extractives with GC/MS are shown in Tables 10 and 11, respectively, with their molecular structure given in Figure 26. Analysis by HPLC/MS has also shown signatures of catechols and tannins present in the water extracted solutions.

Table 10. Composition of water extracted chemicals from young softwood *Pinus taeda* chips (mg/L).

	Concentration (mg/L)	
Extraction Time	**24 hr**	**48 hr**
Fatty Acids		
Palmitic acid	0.16	0.2
Linoleic acid	0.01	0.01
Oleic acid	0.05	0.1
Stearic acid	0.08	0.15
Resin Acids		
Pimaric acid	0.01	0.03
Isopimaric acid	0.10	0.17
Palustric acid	0.05	0.12
Abietic acid	0.73	1.01
Dehydroabietic Acid	9.42	10.05
Neoabietic acid	0.06	0.14

Table 11. Composition of water extracted chemicals from a mixture of hardwood chips (mg/L).

	Concentration (mg/L)			
Extraction Time	**1 hr**	**6 hr**	**24 hr**	**48 hr**
Hydrocarbons				
Pinitol	0.0	1.38	0.58	2.16
1,2,3-trihydroxybenzene	0.0	0.0	6.68	9.69
Fatty Acids				
Palmitic acid	0.0	0.36	0.48	0.48
Stearic acid	0.19	0.22	0.18	0.27
Resin Acids				
Sitosterol	0.0	0.0	0.0	12.88
Stigmastanol	0.0	0.0	0.0	0.98

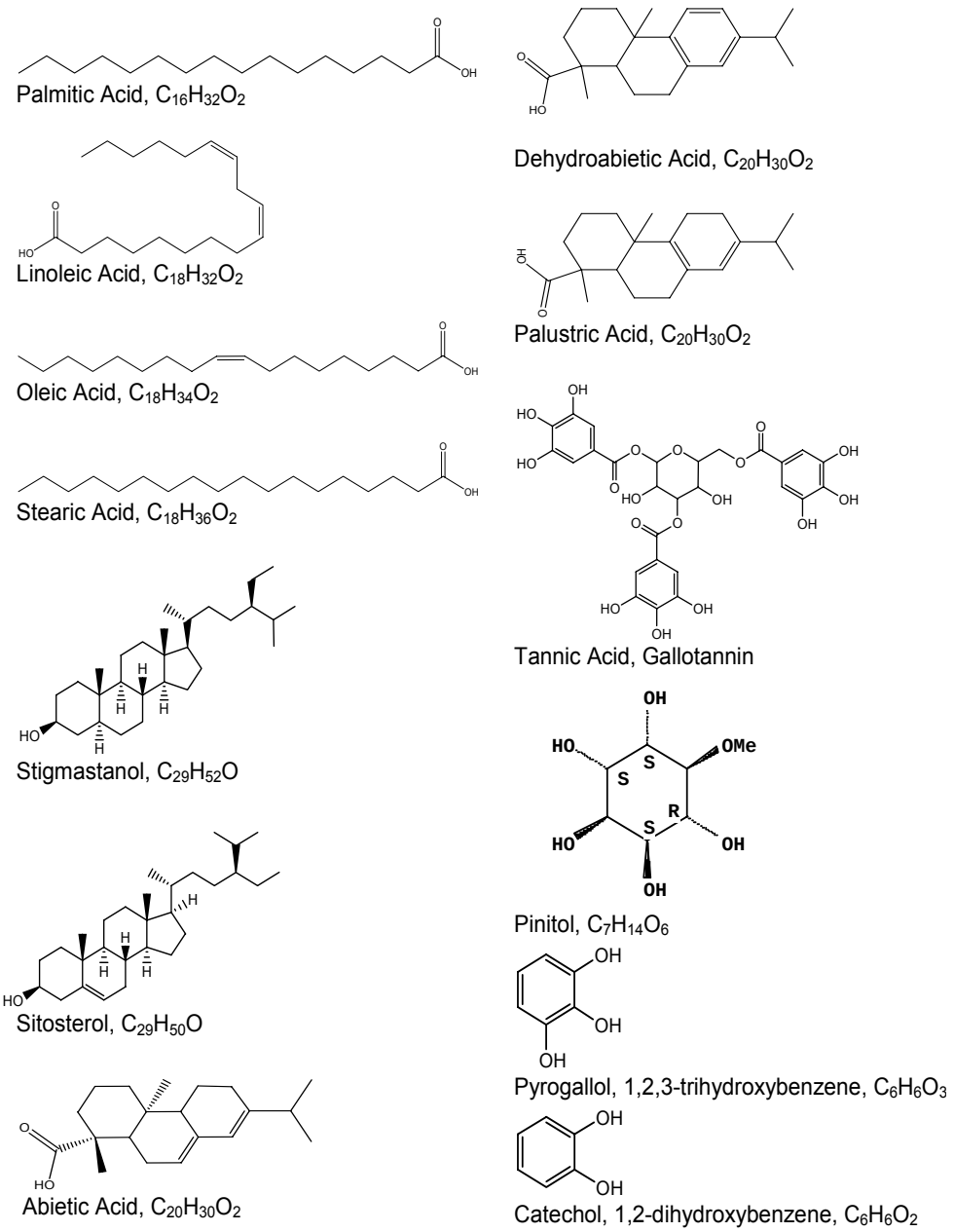

Figure 26. Structures of chemical compounds identified in extraction solutions.

Analysis of the SW-Young and HW-Mix extracts confirmed the presence of long chain fatty acids and resin acids (sterols) in solution. However, species to species variability in organic compounds may have an inhibitory effect, such as the low corrosion rates experienced with Eastern Cottonwood (*P. deltoides*) and Sweetgum (*L. styraciflua*),[37] or an activation effect, such as the increased rates of corrosion for Western Red Cedar (*T. plicata*) and Douglas Fir (*P. taxifolia*),[34] on the corrosivity of their respective BLs.

In SW-Young, resin acids were identified as pimaric acid, palustric acid and abietic acids. In HW-Mix, hydrocarbons α-pinitol and pyrogallol (1,2,3-trihydroxybenzene) were seen with resin acids identified as β-sitosterol and stigmastanol. Sterol esters containing sitosterol and stigmastanol have been seen in Kraft BL[60] and all identified resin acids have been shown to participate in BL tar formation. The ability of long chain fatty acids, hydrocarbons, and resin acids to form esters may enable these compounds to bind to the metal surface potentially covering adjacent sites. Additionally, inhibitors anchoring to the metal through their polar group, with the nonpolar tail vertical to the surface, would allow hydrocarbons to adsorb onto the nonpolar tail, illustrated in Figure 27, increasing both film thickness and hydrophobic barrier effectiveness for corrosion inhibition.[87,88]

Inhibitor film stability is the result of a number of interlaced factors involving both the hydrophobic hydrocarbon chain and the polar portion(s) of the molecule. A change in the hydrophobic portion of the molecule, such as branching and chain length reduction, to increase solubility has been shown to decrease the stability of the inhibitory film. Yet, an inhibitory molecule must be soluble enough to easily disperse within the solution to provide ample coverage of the affected area. However, a strongly adsorbing polar group, or multiple groups on the same molecule, and polymerization of inhibitor molecules promotes stability of inhibitor films.[89] The dependence of chemical structure and concentration on the ability of pyrogallol, catechol, and tannin to affect liquor corrosivity has been investigated previously.[34,37,42,47,48,49]

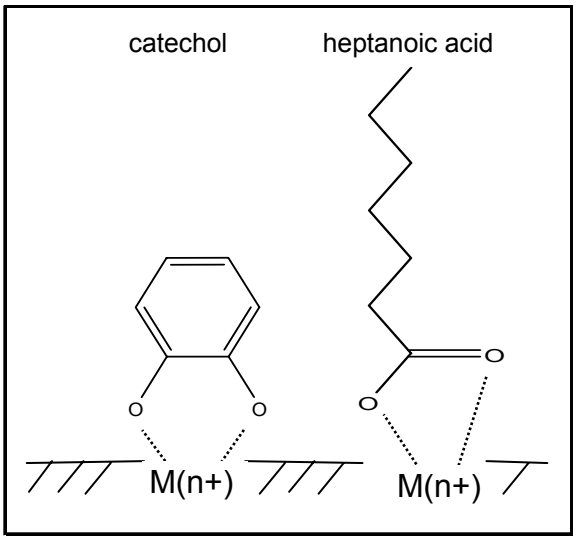

Figure 27. Schematic representation of ligand-metal chelation.

Data in Tables 10 and 11 illustrate a time dependency on the diffusion of extractives from wood chips. However, as shown in Table 11 the extraction of resin acids and 1,2,3-trihydroxybenzene took a longer soaking time before they could be detected in the extraction solution from HW-Mix chips. The longer time period required for diffusion of these chemicals out of the wood chips may be due to the hydrolysis and initial breakdown of the wood structure, namely lignin, or other native compounds, yet no significant hydrolysis of lignin or carbohydrate, cellulose and hemicellulose, is expected at room temperature. As shown in Table 8, the longer extraction time also resulted in an increase in the corrosion rate of carbon steel in the resulting BL from the extracted wood chips. The removal of resin acids and other compounds and/ or their breakdown products in the extraction solution may play a significant role in the increase in corrosion rate of carbon steel in BL. Previous work on catechols,[34,37,44] 1,2-dihydroxybenzes, indicates that trihydroxybenzenes would also negatively impact corrosion rates in BL.

Although the identification of some organic compounds in the aqueous solution was possible the role of these compounds in BL corrosivity is not clear at this time. Further research is needed to understand the role of water

extracted organics in BL corrosivity and whether these compounds are removed from the surface of the chip or diffusing out of the cell structure.

7.3.5. ADDITION OF ORGANIC EXTRACTIVES TO BLACK LIQUOR

To further examine the role of identified extractives in the corrosivity of BL to carbon steel A516-Gr70 selected compounds detected in the extraction solution, namely palmitic acid, tannic acid, β-sitosterol, pyrogallol, and catechol were added to different extracted or non-extracted BLs as described in Table 12. To confirm the effect of added chemicals on liquor corrosivity, tests were also carried out in BLs from the same batch of pulping but without any chemical addition. All BLs were tested at 170°C for 72 hours. Palmitic acid was the only chemical additive, among those tested in this study, to reduce corrosivity, reducing the corrosivity of SW-Old BL by 15%. Catechol, as expected, increased the corrosivity of HW-Mix BL by a factor of ~20, where the corrosion rate for carbon steel increased from ~0.09 to ~1.52 mm/yr, illustrating the ability of the extractives to inhibit passivation of carbon steel with a significant addition of catechol. The addition of tannic acid also resulted in an increase in corrosivity with the addition to SW-Old BL although the 16% increase was significantly less than other compounds tested.

Table 12. Corrosivity changes in black liquors with the addition of chemicals.

Additive	Addition	Wood Species	Extraction Time (hr)	Δ CR (mm/yr)	% Change
Palmitic Acid	1.5 g/L	SW-Old	-	-1.00	-15
Tannic Acid	6.4 g/L	SW-Old	-	1.25	16
Sitosterol	3.3 g/L	HW-Mix	48	3.50	53
Pyrogallol	6.4 g/L	HW-Mix	48	2.40	36
Catechol	6.4 g/L	HW-Mix	-	1.43	1634

However, these results did not conclusively identify an inhibitor which explains the inhibitory property of water extractable compounds in tested wood chips. Further investigations are needed to understand the synergistic or antagonistic effects of water extractable compounds in wood on overall BL corrosivity towards carbon steel. This information is important for chip transportation, chip yard management and in the pre-treatment of chips in steaming, bio-refining and bio-fuel production. In the chip yard and in pre-treatment, removing extractives from chips may result in unexpected increases of corrosivity in the downstream processes in the pulp mill.

Tests with individual chemicals may not show the synergistic or antagonistic effects that may be important in the presence of other inhibitors or chemicals. This is particularly true in BLs, where a large number of organic compounds

may potentially participate in the inhibition or activation reaction. In a previous study, the addition of catechols in unextracted HW BLs showed an increase in critical current density as well as passive current density. Corrosion rates for carbon steel increased from 0.05 to 0.90 mm/yr with an addition of 0.064 g/L of catechol in a Eastern Cottonwood BL.[37,38] Yet, the addition of catechols to synthetic BL, without the presence of organic chemicals, resulted in a significantly lower increase in corrosion rate,[38] i.e. from 0.00 to ~0.02 mm/yr at 0.064 g/L of catechol, compared to that of catechol addition in BL.[34,37]

Results from this study show that the presence of other chemicals may have synergistic or antagonistic effects on corrosion inhibition. Although the removal of extractives from HW chips by water extraction leads to a significant increase in the corrosivity of resulting BLs it is difficult to point to one extracted chemical for this effect. These effects may also vary from one wood species to another. A limited potentiodynamic polarization study as shown in Appendix B - Electrochemical Effects Of Water Extraction also indicates that the removal of extractives during wood chip pre-treatment or storage in the wood yard may affect the capability of anodic protection methods utilized to protect carbon steel equipment in some pulp mills.

7.4. CONCLUSIONS

- Corrosion rates for carbon steel A516-Gr70 in selected BLs vary significantly with wood species as well as the age of the tree. BL from SW-Old was nearly 4 times as corrosive as SW-Young. HW-Mix BL was almost 20 times less corrosive than SW-Young. These variations may be due to the content and concentration extractives in the wood pulped.

- Removal of water extractable organics was found to increase BL corrosivity in tested wood species. However, the role of individual compound or their combined effect towards BL corrosivity is not clear at this stage and needs further investigation.

Chapter 8

EFFECT OF BLACK LIQUOR OXIDATION ON THE CORROSION AND STRESS-CORROSION CRACKING OF CARBON AND STAINLESS STEELS

8.1. INTRODUCTION

In some pulp mills BL is oxidized to control odor as well as to allow an increase in pulp production in recovery boiler capacity limited mills. The oxidation of BL affects the liquor chemical composition, with the oxidation of sulfur to thiosulfate and further oxidation to sulfate as shown in Equations (16) and (17), which can affect the corrosivity of BLs. Increased concentration of thiosulfate may anodically shift the potential of the metal in solution to the active-passive region thereby increasing the susceptibility of the metal to SCC. A material failure due to SCC in an oxidized BL storage tank prompted an investigation into the root cause of the failure and identification of materials suitable for use in the process environment.

$$2Na_2S + 2O_2 + H_2O \rightarrow Na_2S_2O_3 + 2NaOH, \quad \Delta G = -806\ \text{kJ}\ @100^\circ\text{C} \quad [16]$$

$$Na_2S_2O_3 + 2NaOH + 2O_2 \rightarrow 2Na_2SO_4 + H_2O, \quad \Delta G = -889\ \text{kJ}\ @100^\circ\text{C} \quad [17]$$

Corrosion and SCC susceptibility of commonly used materials, carbon steel (A516-Gr70), austenitic stainless steel (SS304L), and duplex stainless steels (DSS2205 and DSS2304), were evaluated for use in 90% southern HW and 10% southern SW BL and an equivalent oxidized BL (BLOX) from the same mill. The non-oxidized BL was collected from a sample trap upon exiting a storage tank immediately prior to the entrance of the serpentine oxidation unit. The oxidation unit was composed of an austenitic stainless steel with a liquor flow rate of 300 – 500 gal/min, elemental oxygen flow of ~25,000 scfh, and an exit temperature of ~150°C. Immediately upon exit from the oxidation unit a sample trap was used to collect the BLOX. According to mill management, the residual sodium sulfide upon exiting the oxidation unit was expected to be less than 10 g/L. Both liquors were analyzed for their inorganic composition to identify the reasons for changes in liquor corrosivity.

8.2. EXPERIMENTAL PROCEDURES

Oxidized and non-oxidized BL from a mill using a 90% HW and 10% SW mixture was collected and shipped in air-tight containers. The liquor of each type was divided into small quantities (1-gallon bottles) under nitrogen, N_2, atmosphere and stored at 4°C. Prior to dividing into small portions, the liquor was stirred for 30 minutes under N_2 atmosphere for uniform consistency in

each bottle. A small portion of BL sample was collected before each test for analysis of sulfide, sulfidity, organics, active alkali, and percent solids in the liquor.

Materials tested in this study include carbon steel (A516-Gr70), austenitic stainless steel (SS304L), and two duplex stainless steels (DSS2205 and DSS2304). Chemical compositions and UNS numbers of these alloys are given in Appendix D – Chemical Composition of Alloys. Round tensile samples, with 1-inch gauge length, diagram shown in Figure 28, were machined from the alloys. Gauge length of tensile samples was polished to a 1-μm finish and the samples were cleaned with acetone to degrease the surface before testing. Two edges of the gauge were marked and measured as initial length. Initial diameter of the sample was also measured. Slow strain rate tests (SSRT) were carried out in a specially designed rig with autoclave. Each sample was weighed prior to placement of sample into the autoclave for testing.

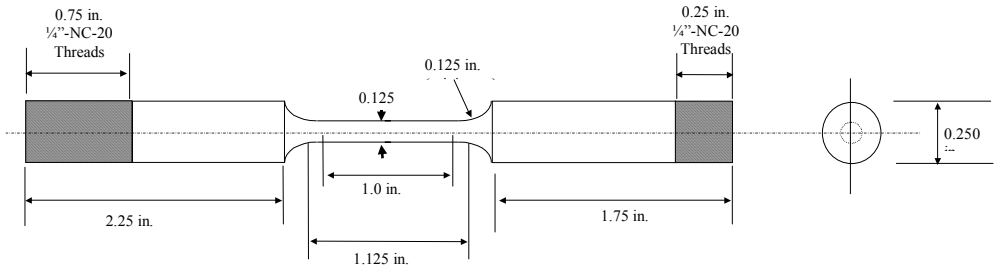

Figure 28. Slow strain rate test specimens (minimum specifications).

8.2.1. SLOW STRAIN RATE TESTING PROCEDURES

Precautions were taken to prevent any oxidation of test liquors while transferring them into the autoclave, shown in Figure 29, under N_2 atmosphere. Autoclave seals were tightened and excess air was removed by passing N_2 through it for 5 minutes. All valves and openings were tightened before increasing the temperature to the test value. Tests were conducted at 100°C and 204°C. An initial strain rate of $2x10^{-6}$ s^{-1} was used for each SSRT in this study. Applied load and displacement data was recorded by a data acquisition system. Slow strain rate tests were also conducted in dry air, shown in Figure 30, at 100°C and 204°C for comparison with liquor tests. In these tests, specimens were surrounded with washed pure sand instead of the

liquor. Sand was used to ensure better heat transfer and test temperature control.

After each test the samples were removed from the autoclave and examined for any visible surface cracks. Final gauge length of the specimen was measured to calculate the percentage elongation (% elongation). Both halves of the specimen were weighed individually prior to removing the oxide film. Final weight after film removal was used to calculate the overall corrosion rate of each material in the tested liquors. Specimens were sectioned, mounted, and polished for further examination and quantification of crack length, velocity, and morphology.

8.2.1.1. Testing Vessels

Figure 29. Slow strain rate apparatus used for controlled liquor environment testing.

Where A is the environmental chamber with 2 liter capacity and B the location of the thermocouple in Figure 29. The autoclave was heated with an external thermal blanket, shown surrounded by insulation in Figure 29, connected to a temperature controller with measurements taken by the thermocouple. Teflon washers were used to isolate the tested specimen from autoclave. Data were recorded by a Sensotec load cell and transmitted to a data acquisition system for further analysis.

Figure 30. Slow strain rate apparatus for controlled temperature dry sand experiments.

Where A is the sampled material, B is the environment containment apparatus, and C is the location of the thermocouple (not shown in Figure 30). Heating wraps used at elevated temperatures are not displayed for Figure 30.

8.2.2. LIQUOR ANALYSIS – GAS CHROMATOGRAPHY

Dissolved gases in oxidized and non-oxidized BLs were analyzed using gas chromatography (GC). For appropriate GC analysis, a gas phase is required. For that purpose, 2 cc of liquor samples were extracted and placed in

previously N_2 purged airtight 20.5 mL vials. The purging was achieved by flushing N_2 into each vial for two minutes. The vial was fitted with two needles: the first was used as a gas inlet and the second an outlet guarantying adequate flow of gas through the vial. A similar setup was used to fill the vial with the liquor aliquot; displacing N_2 volume as the liquid partially filled the vial. The partially filled vial was then placed in a heated water bath set at 96°C for one minute. A 5 cc syringe was then used to collect a gas phase sample from the tested vial.

The gas sample was injected into the inlet receptacle of a Perkin Elmer Gas Chromatographer Arnel No 5763-B. The apparatus is comprised of five columns, two detectors, a thermal conductivity detector (TCD) for light gases and a flame photo detector (FPD) for sulfur bearing gases. Once the chromatograms were obtained for each sample, analyses were conducted to determine both the type and the amount of species present according to previously performed calibrations. Matching retention time with numerous compounds and base line events previously tested in the apparatus then identifies the specie. The concentration of each species was then obtained by performing an integration of the area comprising the matched peak. The

chromatograph is specially configured to analyze light gases and organo-sulfur gases. Columns used to separate test gases are described in Table 13.

Table 13. Gas Chromatography column description.

Column	Description
1	7' HayeSep N 60/80, 1/8" H
2	9' Molecular Sieve 13x45/60, 1/8" Ni
3A	4' HayeSep T 60/80 H
3B	9' Molecular Sieve 5A 45/60
4	6' XE60/H_3PO_4 on Carbonpack B 1/8" TFE

8.2.3. OPEN CIRCUIT POTENTIAL MEASUREMENT

Open circuit potential (OCP) of tested samples was measured in both oxidized and non-oxidized BL at 50°C, 100°C, and 150°C. Cylindrical metal samples were polished to a 1.2-μm finish, cleaned with acetone, weighed and the surface area measured. Steel samples were insulated from the autoclave material with Teflon fittings. OCPs were measured using a pressure compensated external Ag/AgCl reference electrode.

8.3. RESULTS AND DISCUSSION

8.3.1. EFFECTS OF OXIDATION ON BLACK LIQUOR COMPOSITION

Oxidation of BL decreases the amount of reduced sulfur species including hydrogen sulfide and methyl mercaptans. In fact the main reason for the adoption of oxidation by the paper industry was for the control of mill odor generally attributed to hydrogen sulfide and mercaptans. The first measure to check the effectiveness of oxidized mill liquor was to analyze vapors collected from the head-space of the BL storage container at 96°C. The analysis, provided in Table 14, shows a near 90% reduction in methyl mercaptan and an approximate 100% removal of hydrogen sulfide in BLOX compared to the non-oxidized BL, taken from the same mill.

Table 14. Gas chromatography analysis of liquor headspace samples at 96°C.

	Hydrogen Sulfide (H_2S), ppm	Methyl Mercaptan (CH_3SH), ppm
Black Liquor (BL)	60	288
Oxidized Black Liquor (BLOX)	0	31

Further analysis of the two BLs indicated a decrease in the sulfide concentration with a corresponding increase in the concentration of hydroxide

after oxidation treatment, as shown in Table 15. Based on Equations (16) and (17), these results indicate that the mill-treatment resulted in the incomplete oxidation of sulfides in the BL. A complete oxidation would have significantly decreased the amount of sulfide without affecting the hydroxide concentration. However, an increase in hydroxide concentration is descriptive of incomplete oxidation with expected increases in thiosulfate and sulfite concentrations, as indicated by Equations (16) and (17).

$$2Na_2S + 2O_2 + H_2O \rightarrow Na_2S_2O_3 + 2NaOH, \quad \Delta G = -806 \text{ kJ } @100^\circ C \quad [16]$$

$$Na_2S_2O_3 + 2NaOH + 2O_2 \rightarrow 2Na_2SO_4 + H_2O, \quad \Delta G = -889 \text{ kJ } @100^\circ C \quad [17]$$

Table 15. Inorganic composition of oxidized and non-oxidized southern hardwood black liquors.

	Sulfide Na_2S	Hydroxide NaOH	Carbonate Na_2CO_3
Black Liquor (BL), g/L	42.0	13.2	51.5
Oxidized Liquor (BLOX), g/L	5.5	26.1	58.9

Additional reaction paths, or side-reactions, may occur resulting in sulfur species normally converted to organo-sulfur compounds or polysulfides. One such pathway for the production of polysulfides is the reaction given in Equation (22).[70] The formation of organo-sulfur compounds or polysulfide

may change the redox potentials of the solution thereby affecting the corrosion of carbon steels or making stainless steels susceptible to localized corrosion attack depending upon the extent of reactants.

$$Na_2S + Na_2S_2O_3 \rightarrow Na_2S_2 + Na_2SO_3, \Delta G = -9.600 \text{ kJ} @ 100^{o}C \qquad [22]$$

8.3.2. STRESS-CORROSION & GENERAL CORROSION RESULTS

8.3.2.1. Carbon Steel: A516-Gr70

Carbon steel A516-Gr70 samples tested by SSRT method in either BL or BLOX did not show significant effects on mechanical properties at 100°C, as is shown in Table 16. Stress-strain curves in Figure 31 show almost identical mechanical behavior for the three tests. Additionally, the presence of BLs did not have any significant effect on % RA or fracture strain. However, a few small transgranular cracks were found on the carbon steel sample tested in the non-oxidized BL at 100°C. No cracks were found on the sample tested in BLOX. Carbon steel samples did experience general corrosion in tested liquors. The corrosion rates increased from 0.32 mm/yr for the BL to 0.65 mm/yr for the BLOX.

The corrosion rate for the carbon steel was almost an order of magnitude higher for tensile samples tested in BL at 204°C than for samples tested at 100°C. For samples tested in BLOX, the corrosion rate also increased with an increase in test temperature. At 204°C the corrosion rates were lower in BLOX liquors than in BL. Results in Figure 32 clearly indicate that samples tested in liquors had lower ductility compared to the one tested in dry sand. Oxidation of BL seems to have a greater effect on SCC susceptibility of carbon steel at higher temperatures as the fracture strain for BLOX was ~11% compared to ~17% for BL. Crack velocity in BLOX samples was almost three times higher than that in BL samples. However, the maximum depth of transgranular cracks measured for carbon steel samples in both liquors was 10 – 16 μm. A golden-black film, believed to be predominantly magnetite based on thermodynamic calculations in the Pourbaix diagrams, was formed on the metal surface in BL at 100°C and in both BL and BLOX at 204°C.

Table 16. Carbon steel A516-Gr70 susceptibility to corrosivity in black liquor (BL) and oxidized black liquor (BLOX) at 100°C and 204°C.

Temp. °C	Test Environment	Crack Length (mm)	Crack Velocity (mm/s)	% Area Reduction	CR (mm/y)
100	Sand	NA	NA	22.2	NA
100	BL	0.010	1.7E-07	4.7	0.32
100	BLOX	-	-	4.7	0.65
204	Sand	NA	NA	31.1	NA
204	BL	0.010	1.3E-07	1.5	3.53
204	BLOX	0.016	3.3E-07	6.3	1.91

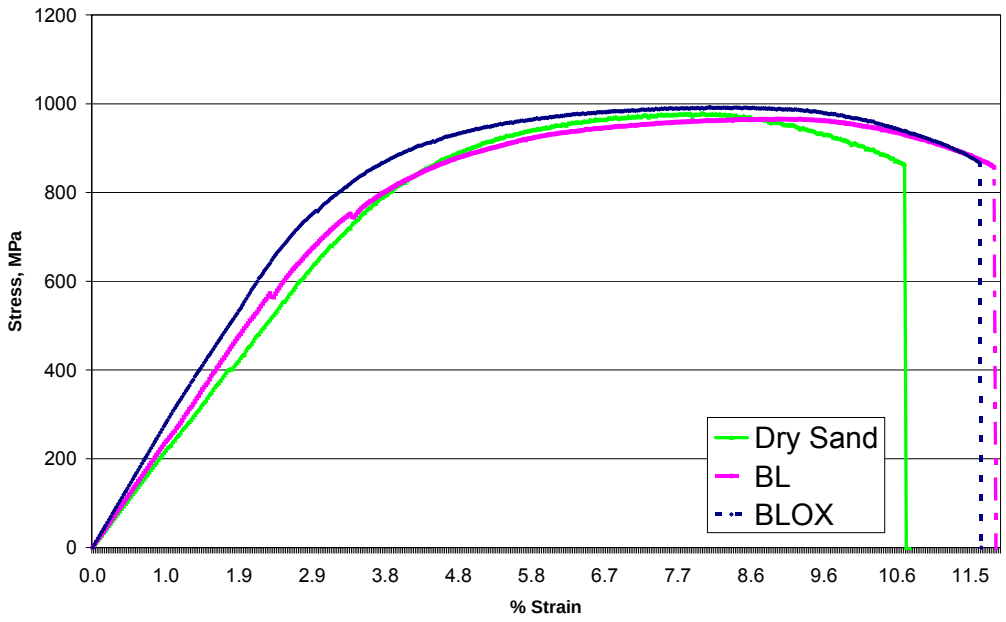

Figure 31. Slow strain rate tests for A516-Gr70 at 100°C in dry sand, black liquor (BL), and oxidized black liquor (BLOX).

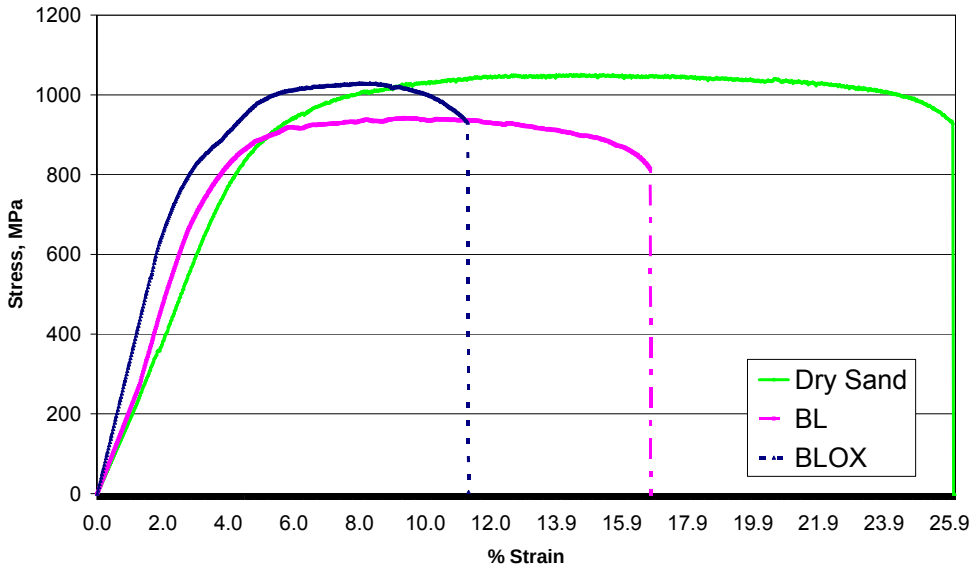

Figure 32. Slow strain rate tests for A516-Gr70 at 204°C in dry sand, black liquor (BL), and oxidized black liquor (BLOX).

8.3.2.2. Austenitic Stainless Steel: SS304L

Austenitic stainless steel SS304L samples at 100°C showed very low corrosion rates compared to carbon steel A516-Gr70. SS304L samples tested by SSRT method at 100°C, as shown in Figure 33, did not show any signs of SCC in either oxidized or non-oxidized BLs. However, SS304L was found to be susceptible to severe SCC at 204°C. The percentage reduction in area for the sample tested in BLOX was ~7% whereas the value was ~21% for BL and ~64% for the SS304L tested in sand at 204°C, as shown in Table 17. The effect of BL oxidation on the ductility of SS304L samples can be seen from the stress vs. strain curves in Figure 34. Crack velocity for samples tested in

BL was $1.4x10^{-5}$ mm/sec whereas the one tested in BLOX was $4.3x10^{-5}$ mm/sec. In samples tested in BL, cracks were branched with a predominately transgranular (TG) mode of cracking, as seen by the micrograph in Figure 35. Fracture surfaces were examined under scanning electron microscope and the fracture surface of SS304L samples tested in BL and BLOX show brittle fracture due to SCC, shown in Figures 36 and 37. Although the cracking mode was predominately TG, some parts of the fracture surface of SS304L samples tested in BL showed signs of intergranular (IG) attack indicating a mixed crack path. Similar crack morphology was found for the samples tested in BLOX.

A black film was found on the surface of all tensile samples tested at 204°C. The corrosion rate of SS304L tensile samples in both BL and BLOX was significantly higher than at 100°C. However, the effect was much more pronounced for samples tested in BLOX, which had a corrosion rate of ~3.17 mm/yr compared to that of ~0.55 mm/yr for the sample tested in BL. These values are very high for austenitic stainless steels, which typically are not expected to undergo general corrosion above ~0.1 mm/yr. The high corrosion rates for the tensile samples are due to continuous damage of the protective film in SSRT tests. This effect is more prominent in alloys which depend

upon the formation of a passive film on the metal surface. When the protective film is damaged through applied strain the overall corrosion rates are significantly higher than for un-strained coupon tests.

Table 17. Austenitic stainless steel SS304L susceptibility to corrosivity in black liquor (BL) and oxidized black liquor (BLOX) at 100°C and 204°C.

Temp. °C	Test Environment	Crack Length (mm)	Crack Velocity (mm/s)	% Area Reduction	CR (mm/y)
100	Sand	NA	NA	69.4	NA
100	BL	-	-	50.4	0.03
100	BLOX	-	-	64.2	0.02
204	Sand	NA	NA	63.9	NA
204	BL	0.584	1.39E-05	21.5	0.55
204	BLOX	1.188	4.34E-05	7.8	3.17

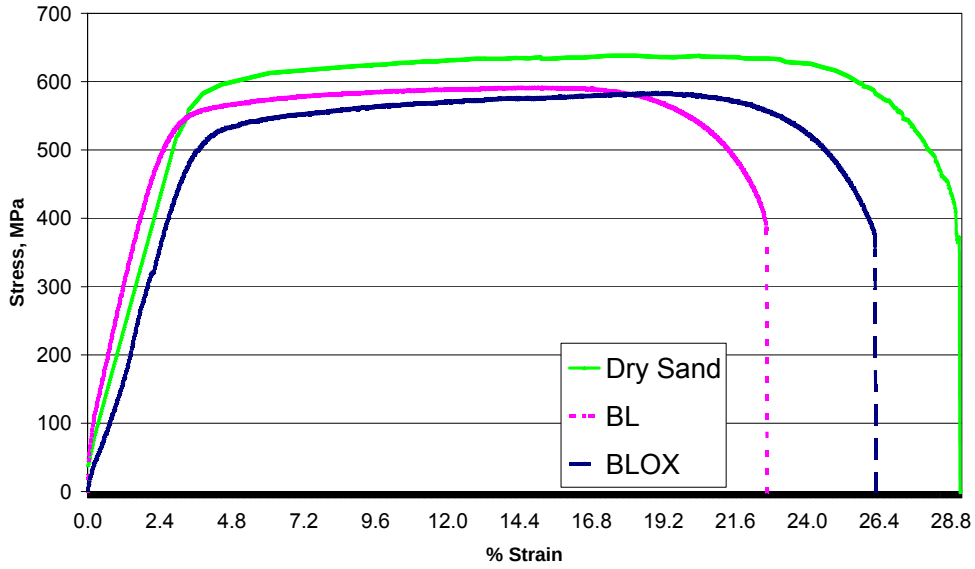

Figure 33. Slow strain rate tests for SS304L at 100°C in dry sand, black liquor (BL), and oxidized black liquor (BLOX).

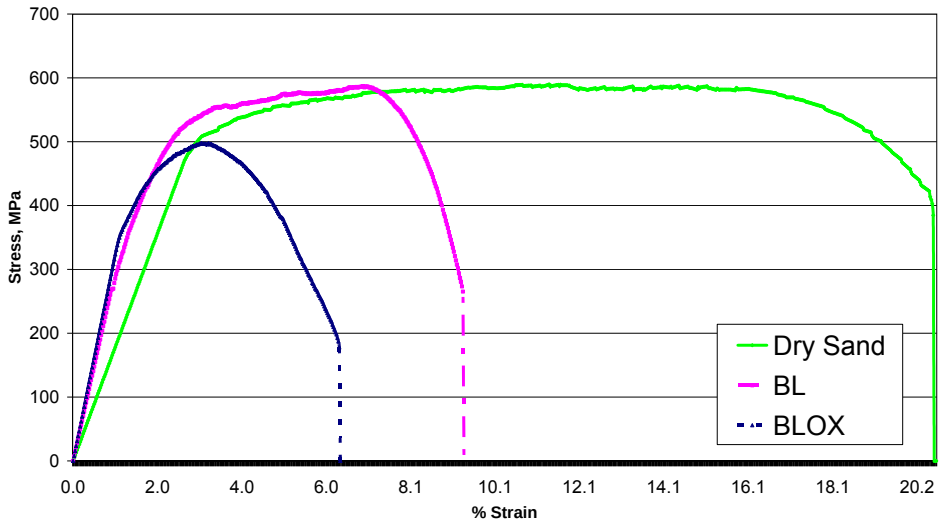

Figure 34. Slow strain rate tests for SS304L at 204°C in dry sand, black liquor (BL), and oxidized black liquor (BLOX).

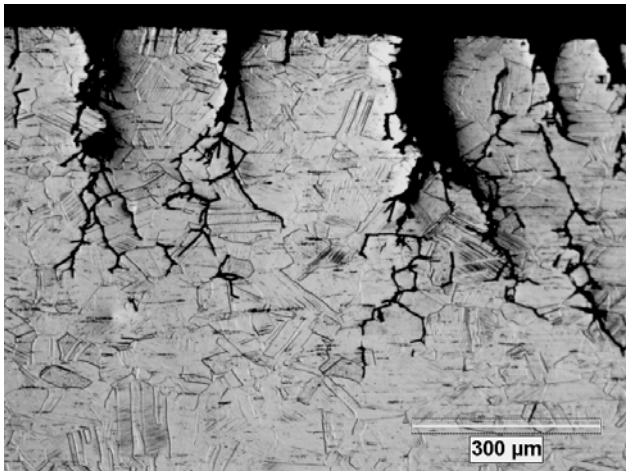

Figure 35. Stress corrosion cracks for the SS304L tensile sample tested in non-oxidized black liquor (BL) at 204°C.

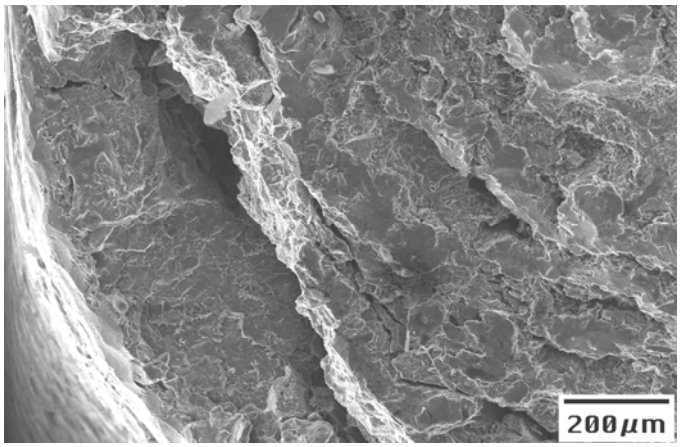

Figure 36. SEM micrograph showing transgranular fracture surface of a SS304L tensile sample tested in non-oxidized black liquor (BL) at 204°C.

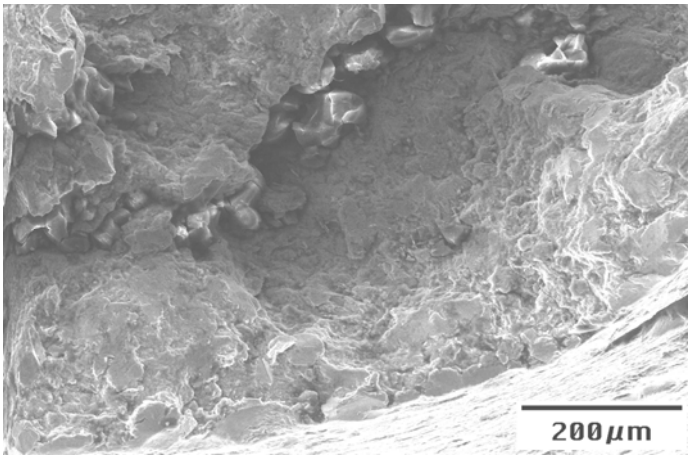

Figure 37. SEM micrograph showing fracture surface of a SS304L tensile sample tested in non-oxidized black liquor (BL) at 204°C.

8.3.2.3. Duplex Stainless Steel: DSS2205 and DSS2304

Duplex stainless steel DSS2205 samples tested at 100°C showed corrosion rates comparable to that of SS304L in both BL and BLOX. However, as shown in Table 18, at 204°C DSS2205 and DSS2304 show an increase in the corrosion rates yet the rates were significantly lower than SS304L in equivalent environments. Although DSS2205 experienced almost double the corrosion rate in BLOX as compared to BL (i.e. from ~0.37 mm/yr in BL to ~0.69 mm/yr in BLOX), the liquor oxidation had a minimal affect on the corrosion performance of DSS2304.

DSS2205 and DSS2304 tested by SSRT method at 100°C and 204°C, shown in Figures 38, 39, and 40, showed no SCC in both BL and BLOX. Fractography of both duplex stainless steels tested in BL or BLOX liquors revealed a ductile dimpled fracture surface with no signs of SCC on the fracture surface, as shown in Figures 41 and 42.

DSS2304 was only tested at 204°C and not at 100°C. However, general corrosion performance of DSS2304 was expected to be better than the DSS2205, which contains molybdenum. In alkaline conditions, molybdenum oxides have been found to undergo transpassive dissolution reducing the protective nature of the passive film and promoting higher corrosion rates compared to their non-molybdenum containing counterparts.[90] This effect was also shown for SS304 and SS316, where the latter containing a higher concentration of molybdenum was shown to corrode at higher rates in pulping liquors.

Table 18. Duplex stainless steels DSS2205 and DSS2304 susceptibility to corrosivity in black liquor (BL) and oxidized black liquor (BLOX) at 100°C and 204°C.

Metal	Temp.°C	Test Environment	% Area Reduction	CR (mm/y)	CR (mils/y)
2205	100	Sand	73.3	NA	NA
2205	100	BL	72.9	0.13	5.0
2205	100	BLOX	72.9	0.05	1.8
2205	204	Sand	84.3	NA	NA
2205	204	BL	61.8	0.37	14.5
2205	204	BLOX	61.1	0.69	27.2
2304	204	Sand	63.2	NA	NA
2304	204	BL	36.5	0.15	6.0
2304	204	BLOX	54.1	0.22	8.8

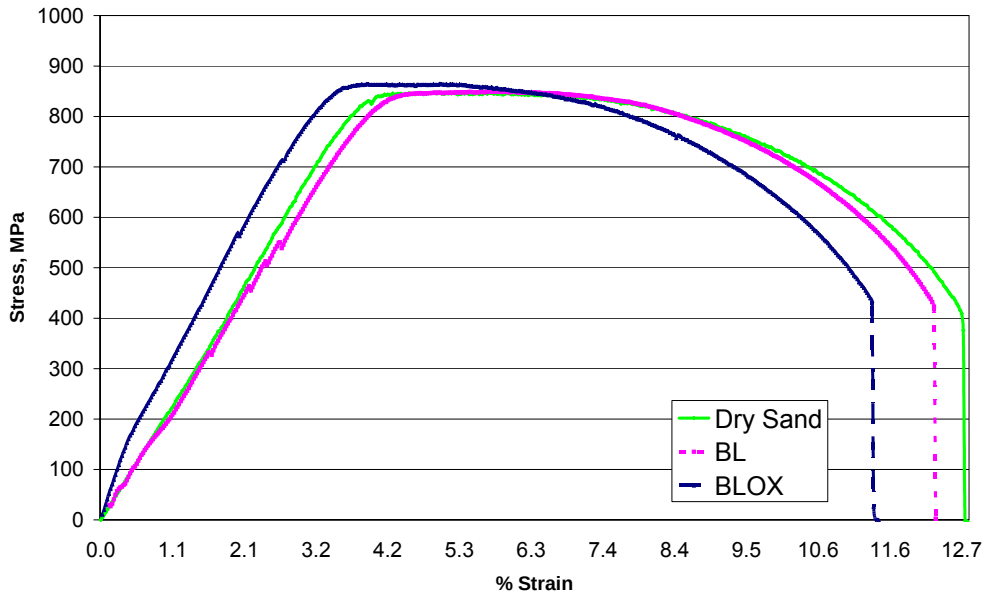

Figure 38. Slow strain rate tests for DSS2205 at 100°C in dry sand, black liquor (BL), and oxidized black liquor (BLOX).

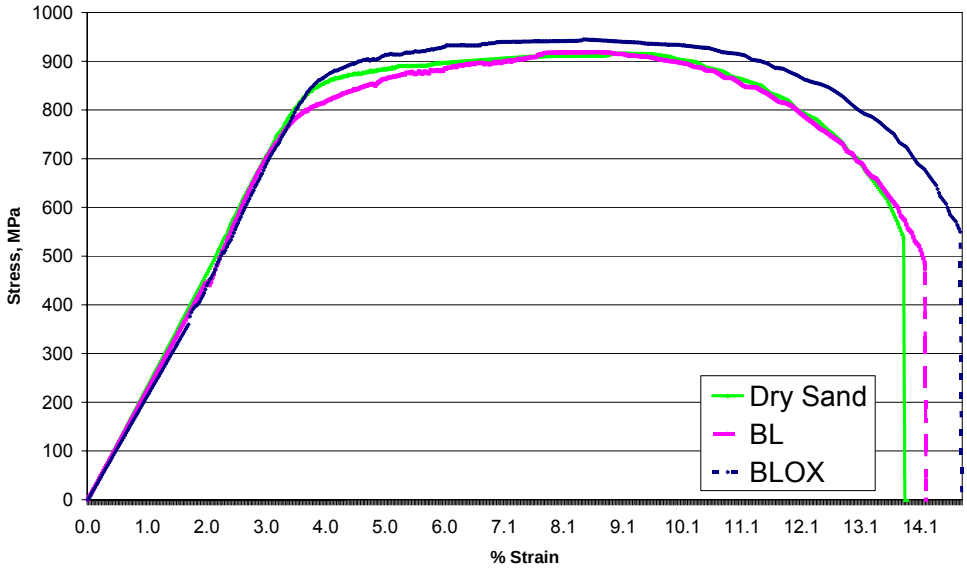

Figure 39. Slow strain rate tests for DSS2205 at 204°C in dry sand, black liquor (BL), and oxidized black liquor (BLOX).

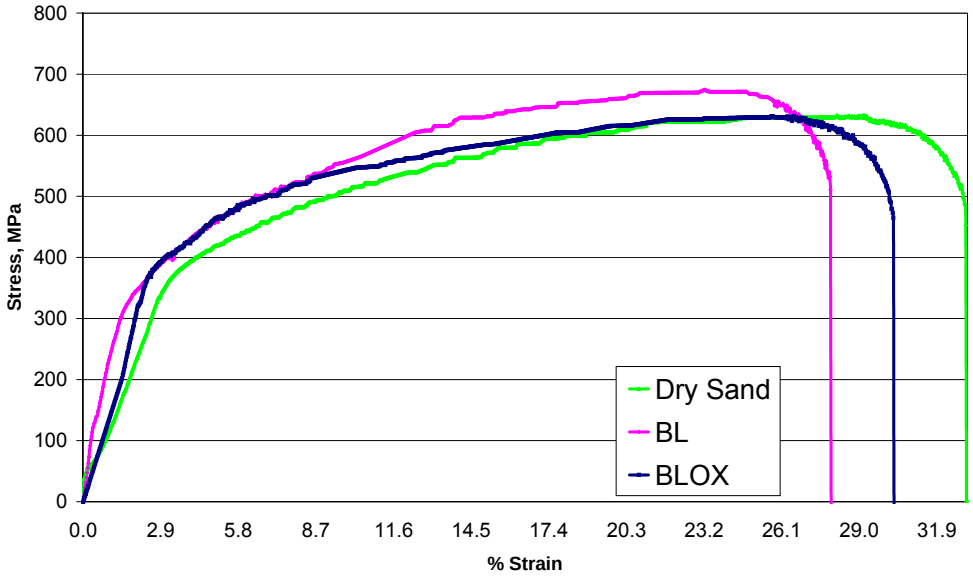

Figure 40. Slow strain rate tests for DSS2304 at 204°C in dry sand, black liquor (BL), and oxidized black liquor (BLOX).

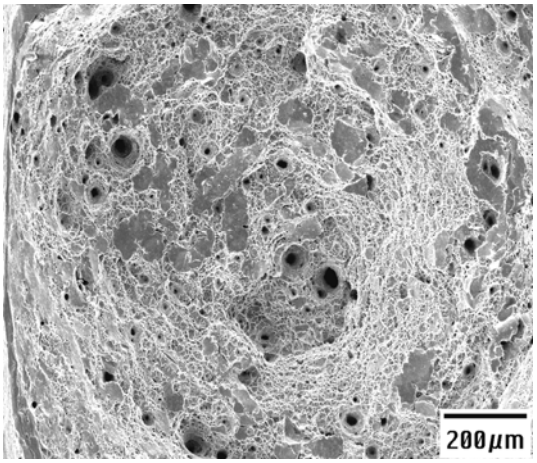

Figure 41. SEM micrograph showing ductile fracture surface of a duplex stainless steel DSS2205 tensile sample tested in non-oxidized black liquor (BL) at 204°C.

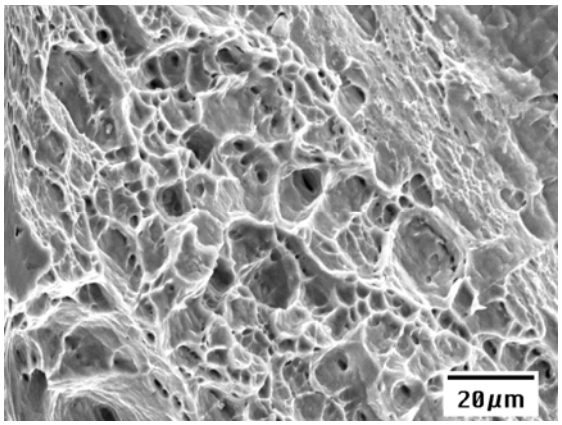

Figure 42. SEM micrograph showing ductile fracture surface of a duplex stainless steel DSS2304 tensile sample tested in non-oxidized black liquor (BL) at 204°C.

Previous work on sulfide containing caustic solutions has shown that SCC of carbon steel occurs in a narrow potential range near the active-passive transition.[78,91,92] Increased temperature and concentration of sulfide and hydroxide changes OCP to cathodic or more negative potentials.[68,93] The presence of different sulfur species in solution also influences the OCP and has a significant role in the ability of metal to passivate in pulping liquors.[65,67,71,72,73,74,75] OCP for tested metals was measured in BL and BLOX at 50°C, 100°C, 150°C, as is shown in Table 19. An increase in temperature shifted OCP to more negative values for all alloys tested, as expected. However, oxidation of BL shifted the potential of carbon steel in the anodic direction (more positive potential) where the OCP for BL at 150°C was -1.11 V (SCE) to -0.927 V (SCE) for BLOX.

Table 19. Open circuit potential of tested alloys with respect to standard calomel electrode (SCE) in black liquor (BL) and oxidized black liquor (BLOX) at 50°C, 100°C, and 150°C.

Metal	Temp, °C	Test Environment	OCP V (SCE)	Test Environment	OCP V (SCE)
A516-Gr70	50	BL	NA	BLOX	-0.858
A516-Gr70	100	BL	-1.084	BLOX	-0.893
A516-Gr70	150	BL	-1.113	BLOX	-0.927
304L	50	BL	NA	BLOX	-0.959
304L	100	BL	-0.840	BLOX	-0.964
304L	150	BL	-0.859	BLOX	-0.970
2205	50	BL	NA	BLOX	-0.875
2205	100	BL	-1.122	BLOX	-0.899
2205	150	BL	NA	BLOX	-0.963
2304	50	BL	NA	BLOX	-0.878
2304	100	BL	-0.873	BLOX	-0.937
2304	150	BL	-0.906	BLOX	-0.949

In previous work by Singbeil and Garner,[94] a narrow potential range for SCC at 100°C was identified which corresponds to the potential peak in polarization studies by Tromans[72] at 92°C. Tromans[72] identified this peak to be for the sulfate to thiosulfate reaction. In the present study on BLs a similar range of potentials were found to be associated with SCC susceptibility. At 100°C, with OCP values of -1.084 V (SCE) for BL and -0.893 V (SCE) for BLOX, only samples tested in BL showed signs of SCC which may indicate that the

open circuit potential for BLOX was more anodic than the active-passive transition region which is typically associated with SCC susceptibility. At 204°C, with OCP values more cathodic than those at 100°C, both liquors showed signs of SCC failure.

OCP data for 304L did not show a direct correlation with SCC in tested solutions. 304L steels were susceptible to SCC at 204°C yet no SCC was found at 100°C. Duplex stainless steels 2205 and 2304 were resistant to SCC irrespective of OCP.

Results from the slow strain rate tests have shown a strong effect of partial BL oxidation on the stress corrosion susceptibility of SS304L above 100°C. Results in the literature on the effect of oxidation on BL corrosivity are confusing as the extent of liquor oxidation for each case could not be compared.[61,62,63,64,65,66,67,68,69,70,71,72,73,74] Changes in the corrosivity of BL depend upon the extent of oxidation. An incomplete oxidation may result in the formation of thiosulfate and an increase in the hydroxide content of the liquor thereby increasing the general corrosion as well as SCC susceptibility of materials used.

Another possible reaction in the presence of thiosulfate is the formation of polysulfide in BL, which is a better oxidizer and may also result in the increased corrosivity of BLOX. This effect was identified by Yeske et al[29] in sulfur containing caustic solutions. However, a complete oxidation of liquors may decrease the overall corrosivity of BL through the formation of sulfate and a reduction in the sulfide content.

8.4. CONCLUSIONS

- Carbon steel A516-Gr70 was found to be susceptible to general corrosion and SCC at 204°C in both non-oxidized and oxidized BLs. However, at 100°C corrosion rates were relatively lower, 0.32 mm/yr compared to 3.53 mm/yr for BL and 0.65 mm/yr compared to 1.91 mm/yr for BLOX, with small cracks found only in BL.

- At 100°C, SS304L tensile samples showed no signs of SCC in BL as well as BLOX and experienced very low corrosion rates, 0.03 and 0.02 mm/yr respectively.

- At 204°C, SS304L was found to be susceptible to SCC in both BL and BLOX. However, crack velocity was significantly higher in BLOX, 4.34E-05 compared to 1.39E-05 mm/s.

- Duplex stainless steels show good resistance to corrosion and SCC in all tested environments compared to the other tested materials. DSS2304 exhibited a lower corrosion rate, 0.15 mm/yr for BL and 0.22 mm/yr for BLOX, compared to DSS2205, 0.37 mm/yr for BL and 0.69 mm/yr for BLOX.

- Corrosion rates for tensile samples tested in BL and BLOX were significantly higher than typically experienced by un-strained coupon tests. This may be due to continuous destruction of the passive film formed on the metal surface.

- Increased corrosivity of BLOX in this study could be attributed to incomplete oxidation resulting in the higher thiosulfate and hydroxide concentrations found in the liquor.

Chapter 9

SUMMARY OF CONCLUSIONS

Earlier research on corrosion in pulping liquors, from published literature, has typically focused on concentrations of 100 g/L sodium hydroxide and 30 – 40 g/L sodium sulfide at temperatures below 150°C. Many of the tested liquors were from actual process streams containing unidentified components and varying levels of liquor oxidation. The mixed results from previously published studies tried to explain the liquor corrosivity as a function concentration of sulfur compounds, namely sulfide, sulfite, and polysulfide; the concentration of hydroxide; and temperature. Results from the present study relate increased temperature and concentration of hydroxide and sulfide as the driving forces of corrosion as related to the potential of the carbon steel A516-Gr70 in solution. Changes to temperature and concentration of hydroxide and sulfide were shown to cause a shift in the potential of carbon steel A516-Gr70 in solution which may increase the rate of corrosion as a result of potentials moving to more cathodic values below that of passivation, in the active region.

An increase in temperature at constant concentration increased the corrosion rate for carbon steel A516-Gr70. Further, at all temperatures tested, increased sulfide content increased the corrosion rate for carbon steel A516-Gr70. In the presence of sulfide the incorporation of FeS into the Fe_3O_4 scale may change the conductivity of the surface film and destabilize the surface corrosion products leading to increased corrosion rates for carbon steel. However, XRD characterization of surface corrosion products was found to be insufficient for the evaluation of passivation and active corrosion behavior of carbon steel in the tested solutions.

At the active-passive transition, depending upon the shift in OCP, carbon steel A516-Gr70 may move to a region of greater stability, with a reduction in corrosion rate, or to a region of greater solubility, which may increase the corrosion rate. It was found that an increase in corrosion rate results in the tested sulfide containing caustic environments was due to a shift in OCP values below approximately -1.00 V (SCE). At OCP values above -1.00 V (SCE) tested environments showed relatively low corrosion rates, below ~0.2 mm/yr. Therefore, any parameter change, such as a change in concentration or temperature, resulting in this OCP shift may change the corrosion behavior of carbon steel. This can provide an indication marker for correlating expected

shifts in corrosion rate with rest potentials below the active-passive transition potential.

Although published literature has identified wood species variability and catechol concentration as significant factors in BL corrosion variability, for greater than 50 years, the focus of research continues to be the inorganic composition of BL. Only recently has a significant effort been made to catalog BL corrosivity among species yet no effort has been made to perform a corresponding comprehensive analysis on the BLs for organic content. It is expected that the lack of organic analysis in BLs in previous corrosion studies is due to the difficulty of quantifying the hundred's of low-molecular weight organic chemicals found in BL coupled with the continued belief that inorganics control BL corrosion. In this study it was found that BL corrosivity is directly related to the wood species pulped. In general the HW BLs had lower corrosivity than SW BLs, which points to the organic constituents in wood chips. It was further found that species-specific water extracted organic compounds from wood chips have a significant role in BL corrosivity.

It was shown that corrosion rates for carbon steel A516-Gr70 in selected BLs varied significantly where wood species as well as age of the tree affected liquor corrosivity. Results show that the BL from SW-Old was nearly 4 times as corrosive as SW-Young whereas HW-Mix BL was almost 20 times less corrosive than SW-Young. These variations may be due to the content and concentration of extractives in the wood pulped which changes with both the age and species of wood. Results have conclusively shown that removing extractives in a cold water bath increased BL corrosivity for all tested wood species. These results are of importance to processes involving chip transportation, chip yard management, and in the pre-treatment of chips in steaming, bio-refining and bio-fuel production. In the chip yard and in pre-treatment, the early removal of extractives from chips is sometimes desired to reduce downstream pulping chemical use and for the enzymatic production of ethanol, yet may result in unexpected increases of corrosivity in downstream pulp mill processes.

Although clarification concerning the role of extractives in BL corrosion may shorten the list of chemical(s) responsible for species to species variability, it does not provide a clear solution to or complete understanding of BL corrosion from tests. To provide a better understanding of factors responsible for

inhibition in BL, based on the analysis of the extracted solutions, identified chemicals were added to BL and tested for their effect on BL corrosivity. Palmitic acid was the only added chemical found to result in a reduction in BL corrosivity, ~16% reduction for SW-Old BL, yet did result in the corrosion inhibition equal to that found for HW-Mix BLs. The inhibition, or reduction, in corrosion by HW-Mix extractives appeared to occur at the metal surface through the formation of a protective film. Extracted HW-Mix BLs, with significant increases in BL corrosion, realized active corrosion of carbon steels rather than the formation of a passive film on the carbon steel surface.

The species to species variability in BL corrosion may be explained by the presence of a group of organic chemicals but changes to the inorganic content of individual BLs may also result in significant changes in corrosivity. Oxidation units were first introduced to control odiferous gasses with the expectation that sulfide oxidized to sulfate would reduce process corrosion in downstream storage tanks and concentrators. Most recently, oxidation units have been installed as a means of providing capacity in a capacity-limited pulp mill as a result of decreased viscosity at higher solids and increasing sulfur recovery efficiencies. In this study it was proposed that the oxidation of BL may result in increased susceptibility of metals to SCC due to increased levels

of hydroxide and thiosulfate. Increased levels of hydroxide and thiosulfate are a result of partial oxidation, and may result in a potential shift to the region of active-passive transition.

Analysis of non-oxidized and oxidized BLs verified the increase of hydroxide and thiosulfate concentrations in the oxidized BL, as is expected in partially oxidized BL. Carbon steel and stainless steels were tested for their suitability in both the non-oxidized and oxidized BL environments at 100°C and 204°C. The negative impact, when compared to non-oxidized BL, on SCC susceptibility of materials exposed to a partially oxidized BL was realized for all metals tested.

Carbon steel A516-Gr70 was found to be susceptible to general corrosion and SCC at 204°C in both non-oxidized and oxidized BLs. However, at 100°C corrosion rates were relatively lower and small cracks were found only in BL test specimens. Austenitic stainless steel SS304L tensile samples showed no signs of SCC in BL as well as BLOX and experienced very low corrosion rates at 100°C. Yet at 204°C, SS304L was found to be susceptible to SCC in both BL and BLOX with significantly higher crack velocities in BLOX.

Meanwhile, high chromium containing duplex stainless steels showed good resistance to corrosion and SCC in all tested environments compared to the other tested materials. At 204°C, DSS2304 exhibited a lower corrosion rate for BLOX compared to DSS2205.

Chapter 10

FUTURE WORK

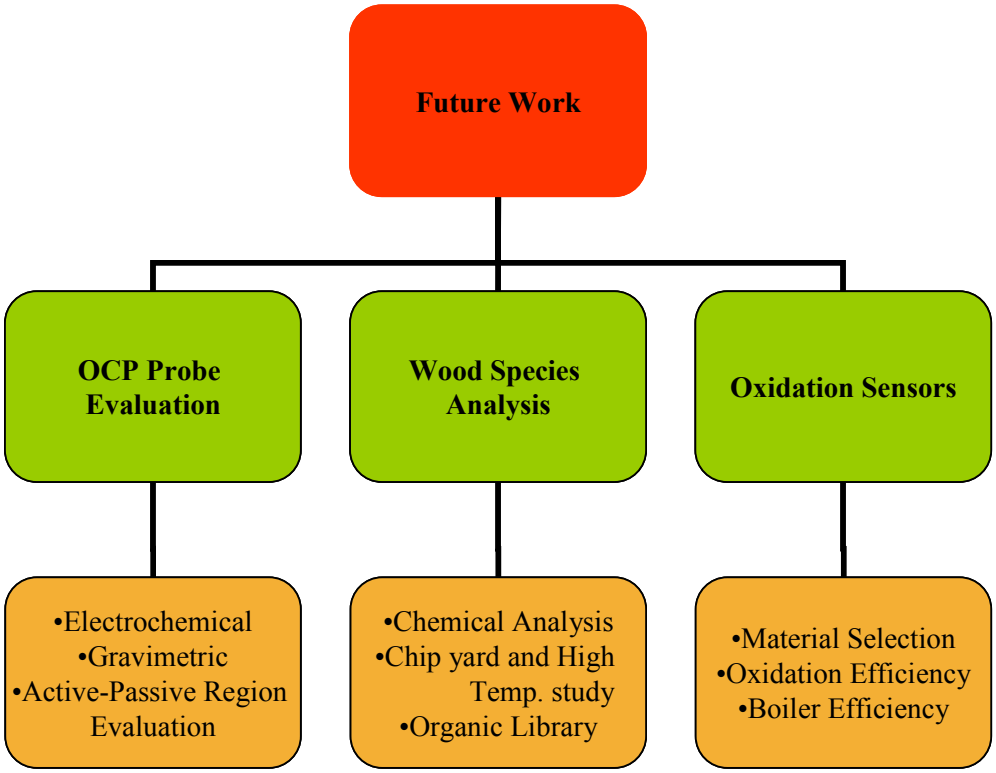

Figure 43. Flow diagram of recommended areas for future research and development.

10.1. OPEN CIRCUIT POTENTIAL AND CORROSION RATE

Further work is needed in order to determine the effectiveness of a probe based on OCP versus corrosion rate in sulfide containing caustic solutions.

One area, in particular, that needs to be addressed is the long-term reliability of a reference electrode at temperatures greater than 100°C in sulfide containing high pH environments. Additionally, such an electrode would need to ensure no contamination of the environment, such as chloride ion leaching, due to its insertion. In the presence of such an electrode further tests concerning corrosion rate versus OCP and temperature could then be utilized to verify expected increases in corrosion rates below -1.00 V (SCE) at all temperatures. Also, the production of such a probe would allow for insertion directly into processes for monitoring of the OCP and provide immediate alerts concerning process parameter fluctuations which may affect process corrosion rates.

Investigation of OCP and corrosion rates is also needed for alloys beyond those of carbon steels, such as austenitic stainless steels and duplex stainless steels. If a similar trend in corrosion rates at a defined OCP can be defined in sulfide containing caustic solution for other metals the ability to monitor corrosion fluctuations as a function of process parameters *in situ* would provide significant industrial benefit and may allow for further definition of solution-metal interface relationships. Investigations into solutions beyond that of sulfide containing caustic solutions also warrant attention. If the OCP-corrosion rate-material relationship exists in more complex solutions such as

BL the utilization of a probe, even at temperatures nearing 100°C, would allow for corrosion rate monitoring in storage tanks for some processes.

10.2. WOOD SPECIES-SPECIFIC ANALYSES

Further work is needed in order to identify water extracted chemicals responsible for changes in the corrosivity of BLs. Such work will need further refinement of analytical testing procedures to ensure no degradation or modification of species-specific chemicals occurs during testing. Additionally, such work is needed to expand current library databases for the identification of low-molecular weight organic chemicals and their degradation or modified products as a result of testing procedures.

A more detailed analytical library along with further investigations into species dependent corrosion rates and water extracted chemical concentrations may allow for the deductive determination of chemicals responsible for corrosivity changes in BLs. However, it appears more likely that the determination of which species-specific chemical additions, whether in concert with other chemicals or by themselves, a result that may also be species-

specific, result in corrosion inhibition will be a result of extractive analysis and an elaborate chemical concentration addition matrix.

Detailed investigations on the impact of wood chip transportation and storage on species-specific BL corrosivity is also needed. Due to current operation procedures in the PPI the variability in storage and transportation times and environments is significant. Further understanding of the impact of storage and transportation on the water extractive content of wood chips, and/ or wood logs, and the impact on BL corrosivity may allow for further process optimization and provide information concerning species-specific BL variability.

10.3. BLACK LIQUOR OXIDATION INVESTIGATIONS

Further work on lower cost high durability materials such as lean duplex stainless steels, an example is LDSS2101, is needed to investigate their suitability for the harsh BL and BLOX environments currently experienced in industry. Yet investigations on individual materials will not proved answers but only short-term solutions. In-depth mechanistic investigations are needed to understand the environment alloy interaction and failure mechanisms in

order to identify and/ or produce materials capable of reliably withstanding fluctuations in BL and BLOX environments.

Methods for more complete oxidation, in-line sensors to monitor the level of oxidation and the related material impact, and industry education are needed to identify material toleration requirements for BL oxidation processes. Additionally, species-specific effects which have been neglected in discussions concerning BL oxidation and corrosion also need investigation. Further, corrosion rate and material failure monitoring of BLs as a function of material, wood species pulped, oxidation levels, solids concentration, and viscosity effects will provide greater detail on the impact of oxidation at different stages of the recovery process, materials required to handle BL variability, oxidation effectiveness, and efficient operating parameters for processes.

APPENDICIES

APPENDIX – A

A. X-RAY DIFFRACTION ANALYSIS

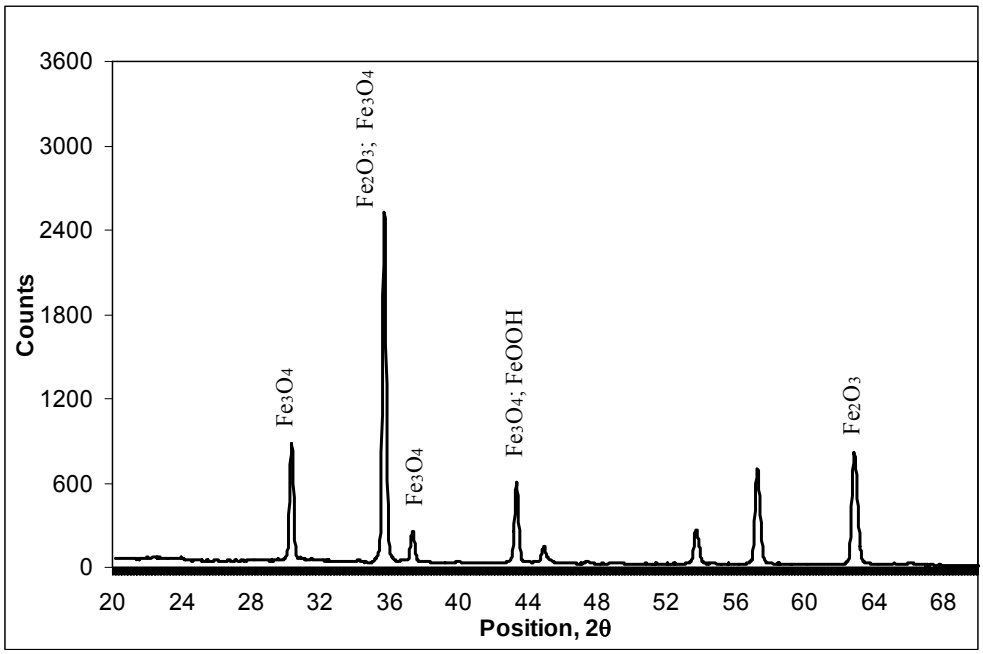

Figure 44. X-Ray Diffraction of surface corrosion product on carbon steel A516-Gr70 in 200 g/L NaOH at 170°C.

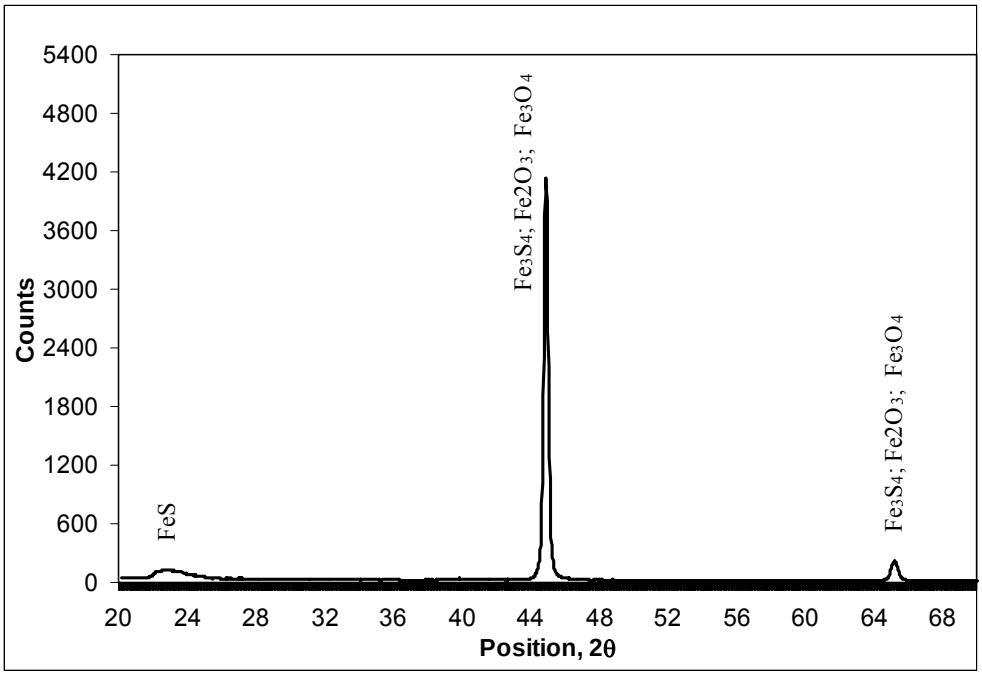

Figure 45. X-Ray Diffraction of surface corrosion product on carbon steel A516-Gr70 in 37.5 g/L Na_2S at 170°C.

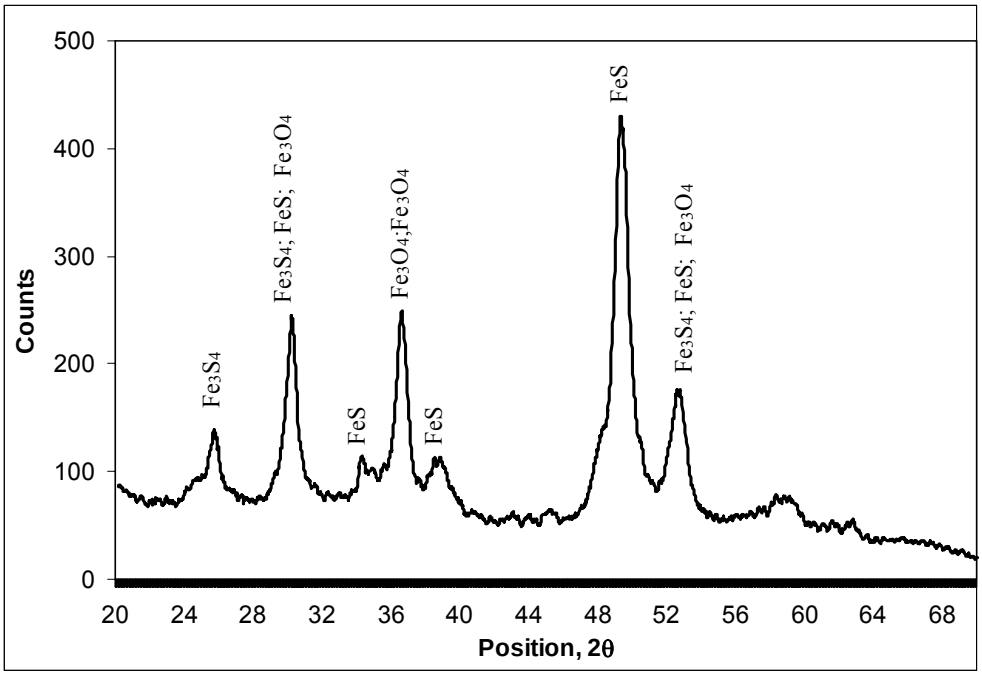

Figure 46. X-Ray Diffraction of surface corrosion product on carbon steel A516-Gr70 in 75 g/L Na_2S at 170°C.

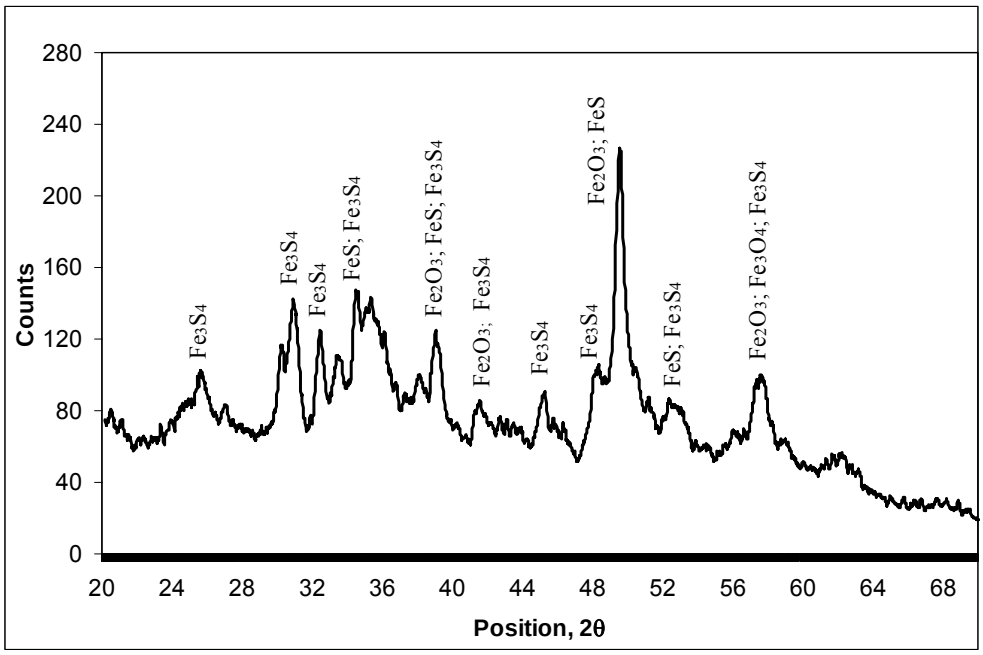

Figure 47. X-Ray Diffraction of surface corrosion product on carbon steel A516-Gr70 in 100 g/L NaOH and 37.5 g/L Na_2S at 170°C.

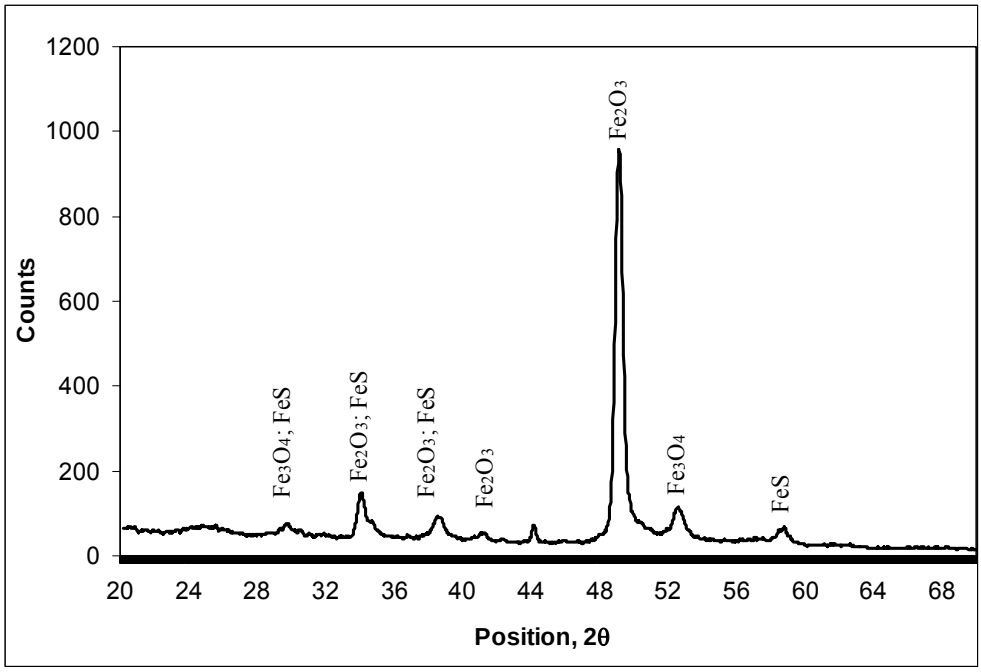

Figure 48. X-Ray Diffraction of surface corrosion product on carbon steel A516-Gr70 in 100 g/L NaOH and 75 g/L Na_2S at 170°C.

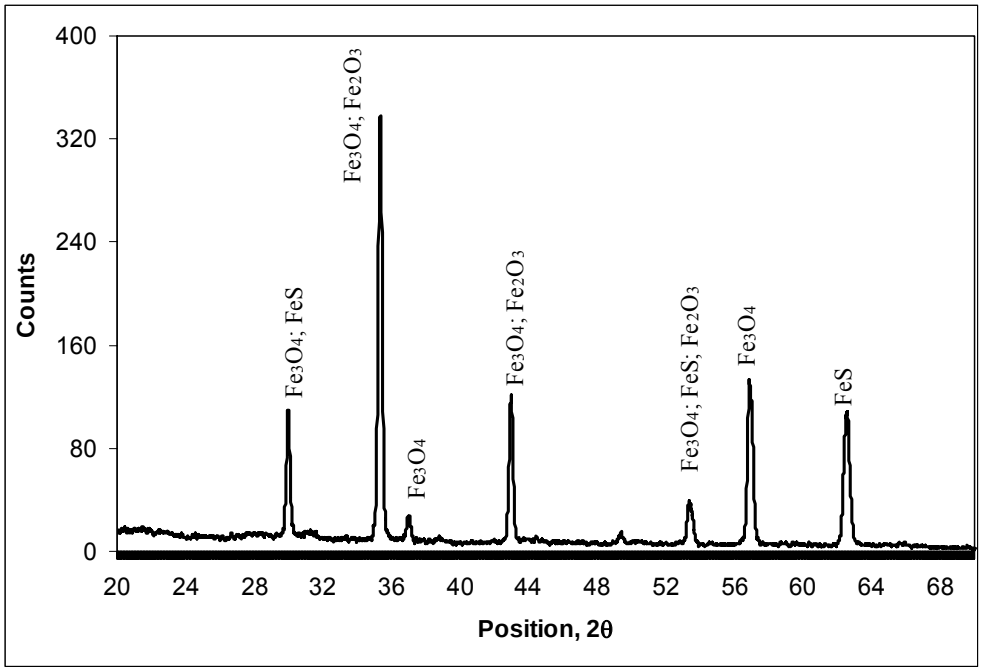

Figure 49. X-Ray Diffraction of surface corrosion product on carbon steel A516-Gr70 in 200 g/L NaOH and 37.5 g/L Na_2S at 170°C.

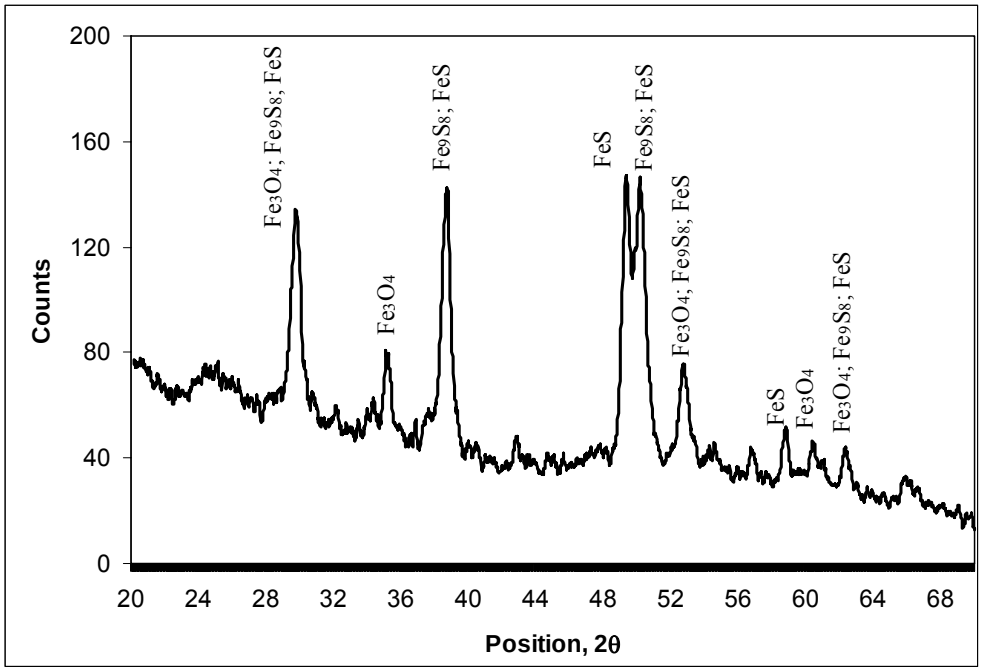

Figure 50. X-Ray Diffraction of surface corrosion product on carbon steel A516-Gr70 in 200 g/L NaOH and 75 g/L Na_2S at 170°C.

APPENDIX – B

B. EFFECT OF WOOD CHIP STORAGE AND EXTRACTION ON A SOUTHERN HARDWOOD SWEETGUM

A southern HW sweetgum of ~35 years old was felled and a wood log sewn at 6 – 10 feet above ground. Sweetgum wood chips were stored at 4°C for approximately nine months prior to study. In previous work Singh et al[37] realized a corrosion rate of ~0.00 mm/yr for a BL prepared from a freshly chipped southern HW sweetgum. Upon removal from cold storage sweetgum chips were visibly wet with a moisture content of ~55%. Wood chips were separated for preparation of a HW-Sweetgum BL and for a 48 hour water extraction prior to pulping. During the water extraction samples of the solution were taken at 24 and 48 hours for analysis using capillary ion electrophoresis, GC/MS, and for determination of percentage carbon analyzed to evaluate thoroughness of chemical evaluation methods. Data, shown in Table 20, indicate an increase in concentration of the lower weight acids oxalic, formic and acetic as well as the presence of higher weight fatty acids palmitic and stearic as seen in the HW-Mix water extracted solution analysis. An evaluation of the total organic carbon in solution indicates a continued increase in extracted organics with time, while also providing a percentage of identified carbon, 2.77% at 24 hours and 1.43% at 48 hours. These results indicate that higher molecular weight organics that our analyses were unable

to quantify, for example compounds such as sterol esters and tannins, may diffuse out of the wood into solution with time.

Table 20. Composition of water extracted chemicals from southern hardwood *Liquidambar styraciflua* chips (mg/L)

	Compounds (mg/L)	
Extraction Time	**24 hr**	**48 hr**
Carboxylic Acids		
Oxalic acid	4.88	8.28
Formic acid	12.09	12.66
Acetic acid	9.84	21.57
Palmitic acid	0.30	0.30
Stearic acid	0.20	0.15
Total Organic Carbon (mg/L)	317	1011

Analysis of the BLs prepared from the stored HW-Sweetgum chips, normal BL and extracted BL, indicates an increase in corrosion rate of ~18% with extraction, from 6.78 to 7.98 mm/yr. The significant increase in corrosion realized from the normal BL in this study when compared to that of Singh[37] may be due to the visibly moist storage conditions of the wood chips resulting in an extraction of the wood chips prior to testing. However, further work needs to be done to clarify species to species variability as well as interspecies variability in BL corrosion as well as extractive content.

APPENDIX – C

C. ELECTROCHEMICAL EFFECTS OF WATER EXTRACTION

To investigate the effect of water extraction on BL corrosivity a potentiodynamic polarization study, with A516-Gr70 carbon steel working electrodes, was performed at 25°C and 90°C in BLs from both extracted and non-extracted HW-Mix chips. A change in temperature from 25°C to 90°C did not have a significant effect on the polarization behavior of carbon steel in extracted and non-extracted HW-Mix BLs producing similar results. However, results in Figure 51 indicate that the polarization of carbon steel does show a difference in the ability of extracted HW-Mix BLs to affect the polarization behavior of carbon steel A516-Gr70 at 90°C.

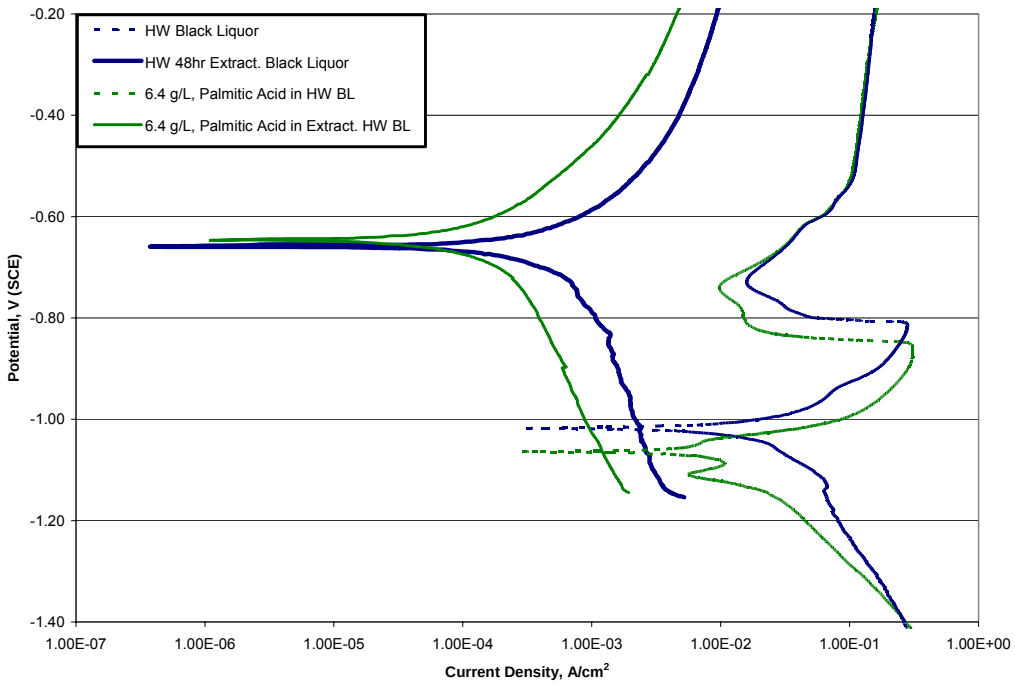

Figure 51. Polarization curve of carbon steel A516-Gr70 in HW-Mix black liquor and extracted HW-Mix black liquor with addition of palmitic acid at 90°C.

The addition of 6.4 g/L palmitic acid was performed to investigate the impact of chemical addition on the polarization behavior of carbon steel in extracted and unextracted HW-Mix BLs at 25°C and 90°C. Although addition of palmitic acid to SW-Young BL resulted in a 15% decrease in the corrosion rate for carbon steel at 170°C, differences in the polarization behavior of carbon steel in HW-Mix BLs were not significant at 25°C and 90°C. It is

possible that an increase in temperature to 170°C would result in an expected shift to more cathodic values. However, polarization tests at 170°C could not be carried out to confirm those effects. The impact of temperature on constituents of both extracted and unextracted liquors is also unclear. Breakdown products or other compounds in solution may act as oxidizing or reducing agents shifting the polarization curves to more anodic or cathodic values. Due to reference electrode instability in sulfide containing caustic solutions at temperatures greater than 100°C no further testing could be performed.

APPENDIX – D

D. CHEMICAL COMPOSITION OF ALLOYS

D.1. Materials For Black Liquor Oxidation Study

Table 21. Alloy composition for tested metals with UNS designation.

UNS #	Alloy	C	Mn	P	S	Si	Ni	Cr	Mo	Cu	Al	V
K02700	516-Gr70	0.48	0.64	0.14	0.016	0.25	0.05	0.04	0.02	0.09	0.02	0.004
S 30403	304 L	0.04	1.66	0.53	18.1	8.4	0.013	0.026	0.39	0.47	0.02	0.06
S 32205	2205	0.022	1.46	0.018	0.005	0.62	4.88	22.8	2.81	0.36	0.02	0.06
S 32304	2304	0.02	1.4	0.03	0.005	0.6	4.2	23		0.3		

REFERENCES CITED

1. D.A. Jones, Principles and Prevention of Corrosion, Second Ed. (Upper Saddle River. NJ: Prentice Hall Inc., 1996).

2. J.T.A. Valvano, ESPN Arthur Ashe Courage and Humanitarian Award Address, http://www.jimmyv.org/rememberingjim/espy.cfm, January (2006).

3. R.J. Boudreaux, Jr., Ode to the Trumpet Man, in memory of Ivan 'John' Douglas Hazlewood, Jr. November (1996).

4. News Scan, Labor, Blast Kills Three at Stone Container Mill, Pulp & Paper Magazine (June 1994).

5. Corrosion Cost and Preventive Strategies in the United States, US Congressional Study FHWA-RD-01-156, U.S. Department of Transportation, Federal Highway Administration, Appendix W – Pulp and Paper (2002).

6. K.W. Whitten, K.D. Gailey, and R.E. Davis, General Chemistry with Qualitative Analysis, 4th Ed., (Fort Worth. TX: Saunders College Publishing, 1992).

7. M.G. Fontana, Corrosion Engineering, 3rd ed., (New York. NY: McGraw-Hill, 1986) p.457.

8. R.G. Kelly, J.R. Scully, D.W. Shoesmith, and R.G. Bucheit, Electrochemical Techniques in Corrosion Science and Engineering, P.A. Schweitzer, Ed., (New York, NY: Marcel Dekker Inc., 2003.

9. J.M. West, Basic Corrosion and Oxidation, (New York. NY: John Wiley & Sons, 1980).

10. P. Kofstad, High-Temperature Oxidation of Metals, eds. R.T. Foley, N. Hackerman, C.V. King, F.L. LaQue, H.H. Uhlig, (New York. NY: John Wiley & Sons, 1966).

11. NACE Glossary of Corrosion Terms. Materials Protection 4, 1 (1965) p.79-80.

12. N.E. Hamner, Scope and Importance of Inhibitor Technology, ed. C.C. Nathan, Corrosion Inhibitors (Houston. TX: NACE, 1981) p.1-27.

13. C.C. Nathan, "Studies on the Inhibition by Amines of the Corrosion of Iron by Solutions of High Acidity," Corrosion 9, 6, August (1952) p.199-202.

14. A. Weisstuch, D.A. Carter, C.C. Nathan, "Chelation compounds as cooling water corrosion inhibitors," Materials Performance 10, 4 (1971) p.11.

15. J.H. Metcalf, Inhibition and Corrosion Control Practices for Boiler Waters, ed. C.C. Nathan, Corrosion Inhibitors, (Houston. TX: NACE, 1981) p.196-219.

16. D.C. Silverman, Practical Corrosion Prediction Using Electrochemical Techniques, in: ed. R.W. Revie, Uhlig's Corrosion Handbook, (New York. NY: John Wiley & Sons Inc., 2000) p.1179-1225.

17. R.H. Jones, R.E. Ricker. Chapter 1. Mechanisms of Stress-Corrosion Cracking. Stress Corrosion Cracking, Materials Performance and Evaluation, ed. R.H. Jones, (Materials Park. OH: ASM International, 1999).

18. J.D. Fritz, B.W. Parks, H.W. Pickering, "Stress corrosion cracking of copper – 18 at.% gold in 1N sodium sulfate – 0.01N sulfuric acid," Scripta Metallurgica 22, 7 (1988) p.1063-1068.

19. M.C. Petit, D. Desjardins, Stress Corrosion Cracking and Hydrogen Embrittlement of Iron Base Alloys, eds. R.W. Staehle et al, NACE-5, (Houston. TX: NACE, 1977) p.1205-1210.

20. R.W. Revie, H.H. Uhlig, Acta Metallurgica 22, May (1974) p.619-627.

21. D.A. Jones, Environment-Induced Cracking of Metals, eds. R.P. Gangloff, M.B. Ives, (Houston. TX: NACE, 1990).

22. J.M. Gere. Mechanics of Materials, Fifth Ed. (Pacific Grove. CA: Brooks/Cole, 2001).

23. C.J. Biermann, Handbook of Pulping and Papermaking, Second ed., (San Diego. CA: Academic Press, 1996).

24. P. Ricca, "A Study In The Oxidation Of Kraft Black Liquor" (Ph.D. diss., University of Florida, 1962).

25. T.T. Collins, Jr., "The Oxidation of Sulphate Black Liquor. A Review of the Literature. The First of Two Parts," Paper Trade Journal 36, March 20 (1953).

26. G.A. Smook, Handbook For Pulp & Paper Technologists, Second ed., (Vancouver. Canada: Angus Wilde Publications, 1992).

27. O. Arpalahti et al, Papermaking Science and Technology, Book 6B, Chemical Pulping, eds. J. Gullichsen, C.-J. Fogelholm, (Atlanta. GA: TAPPI Press, 1999) p.B135-202.

28. L. Peterman, R.A. Yeske, "Thiosulfate Effects on Corrosion in Kraft White Liquor," CORROSION/87 (San Francisco. CA: NACE, 1987).

29. R.A. Yeske, "Closure Effects on Pulp Mill Corrosion," 1985 TAPPI Environmental Conference (Mobile. AL: TAPPI, 1985) p.327.

30. R.B. Kesler, J.F. Bakken, "Corrosion of Mild Steel in Alkaline Pulping Liquors. Part 1. Kraft White Liquor," TAPPI 41, 3 (1958) p.97-102.

31. R.B. Kesler, "Corrosion of Mild Steel in Alkaline Pulping Liquors. Part 2. Neutral Sulphite Cooking Liquor," TAPPI 41, 3 (1958) p.102-109.

32. R.B. Kesler, "Corrosion of Mild Steel in Alkaline Pulping Liquors. Part 3. Special Effect of Sulfite Ion in Kraft White Liquor," TAPPI 43, 4 (1960) p.355-373.

33. C.G. Von Essen, "Corrosion Problems in Sulphate Pulp Mills," TAPPI 33, 7 (1950) p.14-32A.

34. H. MacLean, J.A.F. Gardner, Heartwood Extractives in Digester Corrosion, Pulp and Paper Magazine of Canada 54 (1953) p.125-130.

35. K. Niemelä, "Low-Molecular-Weight Organic Compounds in Birch Kraft Black Liquor," Annales Academiae Scientiarum Fennicae, Series A, II. Chemica, 229, Ph.D. diss., Helsinki University of Technology, Laboratory of Wood Chemistry, SF-02150, Espoo, Finland (1990).

36. K. Niemelä, "GLC-MS Studies on Pine Kraft Black Liquors, Part V. Identification of Catechol Compounds," Holzforschung 43, 2 (1989) p.99-103.

37. P.M. Singh, A. Anaya, K. Frey, J. Mahmood, "Corrosivity of Black Liquors – Role of Wood Species Pulped," 10th International Symposium on Corrosion in the Pulp and Paper Industry, 2 (Finland: VTT, 2001).

38. A. Anaya, P.M. Singh, "Effect of Wood Species on Corrosivity of Black Liquors," Corrosion 2001, paper no. 281 (Houston. TX: NACE, 2001).

39. A. Fries, T. Ericsson, R. Gref, "High heritability of wood extractives in Pinus sylvestris progeny tests," Canadian Journal of Forest Research 30 (2000) p.1707-1713.

40. F. Doussot, P. Pardon, J. Dedier, B. De Jeso, "Individual, species and geographic origin influence on cooperage oak extractible content (Quercus robur L. and Quercus petraea Liebl.)," Analusis 28 (2000) p.960-965.

41. L. Troselius, "Influence of chemical compounds on the corrosion rate of steels in liquors from continuous digesters," VTT Symposium, 10th International Symposium on Corrosion in the Pulp and Paper Industry, 2 (Finland: VTT, 2001) p.455-467.

42. A. Wensley, "Corrosion of Batch and Continuous Digesters," The Proceedings of the Ninth International Symposium on Corrosion in the Pulp and Paper Industry (NACE, 1998) p.27-37.

43. S.J. Pawel, D.W. Townley, D.F. Wilson, M.E. Gorog, "Influence of Douglas Fir Content in the Furnish on Corrosion of a Kraft Continuous Digester," Proceedings of the 2002 TAPPI Fall Technical Conference (San Diego. CA: TAPPI, 2002).

44. S. Kannan, R.G. Kelly, The Role of Dihydroxbenzenes and Oxygen on the Corrosion of Steel in Black Liquor, Corrosion Science 58, 7 (1996) p.1051-1069.

45. S. Afrossman, J. Daviot, D. Holmes, R.A. Pethrick, M. Wilson, "Molecular Design for Inhibition of Titanium Corrosion in Resist Cleaner Systems," Corrosion Science 43 (2001) p.939-950.

46. N. Subramanyan, V. Kapali, S. Venkitakrishna Iyer, "Influence of Hydroxy Compounds on the Corrosion and Anodic Behaviour of Al in NaOH Solutions," Corrosion Science 11 (1971) p.115-123.

47. G. Matamala, W. Smeltzer, G. Droguett, "Comparison of Steel Anticorrosive Protection Formulated with Natural Tannins Extracted from Acacia and Pine Bark," Corrosion Science 42 (2000) p.1351-1362.

48. H.F. Lewis, M.A. Buchanan, D. Fronmuller, E.F. Kurth, "Redwood Products as Inhibitors of Oxidation in Petroleum Hydrocarbons, Inhibition of Oxidation in Mineral Oils," Industrial and Engineering Chemistry 37, 10 (1945) p.988-990.

49. O. Lahodny-Šarc, F. Kapor, "Corrosion inhibition of Carbon Steel in the Near Neutral Media by Blends of Tannin and Calcium Gluconate," Materials and Corrosion 53 (2002) p.264-268.

50. M.M. Osman, M.N. Shalaby, "Thermodynamic parameters accompanying the corrosion inhibition of low carbon mild steel by some commercial surfactants," Corrosion Prevention & Control 50, 3 (2003) p.126-135.

51. W. Skinner, W.S. Ernest, "Influence of flow conditions on corrosion characteristics of mild steel rotating cylinder in solutions of fatty acids," British Corrosion Journal 34, 1 (1999) p.79-80.

52. E.F. Otte, W. Skinner, "Corrosion characteristics of mild steel in aqueous solutions of fatty acids," British Corrosion Journal 30, 2 (1995) p.135-136.

53. M.M. Singh, A. Gupta, "Corrosion Behavior of Mild Steel in Acetic Acid Solutions," Corrosion 56, 4 (2000) p.371-379.

54. M. Abdallah, A.A. El-Sarawy, A.Z. El-Sonbati, “Commercial fatty acid sulphonate as a corrosion inhibitor for mild steel in HCl,” Corrosion Prevention & Control 48, 3 (2001) p.97-100.

55. C.A. Loto, A.I. Mohammed, “The effect of cashew juice extract on corrosion inhibition of mild steel in HCl,” Corrosion Prevention & Control 47, 2 (2000) p.50-56,63.

56. C.A. Loto, “The effect of mango bark and leaf extract solution additives on the corrosion inhibition of mild steel in dilute sulfuric acid – Part 2”, Corrosion Prevention & Control 48, 2 (2001) 59-64,81.

57. C.A. Loto, “Inhibition of cashew juice on the corrosion of mild steel in sulphuric acid,” Corrosion Prevention & Control 52, 1 (2005) p.13-24.

58. M.G. Bestul, I.A. Stine, J.C. McManus, “New tall oil fraction, similar in physical and chemical properties to lanolin, used as soap additive, rust preventive, emulsifier,” Soap and Chemical Specialties 34, 10 (1958) p.49-51,56.

59. A. Gutiérrez, J.C. Del Río, F.J. González-Vila, F. Martín, “Chemical Composition of Lipophilic Extractives from Eucalyptus globulus Labill. Wood,” Holzforschung 53, 5 (1999) p.481-486.

60. A. Gutierrez, J. Romero, J.C. del Rio, “Lipophilic Extractives from Eucalyptus globolus Pulp during Kraft Cooking Followed by TCF and ECF Bleaching,” Holzforschung 55, 3 (2001) p.260-264.

61. L. Ruus, L. Stockman, “Undersökningar Rörande Korrosion I Sulfatkokare” (translation: “Investigations concerning corrosion problems in sulphate digesters”), Svensk Papperstidning 56, 22 (1953) p.857-865.

62. C.B. Christiansen, J.B. Lathrop, “Field Investigation of Corrosion in Alkaline Pulping Equipment,” Pulp and Paper Magazine of Canada, Nov. (1954) p.119.

63. E.W. Hopper, J.B. Morrison, “Experiments with Digester Corrosion Variables,” TAPPI 38, 1 (1955) p.8.

64. D.A. Wensley, R.S. Charlton, “Corrosion Studies in Kraft Mill Liquor. Part 2. Effect of Plain Carbon Steel Composition,” Pulp and Paper Industry Corrosion Problems, Proc. Third International Symposium on Corrosion in the Pulp and Paper Industry, 3 (NACE, 1980).

65. L.H. Laliberté, “Corrosion Problems in the Pulp and Paper Industry,” CORROSION/77, paper no. 165 (San Francisco. CA: NACE, 1977).

66. T.T. Collins, Jr., “The Oxidation of Sulphate Black Liquor and Related Problems,” TAPPI 38, 8 (1955) p.172A.

67. D.A. Wensley, R.S. Charlton, “Corrosion Studies in Kraft White Liquor: Potentiostatic Polarization of Mild Steel in Caustic Solutions Containing Sulfur Species,” Corrosion 36, 8 (1980) p.385.

68. P.M. Singh, O. Ige, J. Mahmood, “Stress Corrosion Cracking of Type 304L Stainless Steel in Sodium Sulfide-Containing Caustic Solutions,” Corrosion 59, 10 (2003) p.843-850.

69. D.A. Wensley, “Corrosion Studies in Kraft White Liquor Tankage,” Pulp and Paper Industry Corrosion Problems, Proc. Fifth International Symposium on Corrosion in the Pulp and Paper Industry, 5 (Vancouver. Canada: NACE, 1986).

70. B. Haegland, B. Roald, “The Corrosion of Steel in White Liquor,” Norsk Skogindustri 9 (1955) p.351-364.

71. M. Yasuda, M. Okada, F. Hine, “Corrosion of Carbon Steel in Hot NaOH Solutions Under Heat Transfer Conditions,” CORROSION/82 (Houston. TX: NACE, 1982).

72. D. Tromans, “Anodic Polarization Behavior of Mild Steel in Hot Alkaline Sulfide Solutions,” J. Electrochemical Society 127, 6 (1980) p.1253.

73. L. Stockman, “Sulfate Digester Corrosion As A Function Of White-Liquor Polysulfide Content,” Svensk Papperstiding 63, 13 (1960) p.425-430.

74. N. Tonsi-Eldakar, “Corrosivity of Kraft Liquors,” CORROSION/80, paper no. 258 (Chicago. IL: NACE, 1980).

75. R.A. Yeske, “Corrosion in the Pulp and Paper Industry,” IPC Technical Paper Series, IPST, paper no. 192, July (1986).

76. T.T. Collins, Jr., “Part 2. The Oxidation of Sulphate Black Liquor,” Paper Trade Journal 36 (1953) p.19-24.

77. D.F. Bowers, “Corrosion Problems in Kraft Liquor Systems,” CORROSION/82 (Houston. TX: NACE, 1982), p.90.

78. D. Tromans, S. Ramakrishna, E.B. Hawbolt, “Stress Corrosion Cracking of ASTM A516 Steel in Hot Caustic Sulfide Solutions—Potential and Weld Effects,” Corrosion 42, 2 (1986) p.63.

79. D.C. Crowe, D. Tromans, “ Reference Electrodes for Use in Alkaline Sulfide Solutions,” Pulp and Paper Industry Corrosion Problems, Proc. Fifth International Symposium on Corrosion in the Pulp and Paper Industry, 5 (Vancouver. Canada: NACE, 1986).

80. M. Pourbaix, “Atlas of Electrochemical Equilibria in Aqueous Solutions,” (Austin. TX: NACE, 1974).

81. R.J. Biernat, R.G. Robins, “High-Temperature Potential/pH Diagrams for the Iron-Water and Iron-Water-Sulphur System,” Electrochimica Acta 17 (1972) p.1261-1283.

82. Outokumpu HSC Chemistry®, Chemical Reaction and Equilibrium Software with Extensive Thermochemical Database, Version 5.1, Outokumpu Research Oy, Finland.

83. D. W. Shoesmith, P. Taylor, M.G. Bailey, B. Ikeda, “Electrochemical Behaviour of Iron in Alkaline Sulphide Solutions,” Electrochimica Acta 23 (1978) p.903-916.

84. M.A. Taras, J.R. Saucier, “Influence of extractives on specific gravity of Southern Pine,” Forest Products Journal 17 (1967) p.97-99.

85. P.R. Larson, D.E. Kretschmann, A. III Clark, J.G. Isebrands, Formation and Properties of Juvenile Wood in Southern Pines, A Synposis. United States Department of Agriculture, Forest Products Laboratory, General Technical Report, FPL-GTR-129 (2001).

86. T207 om-93 Water solubility of Wood and Pulp, TAPPI Test Methods 1996-1997 (Atlanta. GA: TAPPI Press, 1997).

87. C.C. Nathan, Corrosion Inhibitors in Refineries and Petrochemical Plants, in: ed. C.C. Nathan, Corrosion Inhibitors (Houston. TX: NACE, 1973) p.45-60.

88. S. Papavinasam, Corrosion Inhibitors, in: ed. R.W. Revie, Uhlig's Corrosion Handbook (New York. NY: John Wiley & Sons Inc., 2000) p.1089-1106.

89. A.K. Dunlop, Corrosion Inhibitors in Secondary Recovery, in: ed. C.C. Nathan, Corrosion Inhibitors (Houston. TX: NACE, 1973) p.76-88.

90. P.I. Marshall, G.T. Burnstein, "Effects of Alloyed Molybdenum on the Kinetics of Repassivation on Austenitic Stainless Steels," Corrosion Science 24, 5 (1984) p.463.

91. D. Singbeil, D. Tromans, "Stress Corrosion Cracking of Mild Steel in Alkaline Sulfide Solutions," Pulp and Paper Industry Corrosion Problems, Proc. Third International Symposium on Corrosion in the Pulp and Paper Industry, Vol. 3 (Houston. TX: NACE, 1980) p.40.

92. D. Singbeil, D. Tromans, "Effect of Sulfide Ions on Caustic Corrosion Cracking of Mild Steel," J. Electrochemical Society 128, 10 (1981) p.2065.

93. A.K. Agrawal, K.G. Sheth, K. Poteet, R.W. Staehle, "The Polarization Behavior of Fe-Ni-Cr Alloys in Concentrated Sodium Hydroxide Solutions in the Temperature Range 25° to 150°C," J. Electrochemical Society 119, 12 (1972) p.1637.

94. D. Singbeil, A. Garner, "Caustic stress corrosion cracking of pressure vessel steels in dilute alkaline-sulfide solutions," Materials Performance 24, 10 (1985) p.9.

VITA

Patrick E. Hazlewood was born in Jacksonville, Florida in 1974. Within the next eighteen years he would receive an Honorary Citizenship from Sullivan's Island, South Carolina and graduate from Westminster Preparatory Schools of Augusta, Georgia. Patrick began his higher educational studies at the University of Georgia where he was a student athlete and graduated with a BS Chemistry and Bachelor of Science in Biochemistry & Molecular Biology. He insists that his greatest achievement in his four years in Athens was choosing the right time and place to go to dinner in mid-January 1994.

Unfulfilled in an academic laboratory environment, Patrick continued a family tradition and enrolled at the University of Arkansas. While furthering his education with a BS and MS in Chemical Engineering he participated in the founding of the Graduate Student Organization and subsequent subsidization of health insurance for all graduate students. Not having reached his capacity for the academic lifestyle he enrolled in the doctoral program at one of the world's premier educational and research facilities for the Forest Products Industry, The Institute of Paper Science and Technology, now IPST at Georgia Tech. Prior to the impending merger with the Georgia Institute of Technology

and his transition to the School of Chemical and Biomolecular Engineering he received an MS Paper Science and Technology and began studies towards an MBA in marketing and operations at Georgia Tech. Holding the position of President for the Graduate Students in Management he helped form the Men In Business, a growing social networking organization for both male and female business school alumni. Completing his MBA and a Doctor of Philosophy in Chemical and Biomolecular Engineering at Georgia Tech, he now anxiously awaits the challenges ahead of him as part of a global business community and the joy in purchasing season tickets for football at the UNIVERSITY of GEORGIA. GO DAWGS!